AFRL-RH-WP-TR-2016-0060

Depth Acuity Methodology for Electronic 3D Displays: eJames (eJ)

Eric L. Heft, John McIntire,
Frederick M. Meyer, and Darrel G. Hopper

USAF AFMC 711 HPW/RHCV
2255 H Street
Wright-Patterson AFB OH 45433

July 2016

INTERIM REPORT

STINFO COPY

AIR FORCE RESEARCH LABORATORY
711 HUMAN PERFORMANCE WING
AIRMAN SYSTEMS DIRECTORATE
WRIGHT-PATTERSON AIR FORCE BASE OH 45433-7022
AIR FORCE MATERIEL COMMAND
UNITED STATES AIR FORCE

NOTICE AND SIGNATURE PAGE

AFRL-RH-WP-TR-2016-0060 HAS BEEN REVIEWED AND IS APPROVED FOR PUBLICATION IN ACCORDANCE WITH ASSIGNED DISTRIBUTION STATEMENT.

//signed//
DARREL G. HOPPER
Program Manager
Battlespace Visualization Branch

//signed//
ROBERT C. MCKINLEY
Chief, Battlespace Visualization Branch
Warfighter Interface Division

//signed//
WILLIAM E. RUSSELL
Chief, Warfighter Interface Division
Airman Systems Directorate
711 Human Performance Wing

REPORT DOCUMENTATION PAGE

Form Approved
OMB No. 0704-0188

1. REPORT DATE *(DD-MM-YY)*	2. REPORT TYPE	3. DATES COVERED *(From - To)*
24-07-2016	Interim	11 Oct 2012 – 30 Jun 2016

4. TITLE AND SUBTITLE

Depth Acuity Methodology for Electronic 3D Displays: eJames (eJ)

5a. CONTRACT NUMBER
FA8650-08-D-6801-0050

5b. GRANT NUMBER

5c. PROGRAM ELEMENT NUMBER
Multiple

6. AUTHOR(S)

Eric L. Heft, John McIntire,
Frederick M. Meyer, and Darrel G. Hopper

5d. PROJECT NUMBER
5329

5e. TASK NUMBER
11

5f. WORK UNIT NUMBER
H0CK (53291102)

7. PERFORMING ORGANIZATION NAME(S) AND ADDRESS(ES)
USAF AFMC 711 HPW/RHCV
2255 H Street
Wright-Patterson AFB OH 45433

8. PERFORMING ORGANIZATION REPORT NUMBER

9. SPONSORING/MONITORING AGENCY NAME(S) AND ADDRESS(ES)
Air Force Materiel Command
Air Force Research Laboratory
711 Human Performance Wing, Human Effectiveness Directorate
Warfighter Interface Division, Battlespace Visualization Branch
Wright-Patterson Air Force Base OH 45433-7022

10. SPONSORING/MONITORING AGENCY ACRONYM(S)
USAF AFMC 711 HPW/RHCV

11. SPONSORING/MONITORING AGENCY REPORT NUMBER(S)
AFRL-RH-WP-TR-2016-0060

12. DISTRIBUTION/AVAILABILITY STATEMENT DISTRIBUTION STATEMENT A. Approved for public release: distribution unlimited. Previously cleared: 88ABW-2013-2508, 88ABW-2014-0320 88ABW-2014-1130

13. SUPPLEMENTARY NOTES 88ABW Cleared 09/08/2016; 88ABW-2016-4404. Report contains color. Contains Patentable Information (patent being pursued but not approved).

14. ABSTRACT An electronic version (eJ) of the James (J) test of depth acuity is created and evaluated on three different types of 3D electronic displays: one active-eyewear Stereo 3D (S3D) and two non-eyewear full parallax Field-of-Light Display (FoLD) systems. The two FoLD systems are the Actuality Integral Slice (AIS) swept-screen volumetric Perspecta and the Zebra Integral Ray (ZIR) hogel-based ZScape Motion Display (ZMD). The James test is designed so that the only factor examined is binocular single vision (BSV), aka stereoscopic parallax. The James Depth Perception Apparatus (DPA) comprises two vertical white 1cm wide rods (or thin strings) viewed at a reference distance (e.g. 6m) against a black background through a window in a black front. The eJ computer graphics white bar stimuli in this work are designed to visually emulate—within limitations of the S3D, AIS, and ZIR—the white rods in the James DPA. The unique artifacts of the three electronic display types impede creation of a single graphical representation of the two-bar stimuli and complicate cross-type comparisons. A compact variant of the James DPA developed by Howard made the left rod stationary and right rod adjustable by the subject (rather than the administrator) via a hand-crank to match distance via a mechanical string-pulley system. The Howard DPA variant also enabled depth acuity threshold determination by two methods: (a) forced-choice of nearest bar; (b) adjustment of right bar to match left. An AFRL-automated Howard DPA is included in the present study to enable a comparison of real-world stimuli versus the electronic displays. A hand-held computer game controller is used to automate data collection and subject trial initiation. Four software interfaces are developed to control the stimuli positions presented on the three 3D electronic systems and the automated DPA; the right bar is randomly positioned from trial to trial. The four systems (AIS, S3D, ZIR, DPA) are set up side-by-side for a shake-down evaluation using six subjects tested by methods (a) and (b). The subject results are presented, analyzed, and discussed. Binocular depth acuity is assessed on all four systems. The within-type and limited cross-type analyses indicate that eJ is a viable depth acuity metric to guide and assess progress in the development of the emerging FoLD class of non-eyewear 3D visualization systems.

15. SUBJECT TERMS Depth Acuity Metric, 3D Displays, Stereo 3D, S3D, Volumetric Display, Holographic Video Display, HVD, Hogel

16. SECURITY CLASSIFICATION OF:			17.LIMITATION OF ABSTRACT:	18. NUMBER OF PAGES	19a. NAME OF RESPONSIBLE PERSON (Monitor) / 19b. TELEPHONE NUMBER *(Include Area Code)*
a. REPORT	b. ABSTRACT	c. THIS PAGE			
Unclassified	Unclassified	Unclassified	SAR	97	Darrel G. Hopper

TABLE OF CONTENTS

Section **Page**

LIST OF FIGURES

LIST OF TABLES

Table **Page**

ACKNOWLEDGEMENTS

The authors thank Drs. Lawrence K. Harrington and Paul R. Havig II for arranging for the loan of the USAFSAM version of the Howard Depth Acuity Apparatus (DPA) used in this work, and for providing insightful comments during the early phases of this research.

1.0 SUMMARY

Metrics are needed for the Field-of-Light Display (FoLD) class, comprising 3D visualization systems that provide full-parallax imagery viewable by multiple persons without special eyewear (Hopper et al., 2016). The present work explores a quantitative metric for the perception of depth on electronic 3D displays at 6m based on a test and physical apparatus invented by James (1907, 1908), an ophthalmologist working in the UK, which were subsequently used and advanced by other research ophthalmologists in The Netherlands (Schoüte 1910) and U.S. (Howard 1919a, 1919b) (Deyo1922). The 6m viewing distance is chosen so as to enable correlation, for each subject, of depth acuity to lateral acuity measurements per Snellen (1862).

The James test is administered on a physical Depth Perception Apparatus (DPA) comprising two parallel vertical white rods at e.g. 6m ± z viewed through a black-fronted window (that hides the rod ends) against a black background; electric lighting is used to ensure uniform illumination; head position is controlled to eliminate motion parallax (James, 1908). Schoute (1910) reported results for 560 persons and Howard (1919a), for 106 using the James DPA. Multiple variants of the James test and DPA are now in wide use for disciplines ranging from to aviation to sports.

The electronic version of the James test (eJ) developed in the present work comprises computer graphics stimuli designed to visually emulate—within limitations of the electronic displays—a variant of the James apparatus designed by Howard (1919b). The Howard DPA (a) makes the right rod hand-crank adjustable by the subject (rather than the administrator) to match distance via a mechanical string-pulley system and (b) enables threshold depth acuity measurement by the method of adjustment as well as the method of forced choice (James 1908; Howard 1919a).

For eJ, a wireless hand-controller replaces the hand-crank to automate data collection and subject trial initiation. Four personal computer software interfaces control the stimuli (bar/stripe) positions presented on the electronic displays and on an AFRL-automated version of the Howard DPA (Howard 1919b; Meyer et al., 2016). The systems were set up side-by-side for a shake-down evaluation by six subjects tested via two methods: (a) forced-choice of nearest bar; (b) adjustment of one bar (randomly positioned in depth by the software) to match the other. The design and programming of sample images for, and an initial human subject evaluation on, three electronic 3D displays are reported here. These three comprise one Stereo 3D (S3D) class special glasses type and two different types within the FoLD class: the Actuality Integral Slice (AIS) "Perspecta" circular rotating screen scanned volume display (SVD); and the Zebra Integral Ray (ZIR) hogel-based "Zscape Motion Display (ZMD)." The AIS Perspecta and ZIR ZMD (9-Tile table, 1-Tile mobile) are prototype FoLD systems acquired by AFRL in 2005 and 2011.

Figure 1 shows the experimental condition of subjects viewing the displays at a distance of 6m from the reference position of the two thin circular vertical bars. Visual artifacts (unique to each electronic display type) impeded creation of a single 3D graphical representation of the two-bar stimuli and complicated cross-type comparisons (AIS vs. S3D vs. ZIR vs. DPA). The within-type (i.e. across subjects) and limited cross-type analyses (i.e. across displays) reported herein do, however, suggest that eJ is a viable depth acuity metric to guide development of the FoLD class of visualization systems. Figure 2 shows a close-up of the stimuli on the four test devices.

Figure 1. eJames Depth Acuity Experimental Condition at 6m

The stripes representing the bars on the electronic displays (AIS in Figure 2A, S3D in Figure 2B, and ZIR in Figure 2C) are written as white against a black background per James (1907, 1908); the eJ test images are electronic, so this choice can be varied in future work. The DPA (Figure 2D) has black bars against a white background per Howard (1919a, 1919b). The eJ bars are also scaled (in width and height) as a function of their displacement, z, from the reference distance of 6m so that they subtend constant angles at the pupil positions. The physical DPA is designed to prevent viewing of the bar ends. Research by James (1908) and Howard (1919b) shows the bar width adjustment has an insignificant effect on the depth acuity measured for observers. Schoute (1910) replaced the 10mm wooden rods with "medium thick white strings" for similar reasons.

Monocular viewing of the eJ stimuli are also tested to ascertain the effects of artifacts. The present results are consistent with Deyo (1922) who reported monocular depth acuity is worse than binocular acuity by 10X (4X) for subjects having 20/15 (20/20) Snellen lateral acuity.

Howard 1919a) reported instant perception of the nearer bar via binocular single vision (BSV) using a shutter to rapidly reveal the view of real objects (DPA). Present FoLD MoCS results (AIS and ZIR) are similarly fast. However, stereoscopic vision (virtual images) and BSV (real objects) are not the same (Blaauw, 1917, p. 30). The inferiority of the present S3D speeds of depth acuity selection (relative to the AIS, ZIR & DPA results) demonstrates this key difference.

Depth acuity metrology will have to be expanded in future work to address multiple viewing situations. James (1908), Howard (1919c, 1920b on Stereomicrometer); and Howard (1919d, 1920c on semaphores at 100m) examined several distances. Group viewing may involve eye-display distances of meters, compared to arms-length distances for workstations and handhelds.

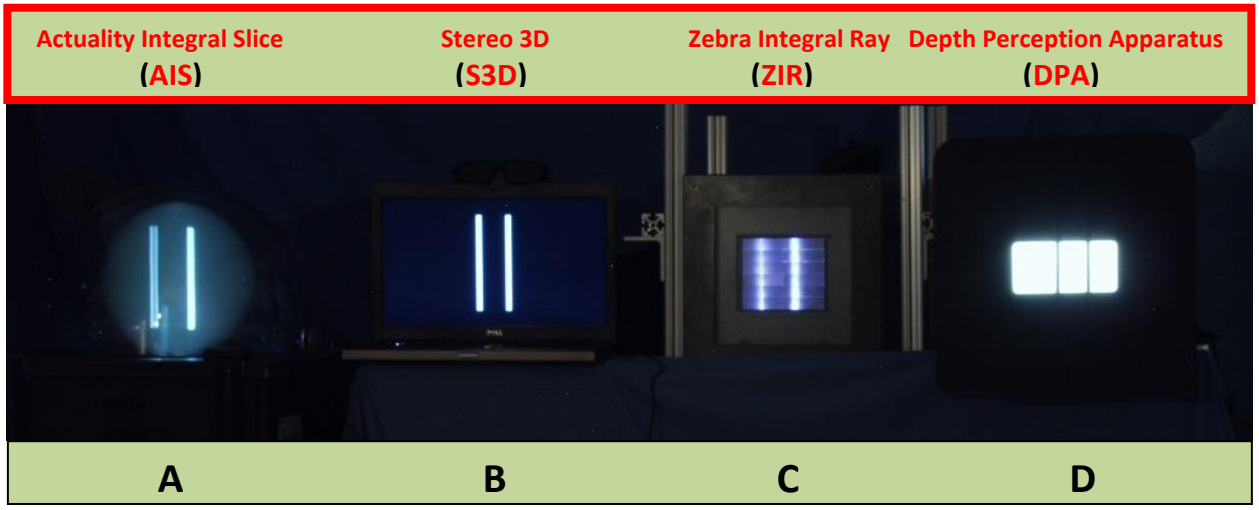

Figure 2. Close-up of Sample Images with Both 10mm Bars at Reference Distance (6m):
(A) Actuality Integral Slice – Perspecta Spinning Screen Scanned Volume Display (AIS);
(B) Stereo 3D – Dell M6700 17.3-in. Notebook with NVIDIA Active-Eyewear (S3D);
(C) Zebra Integral Ray - Hogel-Based Zscape Motion Display (ZIR);
(D) Depth Perception Apparatus - AFRL-automated Howard Six-Meter Stereoscope (DPA)

2.0 INTRODUCTION

2.1 Metrology Gaps for Emerging Field-of-Light Display (FoLD) Systems

The AFRL Battlespace Visualization Branch (USAF AFMC 711 HPW/RHCV) has acquired several examples of a new class of displays capable of producing full-parallax (FP) 3D imagery that do not require eyewear and designed for view by several persons simultaneously as if they were looking as a scaled representation of a physical 3D model or scene. Members of this new, Field-of-Light Display (FoLD), class have common attributes that cannot be characterized with existing 2D display test and evaluation (T&E) methods and standards. New metrics and testing procedures are required as detailed in the AFRL Technical Report entitled "AFRL Display Test and Evaluation Methodologies (AFTEM)" (Hopper et al., 2016). A methodology for depth acuity at a viewing distance of 6 m is reported here to advance performance-based assessments of evolving FoLD technologies. The 6m reference viewing distance was chosen by Snellen (1862) for lateral visual acuity and adopted by James (1908) for depth visual acuity, which is defined as the threshold angle of stereoscopic parallax (aka stereo acuity). Future work will address the separate viewing conditions of 1 m (Howard, 1920a) and 100 m (Howard, 1920b).

AFRL is uniquely situated to lead metrology research in 3D visualization. In-house research addresses both physical measurements on prototype systems and human subject experiments with the aim to create new objective physical metrics based on psychophysical studies of the human vision system (HVS). The FoLD systems currently in-house and extramural programs are described in subsections 2.2 and 2.3. High resolution fixed holograms are available as well.

2.2 FoLD Systems at AFRL

AFRL presently has three FoLD systems as follows:

(a) a volumetric display—Acuality Integral Slice (AIS) Perspecta swept volume system, which computes 2D circular slices of a 3D model for rapid projection via a TI DLP XGA kit onto a spinning screen; developed by Actuality Systems in Burlington MA, bought for $75K during the 2004-2008 period (Reference: Donelan, 2010). (ARS is no longer in production). Video demo: http://www.youtube.com/watch?v=8KaQmn2VTzs (2007, accessed 24 Jul 2016))

(b) a volumetric display—LightSpace Integral Slice (LIS) Depth Cube z1024 system, which computes 2D depth slices of a 3D model for high speed projection via a TI DLP XGA kit into a stack 20 time-sequenced LC-based diffuser screens at 30Hz to generate a 90° FoV; originally developed by LightSpace Technologies (1994-2004, price ~$100K); (July 2016 price: $64.5K) re-developed by EUROLCDS, SIA (2011) as new x-series LightSpace x1403a, replaced by model x1405B. x1405B available from LightSpace Technology, Inc., Twinsburg OH, www.lightspace3D.com (2016). Video demo: http://www.youtube.com/watch?v=RAasdH10Irg (5 Oct 2010). (Reference: Osmanis, 2016).

(c) a hogel-based display—Zebra Integral-Ray (ZIR) ZScape Motion Display system, which computes hundreds of millions of light rays from hogels of a 3D model and projects them via an array of refractive and light-modulating elements into a 90° conical viewing zone at ~1 Hz; a hogel is a model point projected into NxM directions by NxM adjacent 2D pixels. developed by Zebra Imaging, Inc. in Austin TX. (Reference: Klug et al, 2013). (not in production; prototype ZMD1 systems can be purchased for ~$1M). Video demo: http://www.zebraimaging.com/products/motion-displays (accessed 24 Jul 2016)

2.3 AFRL Programs to Develop FoLD Systems and Metrology

AFRL is developing performance based metrics (PBMs) for FoLD systems as part of both its intramural (e.g. this report) and extramural programs. The extramural 3D research comprises primarily SBIRs sponsored by the AFLCMC/HBB Command and Control Operations Centers division at Hanscom AFB MA and AFLCMC/WNU Human System Vison at WPAFB OH. The AFRL extramural program builds on prior investments by DARPA, IARPA, and AFOSR.

One extramural program, *Holographic Lightfield 3D Metrology (HL3DM)*, began Phase I in 2014 with two performers (Adi-Displays Consulting LLC in Portland OR and Rattan Software LLC in Austin TX) with a planned downselect to a single 2-yr Phase II performer (Rattan) from 2016-2018. The HL3DM objective is test and evaluation methodology for holographic lightfield 3D displays with an automated measurement system (a) to support comparisons of prototypes emerging from research, (b) to enable robust calibration, and (c) to perform product acceptance testing. A "Handbook FoLD Test & Evaluation Methodologies" is anticipated by 2018. Transition via incorporation into an international display measurement standard is also planned.

Another program, *Holographic Video Display (HVD)* focuses on SIR systems. One is a Phase II Extension effort 2014-2018 with TIPD, LLC (teamed with MIT Media Lab and Brigham Young U.) to develop a new type of FoLD system, the hogel-based TIPD Integral Ray (TIR) guided-wave scanning type, along with metrics to assess performance. A second HVD Phase II award 2016-2018 to Zebra Imaging Inc. researches a next-generation Zebra Integral Ray (ZIR).

AFRL has a three-year 2014-2017 Cooperative Research and Development Agreement (CRADA) with Zebra Imaging, Inc. entitled "*ZMD Improvements/Analyses and Supporting Fixed Hologram Concepts*" addressing metrics and other topics. The CRADA leverages the 2005-2010 DARPA *Urban Photonic Sandtable Display (UPSD)* and 2010-2013 AFRL *Full Multiplex Holographic Display (FMHD)* programs. AFRL is the DARPA transition partner for USPD and acquired the ZIR systems and spare parts from DARPA via the FMHD program.

AFRL was the technical and contacting agent for the 2012-2013 *IARPA Synthetic Holographic Observation (SHO)* with Ostendo Technologies, Inc. (OTI). SHO leveraged the 2008-2011 DARPA *High Resolution Affordable Emissive Micro-Display (EMD)* and the 2010-2011 AFRL *Ultrahigh Definition Microdisplay (UDM)* programs. Ostendo developed its Quantum Photonic Imager (QPI) micro-pixelated stacked light emitting diode (LED) display under the EMD, UDM and SHO programs. Sechrist (2014) documents the first public demonstration of a QPI device at the SID Display Week 2014 I-Zone and reports that Ostendo plans a commercial display by 2015 (did not happen). An array of QPI devices might be the basis for a hogel-based Ostendo Integral Ray (OIR) Quantum Photonic Imager type of FoLD system once the technology matures.

2.4 Depth Acuity Metric for the Real World – the James Test and Distance Stereoscope

Depth acuity is herein defined as the Binocular Single Vision (BSV) Depth Perception threshold. Binocular Single Vision is the perception of a single image of real objects seen with both eyes. Quantitative metrics for the depth perception threshold can be defined for BSV as illustrated in

Figure 3a. Two objects A and B are at distances LA and LB from the left (L) and right (R) eyes. No depth difference exists if both objects are at points A and T in a plane parallel to the inter pupil distance (IPD) axis, LR. However, if the object at T is moved to position B, the line of sight LT shifts to LB, which crosses the reference plane at point P. The lateral linear distance PT is a quantitative measure of depth perception called binocular Stereoscopic Parallax (Helmholtz, 1856). Another linear metric is the depth difference, TB = z. A third metric is the angle B-L-T, which is known as the Angle of Stereoscopic Parallax (ASP) (James, 1908). The threshold values of either x or z in mm, or of ASP in arcseconds, are quantitative measures of depth acuity.

James (1907, 1908) invented a test and physical apparatus (Figure 3b) that he called a "distance stereoscope," to measure stereoscopic depth visual acuity with the same accuracy as the Snellen (1862) metric for monocular lateral visual acuity. James carefully excluded visual factors other than BSV and designed a test and apparatus that have stood the test of subsequent research. Figure 3b is an annotated reproduction of Fig. 2 in James (1908). Fig. 1 in James (1908) and associated text describes the James DPA as a 380Wx310Hx385L mm box with roof and sidewalls removed; the back included two 190x290 mm wings that, when attached, elongated the back wall to 760 mm wide. James used vertical rods at points A and B having diameter d±δ mm separated by a distance AB, where d=10 and AB = 50mm; δ was adjusted from 0 to 0.5 mm so that the rod diameter subtended a fixed angle of about 6 arcmin at each eye for LA = 6 m. The rods were painted a pure white, illuminated by two electric lamps, and viewed at Reference Distances ranging from 1850 to 6000 mm through a 195x120 mm window (centered in the front wall) against the back wall; the whole of the anterior and posterior walls were covered in black velvet. The depth acuity of subjects was found to vary inversely with their IPD (James considered values from 50 to 70 mm). Influences of rod diameter, illumination, linear perspective (rod ends hidden), parallax (from slight head movements at 6m), and accommodation are excluded and the observer "must form an estimate as to their relative positions from the binocular parallax alone—i.e. from a comparison between the angles subtended at the nodal points of the right and left eye respectively" (James, 1908, p. 1764). James also performed an experiment in which the rods were place horizontally, one 180 mm farther than the other; in this case none of his observers was able to ascertain which rod was nearer at viewing distance LA as small as 2.5m; there was no binocular parallax in this horizontal rod experiment and observers had to rely solely on their convergence innervation. James reported a rough correlation of monocular lateral visual acuity (Snellen test) with his depth acuity results. Applications cited by James include examinations of school children and candidates for the navy, where the visual standard required for both eyes is high. James describes his Depth Perception Apparatus as inexpensive and portable. James states he also designed a small instrument on the same principle to be used at reading distance; Howard (1920a) provides design details for a Stereomicrometer.

Results using the James DPA are similar for many choices of the parameters (d, δ, AT, LA): (10mm, 0-0.5mm, 50mm, 2-6m) by James (1908); (1mm, 0, 50mm, 2-5m) by Schoute (1910); (10mm, 0, 60mm, 6m) by Howard,1919a); and (120mm, 0-33mm, 1m, 100m) by Howard (1920b). Schoute (1910) reports that depth acuity (the threshold BSV) is on average three times as sharp (about 20 arcsec) as expected based on Snellen 20/20 lateral acuity (1 arcmin). Howard (1919a) reports thresholds as low as 3.37 arcsec using his version of the James DPA (Figure 4).

The James test and DPA are still the state-of-the-art for depth perception acuity measurement (Lafayette, 2014) and a suitable basis for developing a depth metric for electronic 3D displays.

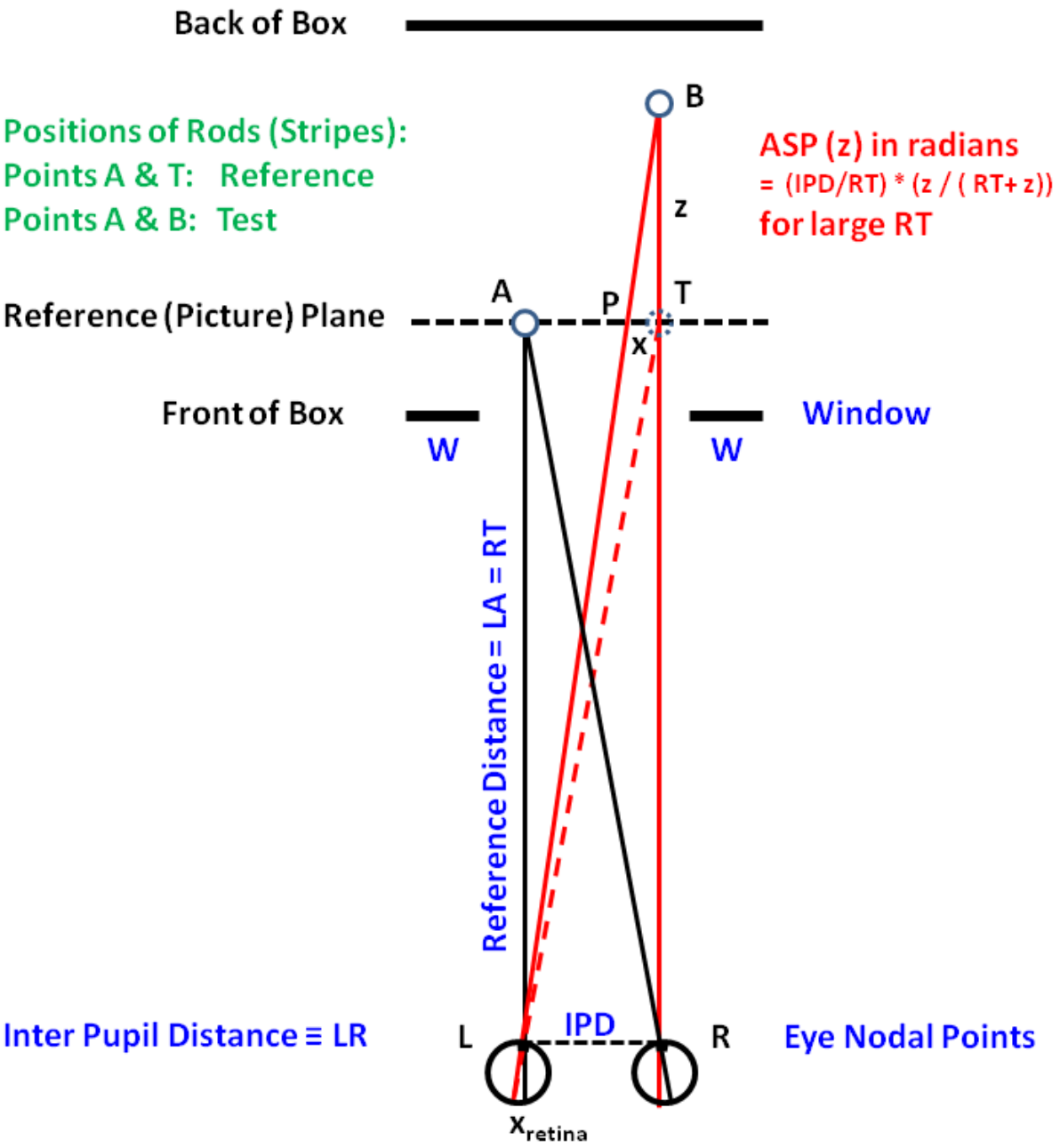

Quantitative Metrics for Binocular Single Vision (BSV) Depth Perception:
(a) Lateral Linear Stereoscopic Parallax (LLSP) ≡ Line Segment PT ≡ x;
(b) Angle of Stereoscopic Parallax (ASP) ≡ Angle P-L-T ≡ Angle B-L-T;
(c) Depth Acuity Metric ≡ ASP (arcsec), or x (mm), or z (mm).

Note1: Schematic drawing is top view (not to scale) of Depth Perception Apparatus (DPA) per James (1908).
Note 2: Line Segment PT ≡ LLSP is also known simply as Stereoscopic Parallax (SP) per Helmholtz (1856).
Note3: Angle B-L-T ≡ ASP is also known as the Binocular Parallactic Angle (BPA) per Howard (1919a).

Figure 3a. Quantitative Metrics for Binocular Single Vision (BSV) Depth Perception.

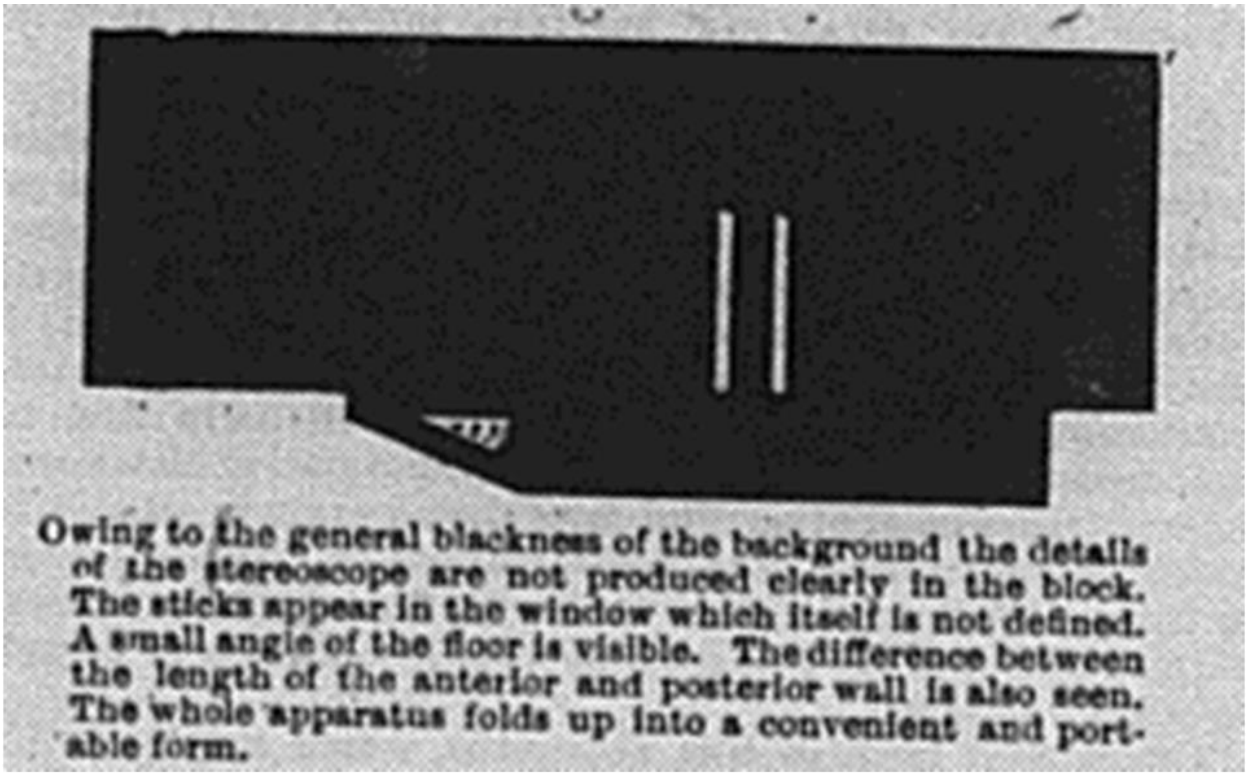

The above figure and caption are Fig. 1 from James (1908) illustrating his "Distance Stereoscope".
Pure white sticks are used as test objects; all other surfaces viewable by the subject are covered in black velvet.
James adjusted the diameter of the sticks to maintain constant size as it was moved from z = 0.
Schulte (1910) used this same apparatus, but with medium thick white threads in lieu of the variable diameter sticks.

Figure 3b. The James (1908) Depth Perception Apparatus (DPA)

Some useful equations based on the James (1908) diagram that served as the basis for Figure 3a are as follows:

ASP (z) in radians = arctan(LR/RT) - arctan(LR/RB) = (IPD/RT) * (z / (RT+ z)) Equation (1)
= LR/RT – LR/RB = (LR * (RB-RT)) / (RT * RB) = (LR * TB) / (RT * (RT + TB))
= (LR/RT) * (TB / (RT + TB))
= (IPD/RT) * (z / (RT+ z))
= 0.0105 * z / (6000+z) in radians for (IPD, RT) = (63mm, 6000mm)

Deyo (1922) reported the ASP(z) values as follows:
= 32.54 urad (6.7 arcsec) for (IPD, RT) = (60mm, 6000mm), z measured as 18.65mm (BSV all)
= 20.82 urad (4.3 arcsec) for (IPD, RT) = (60mm, 6000mm), z measured as 11.93mm (BSVpass)
= 202.5 urad (41.7 arcsec) for (IPD, RT) = (60mm, 6000mm), z measured as 118mm (mono)

Qualified pilots averaged a z threshold of 11.93 mm, which translates to a BSV of 4.3 arcsec.

Fig. 1. A subject making an observation.

The above figure and caption are Fig. 1 from Howard (1919a) illustrating his modification of the James (1908) apparatus and test condition. Flat black wooden rods are used as test objects; all surfaces are painted a dead black; the back side is covered with a sheet of dead white cardboard. The diameter of the rods is not varied.

Figure 4. The Howard (1919a) Version of the James (1908) Depth Perception Apparatus.

Prior to 1910 (and, unfortunately, still to this very day in much of the world literature) it was commonly believed that the smallest distance x= PT (threshold ASP) shown in Figure 3a that could be perceived corresponded to a projected distance on the retina, x_{retina}, equal to the average cone separation (Helmholtz, 1856, 1910). This incorrect belief was established by one researcher (Helmholtz) who determined his own binocular threshold to be $x_{retina} = 4.4$ μm, the size he assumed for the cones; this 4.4 μm retinal distance for a pupil-retinal separation of 15 mm corresponds to and ASP of 1 arcmin, which is the same as the Snellen standard for 20/20 lateral visual acuity. Other researchers overlooked the lack of scientific rigor employed by the well-respected Helmholtz (just one biased and apparently poor-sighted self-observer) and it became "mathematical theory" that cone pitch determined depth acuity and lateral acuity. Work published from 1910 through 1923 firmly established that the depth acuity was much smaller than the cone size of an individual (Schoute 1910; Blaauw 1917; Howard 1919a).

Blaauw (1917) summarizes work to that time and concludes that (a) a sharp distinction should be made between BSV (which provides different lines of sight fused in the brain depending on attention focus) and binocular vision using a stereoscope (which provides a fixed lines of sight fused in the optics and unchanged by mental refocus amongst elements in the field of view); (b) good lateral visual acuity does not mean also good appreciation of depth; (c) every thorough examination should include BSV; and (d) the ophthalmology section of the American Medical Association (AMA) should come to an understanding of the apparatus to be used. Blaauw and other ophthalmologists paid special attention to pilot selection in early 1917: the US had entered WW I and in April 1917 and learned that 90% of British loses the first year of the war were due to physical defects of pilots, not defective planes (8%) or Germans (2%). An independent UK air medical service, focused on care of the flyer, reduced pilot-caused loses to 20% in two years.

The US Army Air Service established a Medical Research Laboratory (MRL) on 19 Jan 1918 at Mineola Long Island NY to develop tests for selection, from amongst an oversupply of applicants, those having physically distinguishing abilities for success as combat pilots, to create the new position of flight surgeon and teach aviation-specific medicine, and to investigate field medical issues related to aircrew.[1] For some 18 months from Jan 1918 through Jun 1919 the brightest experts in various medical disciplines were commissioned and supported with extensive staffs for aviation medical research. One such person was Dr. Harvey J. Howard, an established excellent research ophthalmologist assigned to MRL and tasked with establishing if, or if not, a test for depth acuity should be used in pilot selection. Howard (1919a) used the James DPA and performed extensive experiments to establish depth acuity (BSV thresholds ascertained via the psychophysical method of forced choice) as an important objective test for pilot selection. Howard refers to the ASP in Figure 3a as the "Binocular Parallactic Angle (BPA)," and reports thresholds as low as 3.37 arcsec. After the WWI emergency ended on 11 Nov 1918, Howard and others at MRL published their results and returned to private practice by late 1919. A fewer number of civilian researchers were brought in, but teaching aviation medicine became the focus.

[1] The MRL has existed continuously since its establishment in 1918 and is now the USAF Air Force Material Command 711 Human Performance Wing (711 HPW) at WPAFB OH comprising the same research, teaching and extension mission in the form of its Airmen Systems Directorate (RH), School of Aerospace Medicine (USAFSAM), and Human Performance Integration Directorate (HP). The MRL library is part of USAFSAM library.

2.5 Howard Variation of the James Depth Perception Apparatus (DPA): The Howard DPA

The Howard DPA (see Figure 5) is variation of the James DPA that simplifies test administration and enables depth acuity determination via the psychophysical method of adjustment (by the subject) as well as forced choice. Howard (1919b) exhibited his "Six-Meter Stereoscope" on 17 Jun 1919 at the American Ophthalmological Society (AOS); a conference paper is published in the Nov 1919 Transactions of the AOS (TAOS) and a more detailed paper, in the Dec 1919 issue of the American Journal of Ophthalmology (AJO). Fig. 1 in Howard (1919b) and associated text describe the Howard DPA as a 240Wx200Hx600L mm six-sided box with two compartments. The back 200mm compartment contains electric lamps behind a milk glass partition. The front, 240Wx200Hx400L mm front compartment contained two 180mm long, 10mm diameter vertical rods separated by 60mm. The rods were painted a dead black and viewed at Reference Distance of 6000 mm through a 120Wx100H mm window (centered in the front wall) against the back wall; all interior walls and the front are painted a dead white. Covering the window from behind is a Graflex shutter for time exposures ranging from 1 to 1000 ms. For the method of adjustment a cord/pulley system on the top side enabled the subject to adjust the rods by a turning knob on the pulley wheel. One side was removable for adjustments by the test administrator.

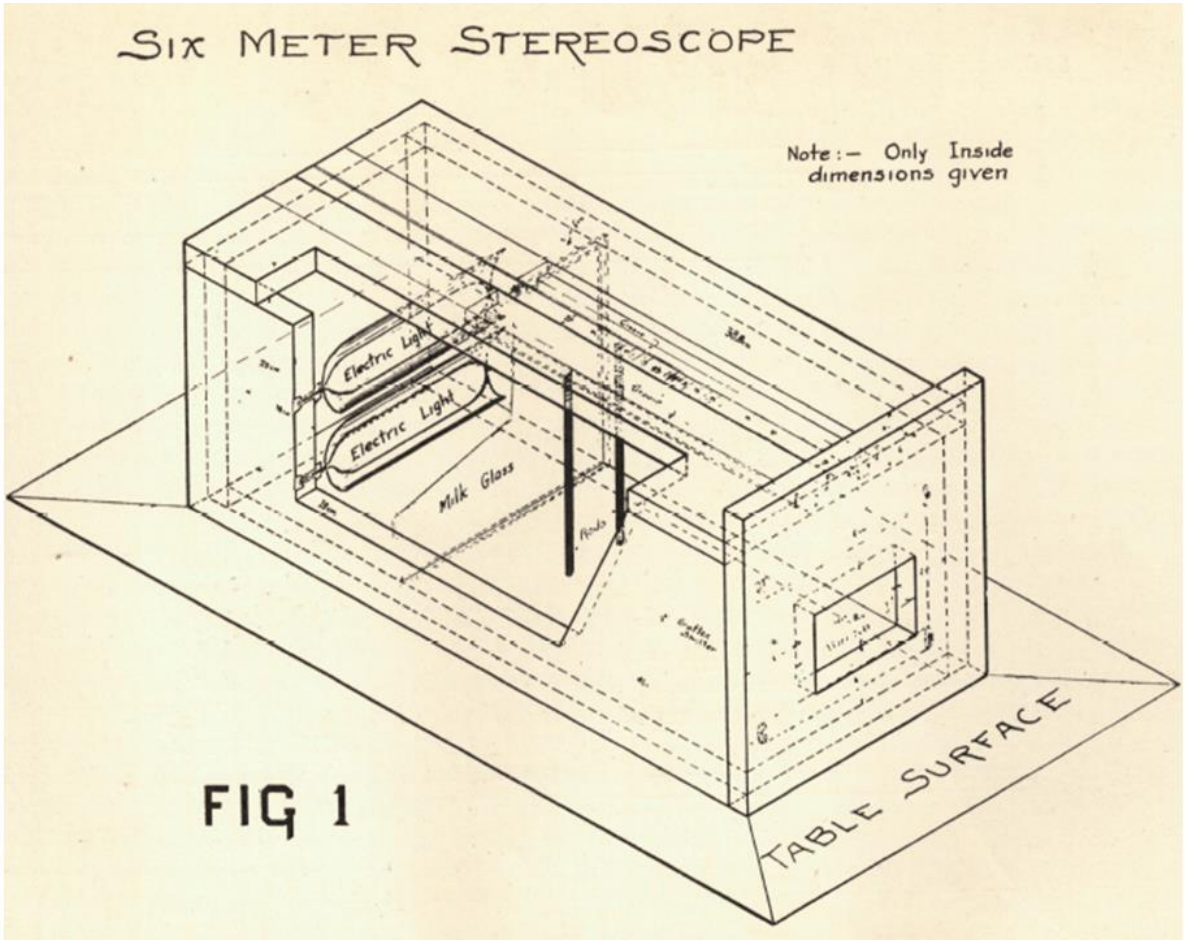

Figure 5. Howard DPA: Compact Version of James DPA Designed by Howard (1919b) for Depth Acuity Testing via Two Methods (Forced Choice, Subject Adjustment)

Modern versions of the Howard DPA shown in Figure 5 are still considered state-of-the-art for depth acuity measurement and are widely used. For example, a commercial automated depth perception apparatus is available $3,427.00 from the Lafayette Instrument Company in Lafayette IN. The Lafayette Depth Perception Apparatus, Model 14012A is a closed internally LED-illuminated box with dimensions 254Wx279Hx686L mm, rod motion accuracy 1mm, power 10A for 110/220 60Hz and an LCD and keypad control plus digital joystick for controlling displacement (www.lafayetteevaluation.com/printview.asp?id=2141, accessed 24 Jul 2016). Lafayette states that "The Depth Perception Apparatus represents the state-of-the-art in sensation and perception measurement technology" and is used to test depth perception acuity for pilots, crane operators, bus drivers, and athletes for use in the employment selection process. The DPA is also used in laboratory research and teaching demonstrations (Lafayette Instrument Co., 2016)

2.6 Deyo Modification of the Howard Six Meter Stereoscope: The Howard-Devo DPA

Deyo (1922) reports measurements she attributes to a Capt Bascom H. Palmer for 100 subjects using a DPA she describes as a 337Wx292Hx552L mm box with top and sides removed per James (1908) and a pulley system installed per Howard (1919b), but on the bottom side rather than the top side. Deyo states that the entire apparatus is painted a dull black and the anterior surface of the back covered with a square of dead white cardboard. Two 152mm long, 9.5mm diameter rods are viewed through a 197Wx89H mm window (centered in the front wall). Following James (1908), the Deyo DPA is placed directly before and beneath the Snellen charts with illumination provided for both by one daylight lamp. The Howard-Deyo DPA and experimental condition are illustrated in Figures 6a and 6b. An average depth acuity of more than z = 30mm (see Figure 3a) disqualifies the subject. Deyo (1922) reports threshold depth differences (z in Figure 3a) for 100 cases averaged $z_{threshold}$ = 18.65 mm (ASP = 6.7 arcsec) with both eyes vs. $z_{threshold}$ = 118 mm (ASP = 42 arcsec) for one eye.[2] The sighting eye is shown to be better than the other, and subjects with 20/15 to have a significantly smaller z (ASP = 4.8 arcsec) than subjects with 20/20. This Howard-Deyo DPA is still widely used.

Some confusion exists in the literature regarding the Howard-Deyo DPA due to a paper by Tefft and Stark (1922) and a textbook by Bauer (1926), who both inserted "Howard-Dolman" as an adjective for the 1922 Deyo-modification of the 1919 Howard DPA (Howard, 1919b). There is no evidence in the literature, none whatsoever, of any publication reporting work on any DPA apparatus or depth perception testing by anyone named Dolman. Details are provided below in the references for (Tefft and Stark, 1922) and (Bauer, 1926). All literature references to a so-called Howard-Dolman DPA should be understood to refer to the Howard Six Meter Stereoscope DPA (see Figure 5) modified as described in (Deyo, 1922). Furthermore, the photographs published as Figures 1 and 2 in Bauer (1926) pertain to the descriptions of the Howard-Deyo DPA and experimental test condition described textually in (Deyo, 1922). Deyo added no adjectives to the DPA that she described and references Howard (1919a) only. The names "Howard DPA" and/or "Howard-Deyo DPA" should replace the term "Howard-Dolman DPA" in all future literature. Furthermore, the term Howard-Dolman DPA has become, erroneously, synonymous with any of dozens of versions of the two bar test invented by James (1907, 1908); all literature references to this two bar test should be understood to refer to James (1907, 1908).

[2] ASP (z) in radians = arctan(LR/RT) - arctan(LR/RB) = (IPD/RT) * (z / (RT+ z)) for large RT.
ASP (z) in arcsec = 202265 * (IPD/RT) * (z / (RT+ z)) for large RT. See Figure 3 for terms.

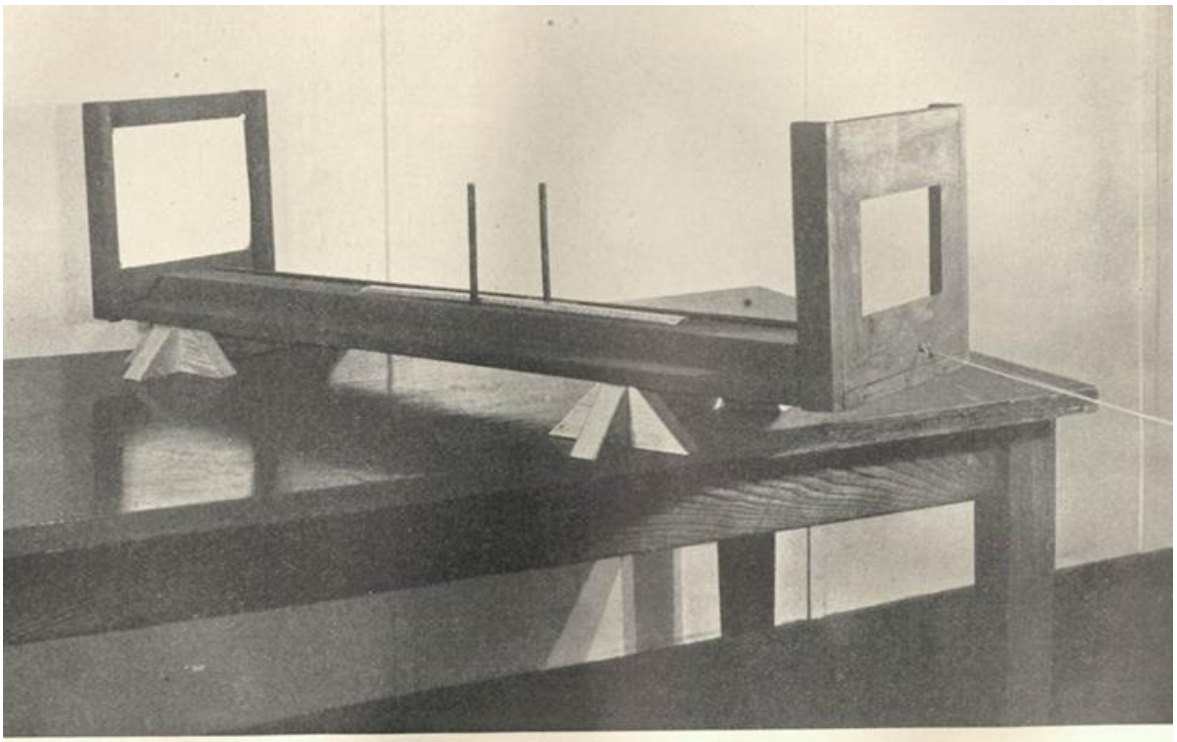

FIG. 1. THE HOWARD-DOLMAN DEPTH PERCEPTION APPARATUS

The above figure is a photographic plate inserted in Bauer (1926) of the Depth Perception Apparatus described by Deyo (1922). The List of Illustrations in the frontmatter of Bauer (1926) reads "Fig. 1. The Depth Perception Apparatus" and Bauer provides no reference to any paper by any person named Dolman. Bauer does reference Howard (1919a, 1919c, 1919d) and Deyo (1922).

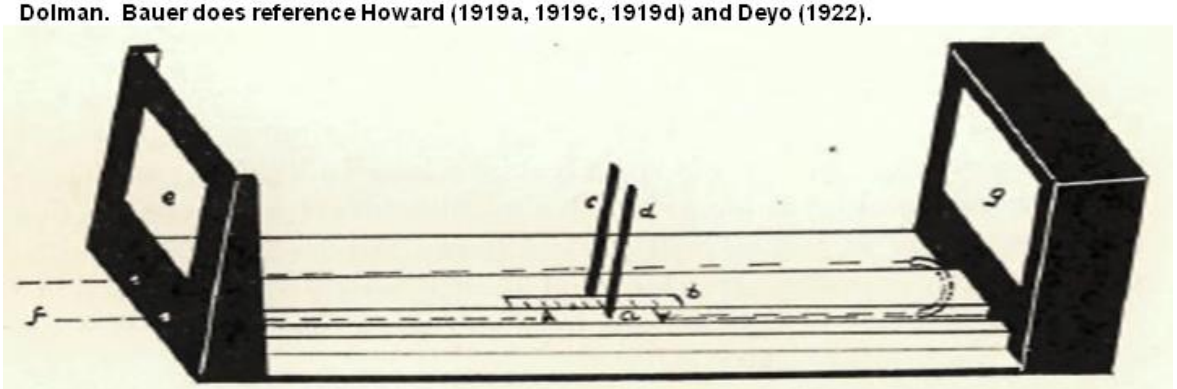

FIG. 6.

Howard-Dolman Depth Perception Apparatus. *a*, slide carrying adjustable rod; *b*, millimeter scale; *c*, stationary rod; *d*, adjustable rod; *e*, aperture through which rods are viewed; *f*, cords for adjusting rod; *g*, modified method of illumination consisting of cabinet faced with ground glass behind which is 50 watt bulb.

The above figure is a photographic schematic drawing inserted in Thorne (1928) of the Depth Perception Apparatus described by Howard (1919b) with the top and sides removed. Thorne references Howard (1919a) but provides no reference to any paper by any person named Dolman.

Figures 6a. Photo and Drawing of the Howard (1919b) Depth Perception Apparatus Modified as Described in Deyo (1922); "Howard-Dolman" Should Read "Howard-Deyo".

FIG. 2. TESTING DEPTH PERCEPTION
The subject is seated 20 feet distant from the rods

NOTE: The above figure is a photographic plate inserted in Bauer (1926) of the test condition and the Depth Perception Apparatus described in Deyo (1922)

Figure 6b. James (1908) Depth Test Condition as Implemented by Deyo (1922).

Thorne (1928) includes a schematic diagram (see Figure 6a, bottom) of the DPA described in Deyo (1922) and states that it is used as an aviation vision test by accepting applicants whose depth acuity ≡ threshold ASP = 9.119 arcsec or less, which for an average American IPD = 64 mm requires z = 25 mm or less.

2.7 Speed and Accuracy of the James Test

The James apparatus built in Mineola by Howard is described by visitors as having extreme precision, with a very slight variation of in the distance of between objects seen at a distance of 6m being *instantly* perceptible to the observer (Howard, 1919a, discussion following 14 Jun 1919 presentation by Howard at 55th Meeting of the American Ophthalmological Society; see Transactions of the American Ophthalmological Society (TAOS) 17, 755-757, Nov 1919).

Andersen and Weymouth (1923) propose a theory to account for the fineness of depth acuity based on a complex percept of position that they propose to call *retinal mean local sign (RMLS)* and state that factors contributing to RMLS include:

> "*1*, the mutual effect of adjacent retinal elements in either retina;
> *2*, the averaging of the successive stimulus patterns on each retinal mosaic caused by the constant slight eye-movements; and
> *3*, the combining of the two simultaneous stimulus patterns presented to the two eyes."
>
> "As a result of these three factors the mean local sign (in the present case of the images of the [two] threads) may be so accurate that a disparity between images of a fraction of a cone-diameter may be correctly perceived."

Empirical evidence has shown that "may be correctly perceived" should read "will be correctly perceived by a normal sighted person" (James 1908; Schuler 1910; Howard 1919a; Devo 1922).

Hirsch and Weymouth (1948a, 1948b) expanded on Andersen and Weymouth sought to combine certain aspects of physiology with the methods of psychophyics.

2.8 Limitations of the James Test for Understanding Image Perception on 3D Displays

Zalevski et al. (2007) summarize depth acuity (aka stereoacuity) research from 1900 through 2002 and note that the lowest, 2-6 arcsec, depth acuity reported for a stimulus comprising two parallel vertical lines horizontally displaced (i.e. the James test) deteriorates by factor of seven or more for a stimulus comprising a square (same two vertical lines, but with two horizontal lines connecting the tops and bottoms). Thus, the perceptual value of 3D displays is also a function of the image composition in practical applications. This issue should be examined in future work.

2.9 S3D Systems at AFRL

AFRL has multiple variants of the Stereo 3D Display (S3D) class of visualization system. However, most laboratory and operational visualization applications opt for 2.5D—3D models

interactively rendered on ever-higher resolution 2D displays—due to the multiple hardware and perceptual limitations of all S3D systems. Problems limiting wider adoption of the S3D class include the (a) objection of most users in most applications to the special eye-selection wear, (b) nausea after just a few minutes, and (c) failure to produce full parallax views with correct BSV for each viewer. All viewers of S3D see the same viewpoint and focus distance (for all pixels) regardless of their position or head orientation in the viewing zone. Donning, doffing, loosing, finding, and tolerating the special S3D glasses (e.g. to see other persons or 2D screens at full brightness results) has driven most usage to episodic scenarios (e.g. sessions of 10 min or less).

There are some important types within the S3D class that attempt to address the aforementioned objections: head-tracked (HTS3D), active-retarder head-tracked (ARHTS3D), stylus-controlled (SCS3D), and combined stylus controlled, active-retarder, head-tracked (STARTS3D). The HTS3D type adds head-tracking to S3D along with software and fast graphical processing to render and update the left/right views to those appropriate to the instantaneous eye positions. The ARHTS3D type integrates an active retarder into the HTS3D screen housing to enable the use of passive polarization glasses to retain the full native resolution of the display (active glasses typically reduce horizontal resolution seen by half). The STARTS3D type adds a separately tracked stylus to the ARHTS3D to achieve a notable trifecta: dynamic user-interaction with 3D data and models with head-motion parallax. The first member of the STARTS3D class is the zSpace Immersive Reality System (www.zSpace.com). AFRL has two zSpace displays.

The Auto-Stereoscopic 3D Display (AS3D) class of visualization system is not used in the present study but is mentioned for completeness. The AS3D class provides multiple horizontal viewing zones that can present adjacent perspectives of a 3D scene (data set, model); up to 200 zones have been demonstrated and up to 16 are offered as consumer products. The AS3D class do NOT require the special eyewear, but provide horizontal parallax only and have objectionable discontinuities between the viewing zones. A head-tracked type (HTAS3D) in which helmet position is tracked and the left/right views dynamically moved to keep the correct view on the correct eye as the viewer moves is available. The first electronic HTAS3D is the one developed by Dimension Technologies, Inc. (www.dti3D.com) under SBIR funding from AFRL in the early 1990s and has recently been awarded a Phase II contract by NASA to further mature their glasses-free cockpit 3D technology. Several modern versions of this 25-year old HDAS3D are available (see e.g. Surman et al. 2006).

2.10 Psychophysical Research on 3D Displays

Psychophysics quantitatively investigates the relationship between physical stimuli and the sensations and perceptions they effect. In this study it is posited that the defining characteristic of depth perception should be a key metric for the characterization and comparison of various classes and types of 3D display. The specific psychophysical measurement selected here is the James (1908) two vertical bar test. Lloyd (2012) applies this test to S3D display with graphically generated bars as the stimuli and reports that "disparity thresholds (5 to 10 arcsec) are obtainable on electronic [S3D] displays with pixel pitch [at the eye nodal point] as coarse as 2 arcmin, but only if sufficient antialiasing is applied." Thus, significant attention is required in the design and programming of the electronic versions of the graphical stimuli for the electronic James (eJ) test.

3.0 METHODS, ASSUMPTIONS AND PROCEDURES

3.1 Software Suite for Graphical Stimuli Emulating the James DPA Sticks

The eJames Software Suite (eJSS) developed for the present effort includes all the code required to produce a virtual model of a typical physical two-vertical-stick (two-bar) James test and the necessary interfaces to set-up and run automated evaluations as illustrated in Figure 1. In the present report the eJSS is applied to an AFRL-automated physical Howard DPA, and to three types of electronic 3D displays: stereo, volumetric, and integral-ray.

The software suite uses OpenSceneGraph, a high performance application programing interface (API), to generate 3D objects in OpenGL (a lower level API), resulting in the desired virtual model. The eJSS stimulus generation interface allows the researcher to adapt the model for a specific display and experimental design. A wide variety of design variables are supported including subject viewing distance, subject inter-pupillary distance, display type (stereoscopic or volumetric), physical display size/volume, stimulus lighting model, stimulus duration, number of trials, trial initiation cue, inter-trial rest period. Psychophysical methods supported include methods-of-adjustment (MoA), staircase, and constant-stimuli (MoCS), aka forced-choice.

The eJSS interface to the AFRL-automated physical Howard DPA uses the virtual model to generate a set of software commands that an Arduino microcontroller (www.arduino.cc, http://en.wikipedia.org/wiki/Arduino) translates into low level electric motor commands. These microcontroller commands configure the physical Howard DPA to match the virtual model.

The eJSS interface to the stereo display uses two virtual cameras to render the model into stereo bit maps appropriate for the targeted display and subject viewing geometries. Full screen antialiasing is supported by the use of NVidia Quadro video cards.

The eJSS also allows direct access to the model by display systems that ingest (handle) OpenGL data. Examples in the present work are the Actuality Integral Slice (AIS) circular rotating-screen Perspecta volumetric display and the Zebra Integral Ray (ZIR) hogel-based Zscape Motion Display (ZMD). Subjects perform the experimental task through a standard video game controller. At the end of each experimental trial the subject response is automatically exported to the data collection spread sheet.

The James test is described in the introduction (see Figure 3 and associated text). The Howard (1919b) variant of the original James Depth Perception Apparatus (DPA) enabled the psychophysical method of adjustment (MoA) in addition to the forced-choice method (MoCS). Both methods are automated by the eJSS. In addition, the software enables (a) scaling of the stimuli, (b) arbitrary variation of the position of both bars, (c) and choice of white bars on black background per James (1908) or black bars on white background per Howard (1919a, b, c, d). All data collected in this study uses the James choice of white bars against a black background for the electronic displays (see Figure 2A, 2B, 2C). The DPA used is difficult to photograph (see Figures 1, 2) with the electronic displays due to the all-white interior surfaces and length-of-box interior lamps used by USAFSAM (see Figure 7a) for its in-house variant of the Howard DPA.

3.2 Display Class & Type: Physical Apparatus & Two Vertical Sticks

The James (1907, 1908) depth test is maximally dependent on instantaneous binocular parallax. Monocular depth cues are reduced to the greatest extent possible. Two vertically oriented sticks (aka strings, rods, dowels, bars) are viewed through a window to hide their ends to eliminate the perspective) cue. The sticks are presented in maximum contrast to the background to reduce lighting variations. A 6m viewing distance of narrow 10mm (or less) diameter sticks is common to limit accommodation and vergence cues. The observer is advised to keep their head steady (no large head motions during testing) to eliminate motion parallax as a significant cue. The observer is not shown the sticks during the time they are being moved to their initial position for an experimental trial to enable stationary stimulus presentation. Observers typically perceive depth differences rapidly before accommodation can occur.

3.2.1 Device Under Test: AFRL Computer-Automated Howard DPA

A DPA based on the design published by Howard (1919b) was built by personnel at the USAF AFMC 711 HPW United States School of Aerospace Medicine (USAFSAM). The USAFSAM physical apparatus is a six-sided 260x260x800mm (inside) wooden box painted white inside and black outside, with interior illumination provided by two fluorescent bulbs that run along the top of the 800mm inside walls (see Figure 7a). Two 500mm rails, parallel with a 50mm center-to-center spacing, straddle the centerline of the floor. On top of each rail sits a 10mm diameter vertical black rod. The left rod, as seen from the viewing window, is fixed in position half-way down its rail; the apparatus is typically placed such that the fixed rod is 6m from the eye nodal points of the subject. The right, travelling rod is adjusted by a loop of cable running from the observer through holes in the front of the box, through the base of the right rod, and around a pulley at the back of the box. A bent wire attached to the base of the movable rod passes through a horizontal slot in the right side to indicate position on a scale mounted on the outside. A 160x80 mm viewing window centered in the front end limits the view of the observer to just the middle of the two rods (see Figure 7b). An experiment requires the test administrator to cover the window, move the right rod, and remove the cover; the observer then declares which is closer (method of forced choice using constant stimuli) or uses the cable to adjust the right rod until the depths are perceived to match (method of adjustment).

The 711 HPW/USAFSAM Howard DPA was manually operated, which slowed clinical use and severely limited the potential for use in human perception research. The AFRL Battlespace Visualization Branch (711HPW/RHCV) agreed to automate this device in exchange for its use in electronic 3D display research.

Key automation features installed by AFRL 711 HPW/RHCV in the physical apparatus include: (a) rotary solenoid actuated shutters to occlude the window under computer control; (b) a photoelectric switch for use in system calibration; and (c) an Arduino microcontroller to translate directions from the eJ software into executable commands for the electric motors. The microcontroller also enabled automated data collection by reporting the position of the movable rod back to the eJ software. The addition of a solenoid and microcontroller necessitated supporting infrastructure improvements including shielding/grounding of power circuits and the installation of a cooling fan. A report on the AFRL-Howard DPA is planned (see Meyer et al.).

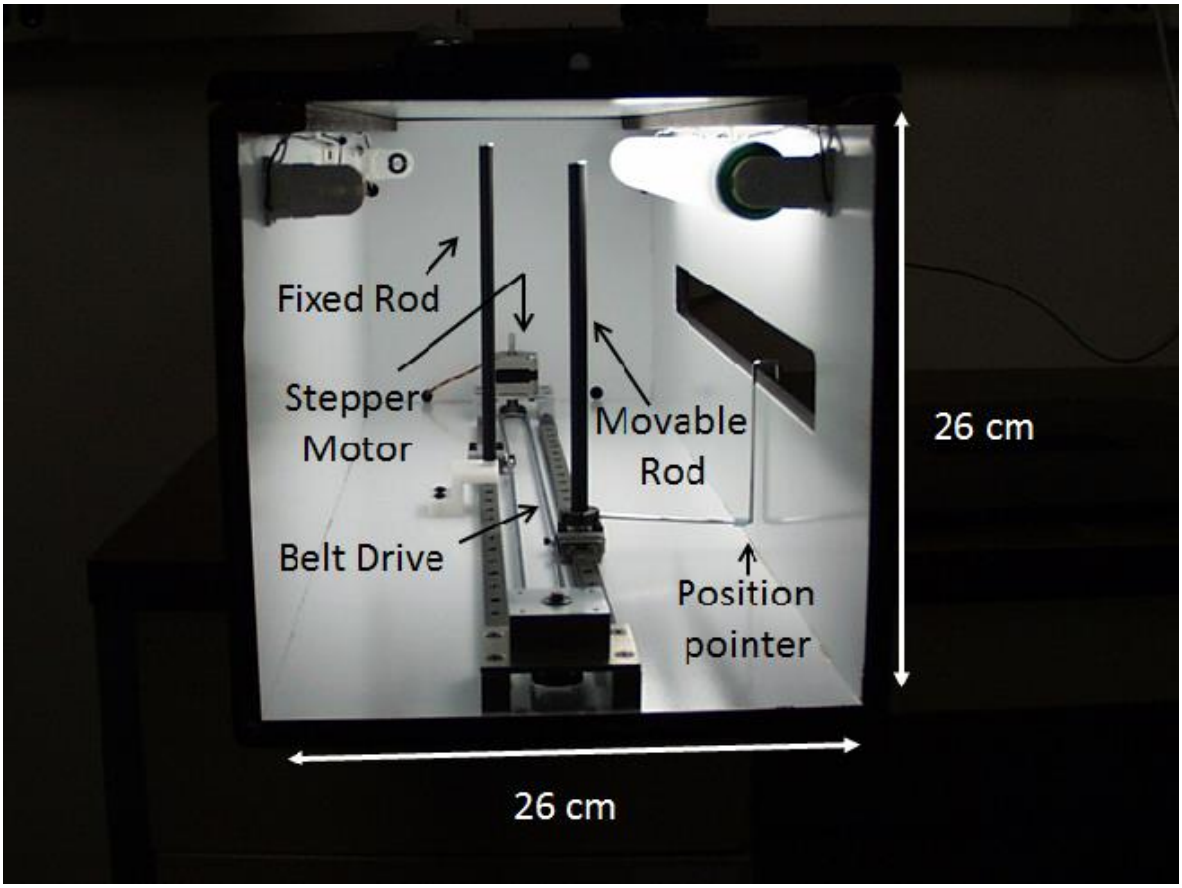

Figure 7a. Inside View of AFRL-automated USAFSAM Howard DPA

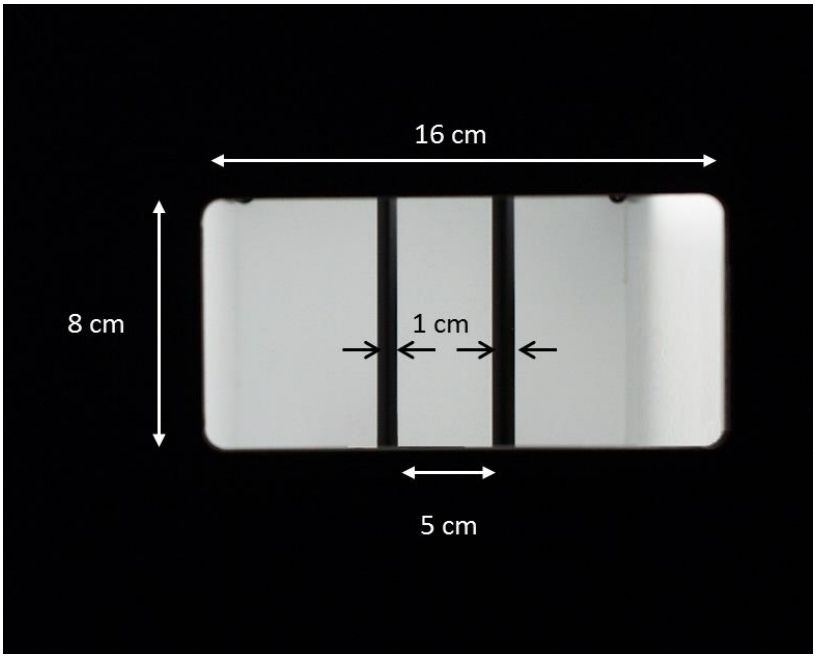

Figure 7b. Subject View of Rods in AFRL-automated Howard DPA

The interior view in Figure 7a shows the belt drive and stepper motor that are now in the device (replacing the cable and pulley). Electronically controlled doors occlude the subject view while computer random number generator commands and moves the right rod to its next position. For testing using the method of adjustment, the doors fly open under computer control and the subject adjusts the position of the right rod using a computer game controller whose inputs are processed by the eJSS and sent via the Arduino microcontroller to the stepper motor. For testing using the method of constant stimuli (forced choice), the subject simply presses a left or right button on the hand-controller to indicate which rod is perceived to be closer. Both methods can be used to determine the just noticeable difference (JND) depth, or threshold depth acuity, of the subject.

3.2.2 Calibration of the AFRL-Automated Howard DPA

The motor step size is calculated by moving the rod a measured distance and dividing by the number of steps incurred. An infrared LED and photo-electric switch is installed on opposite sides of the right rail, at the limit of the forward most rod position. Each time the system goes through the power-up sequence the stepper motor automatically moves the rod forward until it activates the photo-electric infrared LED, thereby defining the reference position (i.e. the forward-most position) for the right rod. Once is reference position is defined the microcontroller keeps a running count of the number of motor steps between the reference position and current location. The current rod location could then be calculated by multiplying the number of steps by the step size in mm. Confirmation of system calibration is accomplished by using the stimulus generation interface of the eJSS to generate a series of experimental trials. When the trials are run the starting location of the virtual model is compared to the starting location of the rod in the physical Howard DPA. Trials terminate with the rod in a variety of locations distributed throughout the length of the right rail. Final right rod locations are compared to the recorded position in the automated data collection spread sheet and a lookup table is generated. Positioning accuracy of <1mm is confirmed for the AFRL-Automated Howard DPA.

3.3 Display Class & Type: S3D & Eye Selection Glasses (ESG)

Stereo 3D displays (S3D) attempt to add image disparity to monocular cues. The appeal of stereo is often described as "intuitive," but it has long been known that S3D is NOT a sufficient approximation of real world 3D vision (Blaauw, 1917). The subtle differences between left/right images captured by cameras or generated by computers (full images at a fixed focal distance and view-direction) are inadequate to fully generate the perception of depth (binocular stereopsis). In practice, the perception created by S3D is dramatic but unpredictable from person to person and from scene to scene. And for over 100 years there is a widely reported frequent discomfort associated with stereo viewing. Stereo cues provide neither shape constancy nor a quantitative depth perception metric (Westheimer, 2011; Johnston, 1991; Scarfe and Hibbard, 2008). These failures are caused the inability of S3D to represent a consistent and complete set of depth cues. At least part of the discomfort reported is due to conflicting sensory cues for accommodation and vergence (Blaaw, 1917; Hoffman et al., 2008). Other sensory conflicts may also be important including binocular parallax-motion, blur-disparity, binocular optical asymmetries, or higher-level cognitive conflicts (Patterson, 2009).

3.3.1 Rendering for Temporally Multiplexed Left/Right Eye S3D Perspective Views

Stereo rendering is based on a pair of virtual cameras. The virtual camera used in graphic rendering is analogous to a photographic camera capturing a real scene. In both types of cameras, the camera position defines how the monocular 3D perspective cues will be rendered. The magnification or zoom setting determines the field of view and focus distance. The spatial relationship between the virtual camera and the lighting model creates shadows and highlights. Since a virtual camera is not burdened by optical limitations, depth of field is not a basic attribute of virtual cameras. However, a depth of field function can be incorporated into the rendering algorithm if desired. When directly viewing an object, motion parallax is derived from the object location and the observer location. Moving the camera captures motion parallax cues, however, in graphics the monocular depth cues are all determined by the virtual camera settings and its position in the model space. Furthermore, the camera-captured cues are independent of the variable positioning of the observer relative to the display. It is possible to align the virtual cameras and eye positions by (a) fixing the observer or (b) monitoring their movement and updating the rendering viewpoint accordingly. Rendering by virtual camera produces a 2D bitmap comprising a set of digitally encoded intensity values across an array of locations. There are significant analogies between stereo rendering and stereo photography: the boundaries of good stereo practice are still defined by the limits of the human visual system. Stereo rendering increases the graphics processing over that required for 2D to a relatively small extent. Real time stereo rendering at high definition spatial, temporal, and color resolutions is not a challenge for current computer technology.

3.3.2 Display Under Test: Dell M6700 S3D System with Liquid Crystal Glasses

From 2012 to 2013 Dell produced a professional class S3D notebook computer system based on a high end M6700 laptop that integrated a 17.3-in. 120 Hz UltraSharp™ active matrix liquid crystal display (AMLCD), an NVidia 3D Vision Pro S3D kit, and a 4 GB NVidia Quadro K4000M discrete graphics card. The native resolution of the AMLCD panel was 1920 (horizontal) x 1080 (vertical) with a screen size of 381 mm (horizontal) x 215 mm (vertical). The

system requires the wearing of electro-optical liquid-crystal active shutter glasses that rapidly oscillated between transparency and opacity in synchrony with the display oscillation between imagery for each eye (at 60 Hz per eye).

3.3.3 Calibration of S3D Display

The stimulus generation software interface was used to create a model of the physical DPA rods for stereo rendering. A viewing geometry for the stereo virtual cameras was defined and expected left/right eye image seperations were calculated for a series of rod positions using well-established retinal disparity equations. A general discussion of these equations can be found in publications by Cormack and Fox (1985, 1986), wherein the term "half image" is used for the left- and right-eye images which were both were printed on the same page (in different colors) for their work. The half image separations were then divided by pixel pitch to calculate the expected pixel shifts for the stereo images pairs. The predicted shifts were compared to measured shifts from the displayed stereo image pairs. To measure the shifts, high resolution digital photographs of the rod images superimposed with a millimeter rule were taken and visually analyzed as pictured in Figure 8. In the measurement trials, the left and right rods were stepped through the series of depth locations in unison in order to verify uniformity of display depth response for both rods. Anti-aliasisng was deactivated during these measurements to improve the readability of the photographs, as a result display response in pixel shift was a step function. Assessment of pixel shift was accomplished by counting the number of pixels between the edge of the rod image for the stereo pairs. Since the step from one pixel shift increment to the next did not occur simultanously for both the right and left rod edges, both sides of the rod had to be measured. The period between the first edge shift and the second edge shift was considered a half pixel shift. The measured pixel shift as a function of the modeled viewing distance is graphed in Figure 9. These measured pixel shifts were converted to depths using the retinal disparity equations. The modelled rod depth is plotted against the displayed rod depth in Figure 10; a slope of 1.02 is computed by regression analysis with a 95% confidence interval of 1.00 to 1.04 and R-Squared of 0.99.

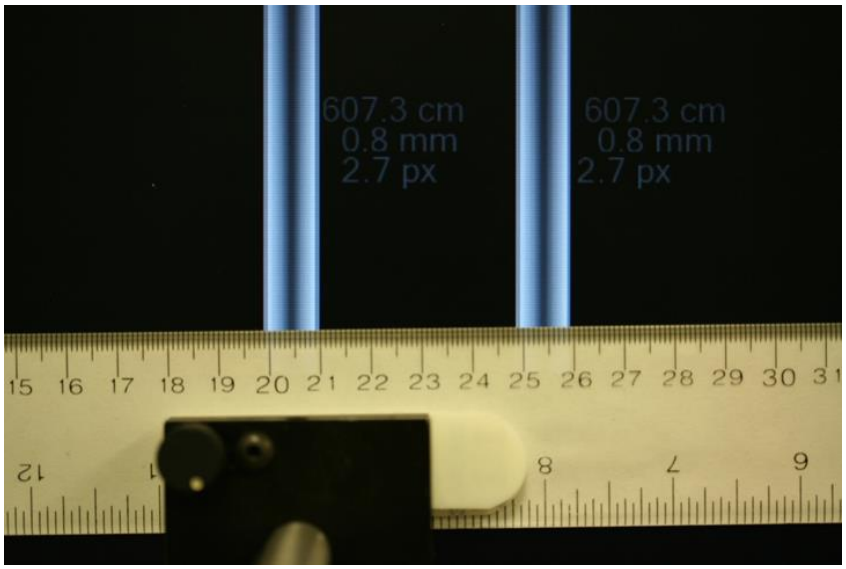

Figure 8. Photo of Superimposed Stereo Pairs Used to Assess Pixel Disparity

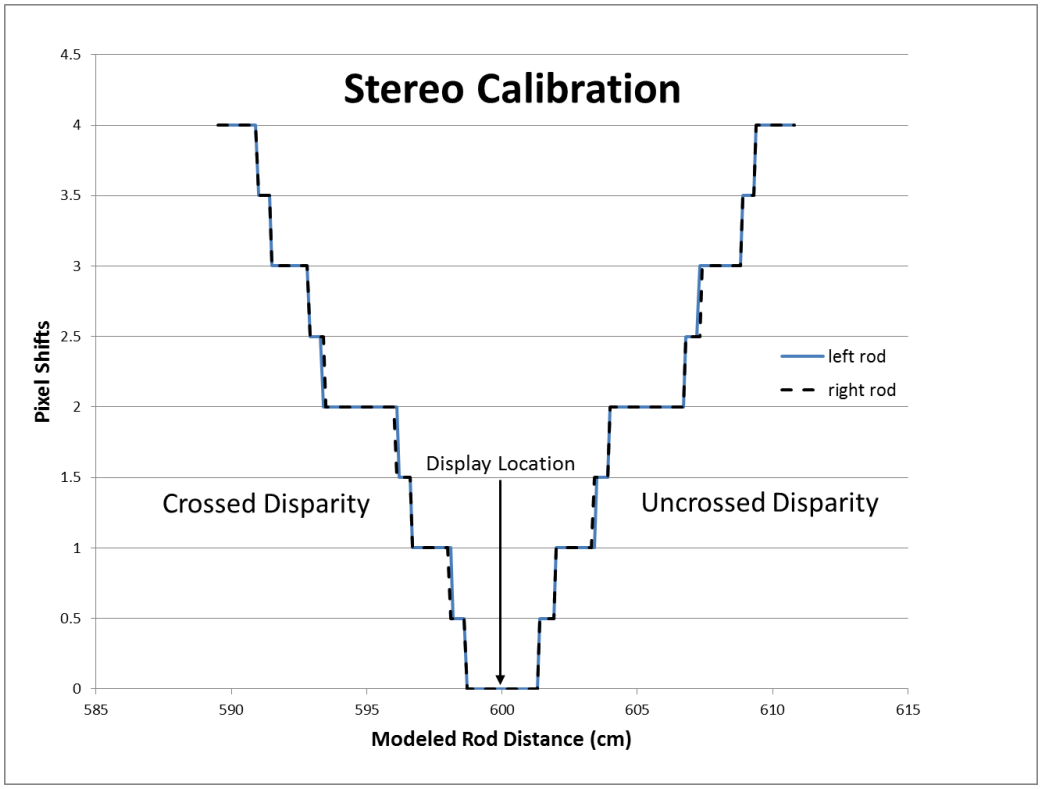

Figure 9. Measured Pixel Shifts for Modeled Rod Distances

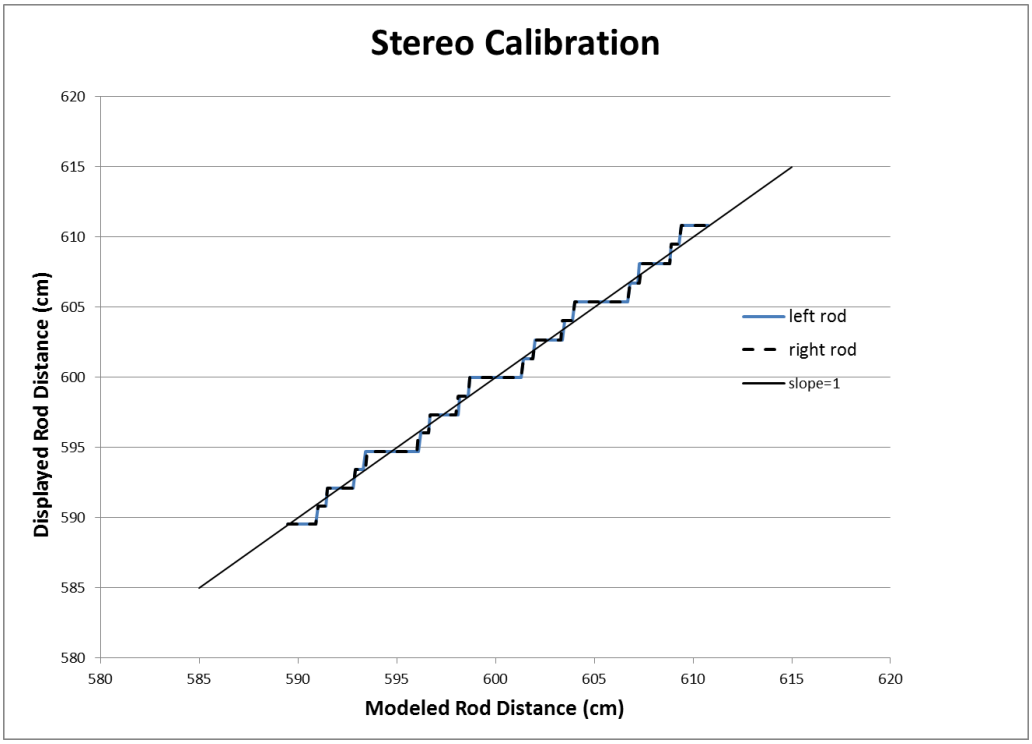

Figure 10. Virtual Model Rod Distance Plotted Against Stereo Displayed Distance

3.4 Display Class & Type: FoLD & Temporally Scanned Volume (TSV)

A temporally scanned volume (TSV) display produces a full-parallax image within a defined 3D space that is viewable with the unaided eye. The display volume is divided into addressable volume elements (voxels). Ideally, each voxel emits light into all directions (4π sr) representative of the corresponding element of a translucent 3D model. The TSV type belongs to the FoLD class of 3D displays.

Volumetric systems have been built in a variety of design approaches based on then-available materials and components including: (a) emissive voxel elements, such as moving light emitting diode arrays (see e.g. Ito et al., 2007); (b) multiplexed 2D images, such as the LIS Depth Cube z1024 and x1403a comprising a sequentially projected stack of some 20 parallel liquid crystal diffusing planes (Osmanis, 2016, www.lightspace3D.com); (c) direct write green laser beam modulated as scanned from above (or below) onto a spinning helical screen (Psaltis, 1992, 1994, 1996); (d) direct freeform volumetric line writing by scanning the intersection point of two infrared lasers in a two-photon up-conversion medium (Downing et al., 1996); and (e) projection of 2D slices of a 3D model onto a transflective moving screen, as in the AIS Perspecta (Donelan, 2010). In reality, each voxel is blocked in some directions by mechanical structure design features of each of these TSV-type display systems.

All TSV-type 3D display systems involve presentation of a complete 3D frame of the voxel array over time and rely on slow retinal chemistry to achieve the human perception of a complete image. This temporal characteristic is familiar from scanned 2D display types, including the cathode ray tube (CRT). All volumetric systems have temporal and spatial visual artifacts due to the limitations of the component devices available when they were designed: graphic and logic processors, optics, light emitting and modulating devices, signal compression and interconnections, and mechanical movement. For example, both the LIS Depth Cube and AIS Perspecta leverage, but are performance-limited by, the 2D display DLP kits released by TI to third-party developers; the 2D DLP image resolution is far too low to support high definition volumetric display systems.

Some specific challenges for the AIS Perspecta swept-volume approach include: (a) large screen acceleration forces; (b) synchronization; (c) dead zone at the screen spin axis; (d) inability to generate opaque surfaces (Brundell et al. 1993); and (e) ambient light reflections from the white screen (contrast reduction) and from the two clear concentric domes over the spinning screen (safety feature). However, for some datasets, translucency is a desirable feature and in some applications the room lights can be sufficiently dimmed to avoid ambient light reflections. The imaging quality available on the AIS Perspecta is illustrated in Figure 11.

3.4.1 Rendering for Rotating Screen TSV

3D models may be approximated as a series of planes sampled in either a Cartesian or spherical coordinate (e.g. parallel planes along the z-axis going away from viewer, or intersecting planes along the φ-axis spinning about the vertical y-axis). Each sample plane, or slice, of the dynamic 3D model comprises a set of voxels that can then be rendered as a bitmap for projection at the

appropriate moment in time. The number of bitmaps can reach into the hundreds creating a significant computational burden that must all be accomplished within 33 ms for a system frame rate of 30 Hz. The 3D-viewpoint is selected by self-motion of the viewer with respect to the display. Thus, this approach is not dependent on a single-viewpoint virtual camera capturing a view from within the model (virtual) space.

3.4.2 Display Under Evaluation: Actuality Integral Slice (AIS) Perspecta

The AIS Perspecta was a low volume commercial display that was produced roughly between 2002 and 2007 (Donelan, 2010). The display evaluated in this study was purchased by AFRL to support 3D research in 2005Q1. The AIS Perspecta has a two-sided screen that has equal front surface diffuse reflection and back-surface diffuse transmission characteristics. The screen rotates on a vertical spin axis at 900 rpm to producing a 30 Hz volumetric frame rate. Some 198 planar slices of the model, evenly spaced from 0-360º in spin-angle φ, are projected at 768x768 pixel resolution onto the screen from a Texas Instruments 1024x768 pixel Digital Light Projection (DLP) engine during each revolution. The image processing and projection rate required is 2970 slices/s = 1.75 Gpx/s = 42 Gb/s. The diffusely reflecting characteristic of the screen, and the specular reflections from the two concentric protective spheres surrounding the spinning screen, make the AIS Perspecta vulnerable to significant image degradation due to reflections of ambient illumination.

3.4.3 Calibration of the AIS Perspecta

A low power, red laser was fixed perpendicular, on a sliding optical mount, to a scaled optical rail as pictured in Figure 12. Distances, parallel to the optical rail, could be measured inside the display volume by simple geometric relationships. First the laser was positioned on the rail so that the laser intersected the point of origin for the distance to be measured in the display. The starting position for the laser on the rail was recorded and then the laser was positioned so that it intersected the point of termination for the distance to be measured. Again, the position of the laser on the optical rail was recorded. Since the opposite sides of a parallelogram are equal, the distance between the starting and ending position of the laser on the optical rail is equal to the distance between the points of origin and termination in the display feature (rod in this case). For example, the width of a rod could be measured by sliding the laser along the scale until it is pointing at the right edge of the rod, then the laser is moved along the scale until it is pointing at the left edge of the rod. The rod width is then equal to the difference between the laser locations. for the right and left alignments. The AIS Pespecta was commanded to produce the white James rods at a variety of locations in the volume addressed by the display. Measurements of the rods were taken from the viewing direction of the observer to insure that the rods were the correct size and separation. Then the laser and rail was rotated 90º around the display center. Multiple measurements were taken with rods at different depth locations to confirm that stimulus location commands resulted in the expected stimulus movements.

Figure 11. Aircraft Model Displayed in 2D on Flat Panel (left) vs. in 3D on AIS Perspecta (right)

Figure 12. Remote Measurement of Rod Images on AIS Perspecta Using Orthogonal Laser Translation

3.5 Display Class & Type: FoLD & Spatially Integrated Ray (SIR)

An ideal electronically-generated 3D display would produce an image that is equivalent to real objects viewed in the real world. The concept of lightfield has been used to design capture techniques to image real world scenes in x-y-z space (e.g. scien.stanford.edu, accessed 24 Jul 2016). Traditional 2D cameras capture an image x-y focused at a single depth z. A 2D image may be approximated as a discrete array of rays originating at a set of *adjacent* solid angle samples (i,j), i=1-N_x, j=1-N_y. Similarly, 3D image may be approximated as a discrete set of rays originating at a set of *adjacent* solid volume elements (i,j,k), i=1-N_x, j=1-N_y k=1-N_k.

Display systems of the FoLD class, SIR type are designed invert the lightfield capture process. The design objective is to generate an approximation of the lightfield that a 3D model would generate if it were a real object imaged with a lightfield camera in x-y-z space. Common approaches generate perspective views comprising **h x v** *aperiodic* sets of spatial rays (aka pencil beams). The spatial rays comprising a view originate at *non-adjacent* view pixels within an extremely large **N x M** pixel array grouped into **n x m** subarrays, where **h = N/n** and **v = M/m**. Each **n x m** pixel subarray together with its associated microoptic element forms the physical realization of a 3D model facet projector (aka hogel) schematically illustrated in Figure 13.[3] Each hogel directs **n' x m'** rays of light, where **n' ≤ n** and **m'≤ n**, into **n' x m'** angular directions **($\theta_{n'}$, $\varphi_{m'}$)**; each ray represents how one 3D model point would appear in each angular direction.

The pupil (of an eye or camera) located a particular position in the design viewing zone, **(Θ, Φ, d^{min}, d^{max})**, captures about **h x v** *irregularly* spaced rays originating from *non-adjacent* pixels, with typically just zero, one, or two rays from each hogel. The pupil of the other eye, located at an average human population interpupillary distance of 65 mm away, captures a different set of **h x v** *irregularly* spaced rays from a different hogel set that generate the image viewable from that pupil position. The perceived image detail at each pupil perspective location is approximately **h x v**. All rays are simultaneously present whether a person has positioned their head (or a camera aperture) there or not. Thus, the correct 3D perspective view is presented to either eye of one or more persons naturally as they move their heads throughout the field-of-display. Challenges include: computation of pixel drive signals from the 3D model; construction of large array of 2D pixels by tiling microdisplays; fabrication of high quality miniature projection optic elements and accurate registration over the pixel plane, total space-weight-power, and acceptable image update rate, control interface, form factor and noise profile.

Ideally, a SIR display would have an imperceptibly small hogel pitch, with each one producing a sufficient number of beams to fill the display volume at an average angular pitch less than that subtended by the average pupil size at the maximum design viewing distance. Practically, each hogel can only produce a limited number of beams and some viewing positions (solid angle direction and distances) may fall into the space between two rays and no light from any hogel enters the eye for that model point. These hogel drop-outs in the projected field of light rays

[3] The term holographic element (hogel) has been used for some 20 years (Benton and Bove, 2008). The word holographic would be apt provided the size of the extremely large pixel array **N x M** were to be on the order of 1 Tpx with ~5 nm pixel pitch with ~1μm nanooptic element pitch, and provided a future generation supercomputer is capable of rendering model points into hogels at 60Hz. Current systems underperform by a factor of ~10^{10}.

vary with changes in the viewing position (head motion) or the 3D model (dynamic update), thus creating discontinuities that degrade the perceived display quality. Light-field discontinuities are mitigated by the inability to completely collimate the beams.

Practically, a perfectly collimated rays are not possible and a tolerance for optical errors and diffusion are required as part of the design SIR display design. The degree of beam collimation is determined by many factors including pixel size, lens focal distance, and pixel-optics alignment. All light beams have some divergence and a non-uniform beam profile. Divergence may cause a particular direction to receive a mixture of energy from two adjacent beams resulting in an intermediate perception so that beam divergence serves as an interpolation function, smoothing out the discontinuity between the designed ideal ray directions. While the smoothing associated with beam divergence may be a benefit it comes at a cost: ray crosstalk that may be perceived, for example, as non-uniform coloration and reduced contrast.

Example FoLD SIR System: The ZIR 9-Tile ZMD has a large 23040 x 18,432 (424,673,280 px) pixel array comprising 100 x 100 px subarrays, within which the center 76 x 76 px patch generate 5776 rays representing a single model point as viewable from 5,776 directions as illustrated in Figure 13. The total number of addressable pixels (= rays generated) is 245 Mpx

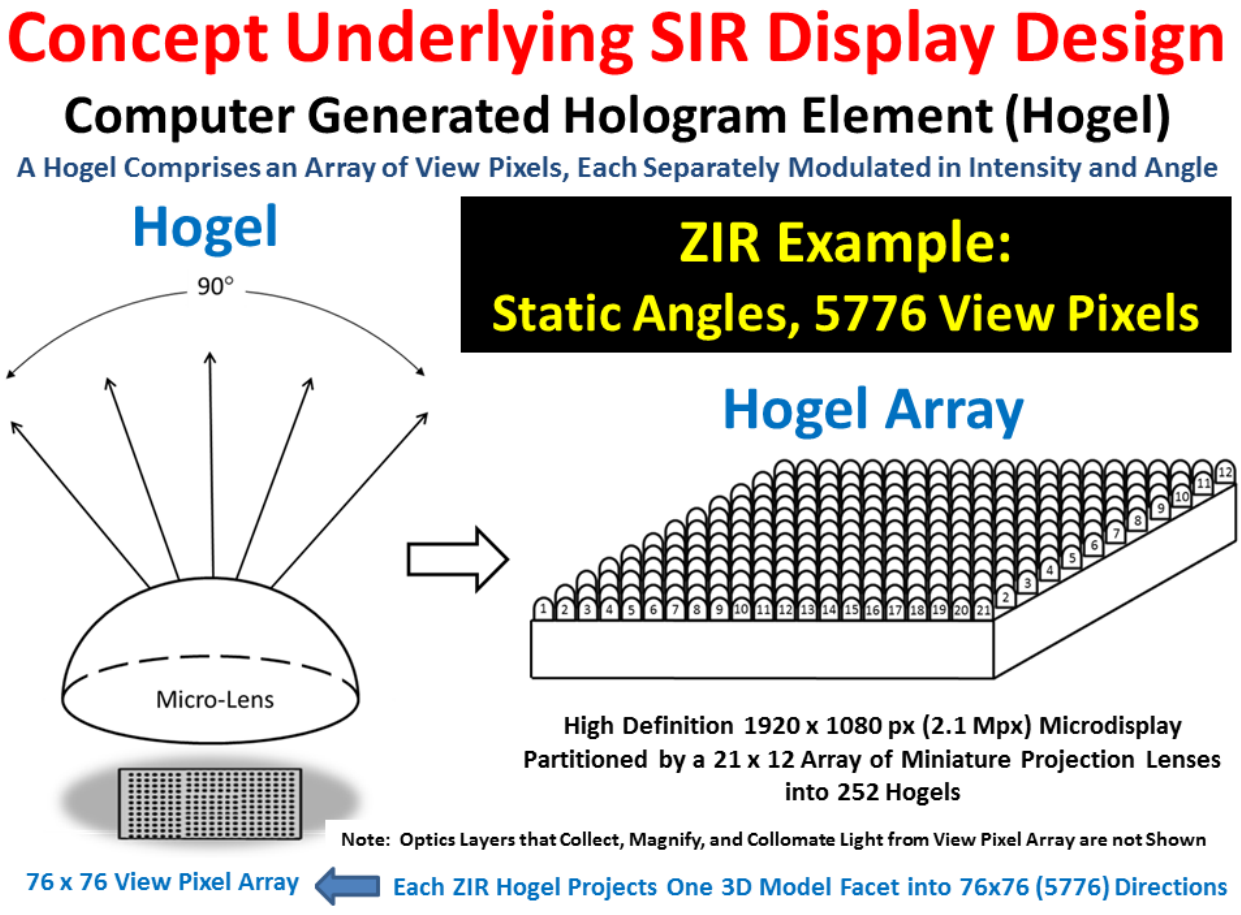

Figure 13. Schematic of a Hogel within a Spatially Integrated Ray (SIR) Display

(230.4x184.32x0.76x0.76 px). The ZMD processing system must compute, from a 3D model, the correct values with which to address each of 245 Mpx to produce 245 Mrays projected into the viewing zone. Each ~5mm pupil (human eye or camera) located within the design viewing zone (90 x 90º pyramidal field and 0.5-1 m distance from the pixel plane) collects a maximum of 230 x 184 (42,320) *irregularly* spaced rays. This image resolution which equates to a so-called equivalent 2D display resolution that is less than the early qVGA (320x240 pixel) digital video display standard. However, this 230 x 184 perceived image resolution is projected in full parallax simultaneously across the 90 x 90º pyramidal field-of-view at a frame rate of 1-10 Hz. The ZIR 9-Tile ZMD system includes a processing system comprising 27 circa 2008 networked, custom-packaged workstations (CPU, GPU, FPGA, HD) drawing 1 KW. The workstations receive are controlled by a client PC running the 3D model and a custom SIR operating system called Argon that Zebra Imaging Inc. developed for its ZMD system (Klug et al, 2013).

Photographs of ray bundles (lightfield approximations) generated from a 3D model and rendered into (a) a monochrome photopolymer hologram (1 mm hogel pitch, 512 x 512 rays/hogel) and (b) the ZIR 9-Tile ZMD SIR system (1.64 hogel pitch, 76 x 76 rays/hogel) are shown from the same perspective for comparison in Figure 14. The lower quality of the image from the electronic pixelated ZIR system relative to the hologram is obvious. The effective hogel pitch and non-uniformity are much less in the hologram than the ZIR. Light from an object not only has a direction and intensity but it also forms of a wavefront. It is the curvature of the wavefront (from the hologram) that determines the optical distance to the origin of the beam. A beam with a uniform wavefront can be well-focused by the eye according to its point spread function (PSF). Therefore, for a perfectly collimated display and a well-focused eye, the size of the PSF relative to the hogel pitch determines whether the image is perceived as smooth and continuous or as a discrete collection of spots. Taking the limitations of hogel optics into consideration, an imperfect light ray field is, in fact, produced comprising a mixture of wavefront directions/curvatures and corresponding optical distances. Consequently, the viewer may not focus the light optimally, resulting perception of a blurred image. Defocus is a well-known method of low pass filtering of coarsely sampled images and may benefit SIR displays like ZIR.

3.5.1 Rendering for a SIR Display

One logical approach to rendering a 3D model is to create a virtual camera for at the center of each hogel with a virtual pixel corresponding to each beam direction. This approach creates a virtual miniature camera array that parallels the physical hogel miniature projector array and is analogous to the relationship between integral cameras and integral projection. However, the hogel miniature virtual cameras do not have the same constraints as integral cameras. For example, an integral camera can only record the reflections in focus off of physical surfaces in front of the apertures and a set focus distance. In contrast, virtual cameras can select any surface to record, first, last or any surface in-between. Therefore the 3D model being rendered can be in front, behind or straddle the virtual camera array. Integral cameras record the reflection off the first surface regardless of distance; virtual camera views can be truncated at any distance and angle. This truncation of the viewing cone results in a frustum-shaped FoV. If the camera view is truncated both in front of and behind the camera array, the camera FoV can be described as having a double frustum shape. The computational demands for lightfield rendering are huge. Rendering rates sufficient for interaction and smooth motion video are difficult to achieve.

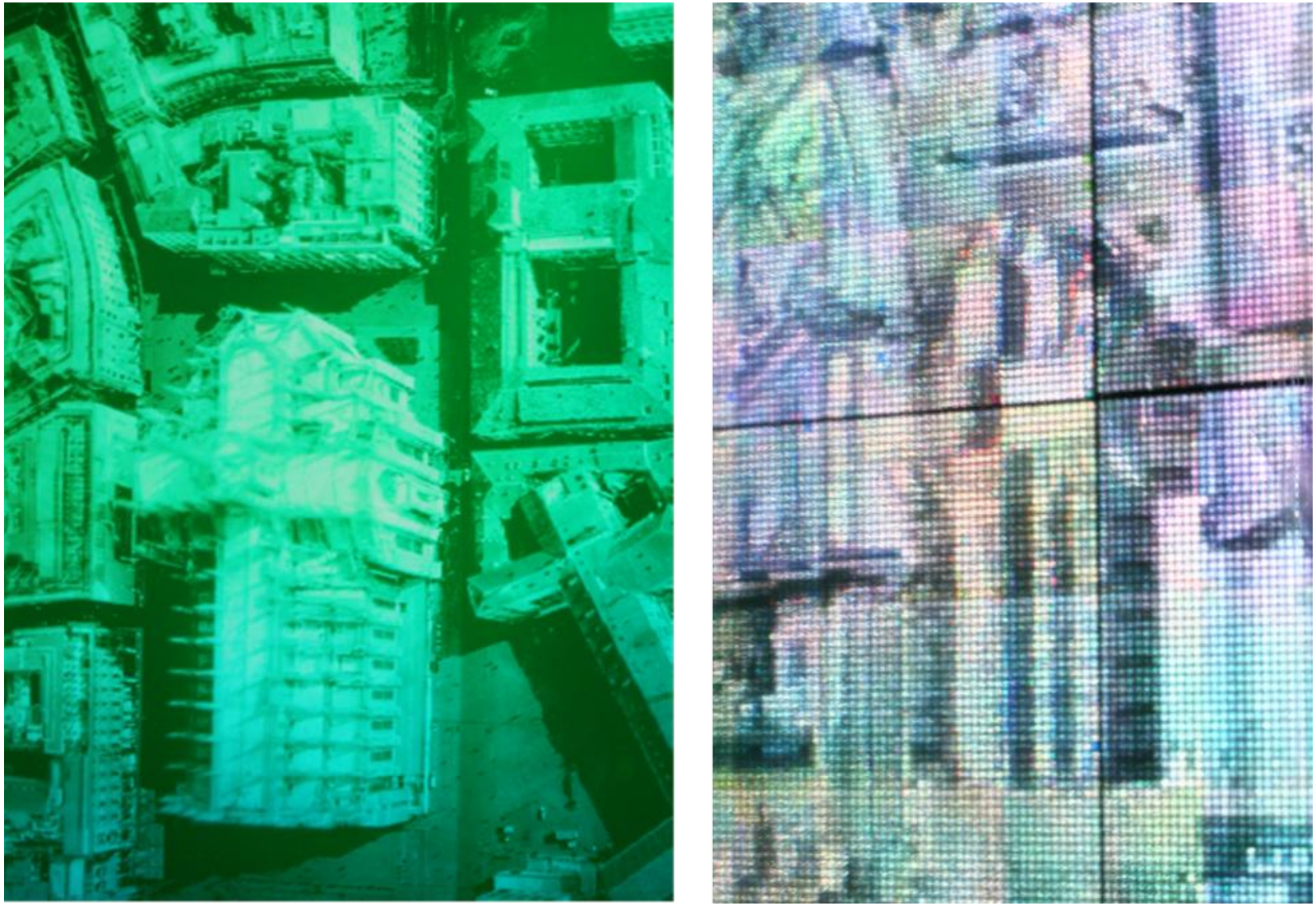

Figure 14. Photographs of Lightfields Produced from a 3D Model Written into a Hologram (left) and ZIR 9-Tile ZMD (right)

3.5.2 Device Under Test: Zebra Integral Ray (ZIR) 1-Tile Zscape Motion Display (ZMD)

The light-field display used in this effort was the mobile, 1-Tile version of the ZIR 9-Tile ZMD developed by Zebra Imaging Inc. of Austin TX under the DARPA Urban Photonic Sandtable Display program. The ZIR 1-Tile ZMD comprises a rectilinear 84 x 72 array of hogels (hogels) that project ray bundles representing each of 6,048 3D model points. Each 1.64 mm diameter hogel projects quasi-collimated rays whose intensity is individually modulated into 5,776 fixed directions, as illustrated in Figure 13. These rays span a 90x90° (2.1 sr) square pyramidal viewing zone whose axis is perpendicular to the planar hogel array. The hogels were implemented in a so-called ZIR ZMD "Tile" comprising (a) a 4x6 array of Seiko-Epson high definition 1920 x 1080 px (2.1Mpx) transmissive active matrix liquid crystal microdisplays, covered by (b) a miniature projection optics lens array and driven from beneath by (c) drive electronics. The Tile-sized miniature projection lens array was overlaid on the 4x6 microdisplay array with an optical pitch and alignment such that a 21 x 12 (252) miniature project lens subarray overlaid each microdisplay, completing a corresponding 21 x 12 subarray of hogels (Klug et al., 2013).

The lightfield is low pass filtered by a diffusing screen placed about 25 mm above the top of the miniature projection lens layer. The ZIR image processing system ingests OpenGL scene descriptions (shunted by the Zebra Argon operating system from the client PC to the ZMD) and distributes the data to a three-slice parallel computing engine. Each Tile comprises three so-called "Slices, each comprising a workstation driving a 4x2 subarray of the 4x6 microdisplay array. Each workstation is housed within a 30 x 6 x 6 in. frame containing a component stack comprising a 20 GB hard drive, a CPU motherboard, GPU daughterboard, and an FPGA card programmed to generate the drive signals required by the microdisplays. This rendering engine implemented a double square frustum camera modeled on the square pyramidal emission zone of the display. Image update rate is better than 4 Hz for simple, but < 1 Hz for complex, 3D models. The microdisplays can be operated in color sequential mode with the built-in RGB light-emitting diode (LED) backlighting system to generate some 4000 colors. The maximum luminance is 200 cd/m^2 with a 70:1 contrast ratio under a dim room illumination condition.

The ZIR 1-Tile ZMD system can be scaled to form larger display systems if desired, such as the 3 x 3 Tile (ZIR 9-Tile ZMD) system described above.

3.5.3 Calibration of the ZIR 1-Tile ZMD

Initial calibration of the ZMD was accomplished by Zebra Imaging Inc., but visual inspection of the James two-rod stimulus implementation on the ZMD suggested that the display had a noticeable tilt to objects coming up out of the display surface. Attempts at AFRL to recalibrate the display using the Zebra automated procedure proved difficult and produced large patches of non-aligned hogels. The Zebra calibration tool allowed for the manual adjustment of individual hogels, but was labor intensive. An alternative method of calibration was developed at AFRL by one author (Heft) that allowed for optimum display uniformity and image quality. Calibration of the display via the Heft method is a two-step process. First, an intra-hogel alignment of the hogel optic and the hogel pixel array is accomplished to optimize imaging performance. Then scaling factors were calculated for the OpenGL coordinate system to insure that the ZMD display volume was uniform and accurately scaled for displaying the James rods.

3.5.3.1 Intra-Hogel Alignment of the ZIR 1-Tile ZMD. After the micro-lens array is overlaid on the micro-display, thereby fixing the hogel locations, the optimal 76 x 76 pixel array from the microdisplay must be assigned and aligned to each hogel. The best pixel array is determined by the intercept of the optic axis of the microlens with the microdisplay surface. The intercept also serves as the origin of the coordinate system from which pixel position and therefore beam direction can be estimated. Determining the optical axis intercept was an iterative process. A small cluster of pixels is illuminated under each hogel micro-lens. The centroid of the cluster functioned as a cursor which could be moved. A high resolution camera is positioned 6 ft from the display surface (optimal camera distance is dependent on ZMD size and camera resolution) with its optic axis perpendicular to the center of the ZMD surface. Using this cursor/camera combination, intensity as a function of location is recorded. For the hogels in the center of the ZMD, directly in front of the camera, the intensity function is unimodal with the maximum intensity recorded when the cursor and micro-lens optical axis are coincident. For non-center hogels, the intensity function was also unimodal, but—due to the slightly oblique camera view—the maximum intensity occurs at a slight misalignment of the axes of the curser and micro-lens optic. Therefore, the cursor location at maximum recorded intensity is taken to be the best estimate of the micro-lens optic axis and the center of the optimal pixel array.

In the manual Zebra Imaging calibration procedure, the movement of the cursor is made using key strokes and mouse inputs. This manual procedure is automated here using OpenCV and AutoHotKey to emulate the manual inputs. Figure 15 shows a series of images taken while OpenCV and AutoHotKey inputs drove the cursor to the maximum intensity location.

The automated iteration process took many hours due to the large number of hogels involved. Figure 16 shows the original appearance of the cursors (calibration pattern) side-by-side with the test pattern after the top two-thirds of the hogels had been aligned. Figure 17 shows the test pattern after alignment. The residual variation in cursor intensity is disappointing, but overall the imaging performance of the display is substantially improved. After the alignment is complete and the center of the pixel array determined, the individual pixels can be mapped to a beam direction using the pixel location and a standard hogel beam distribution model.

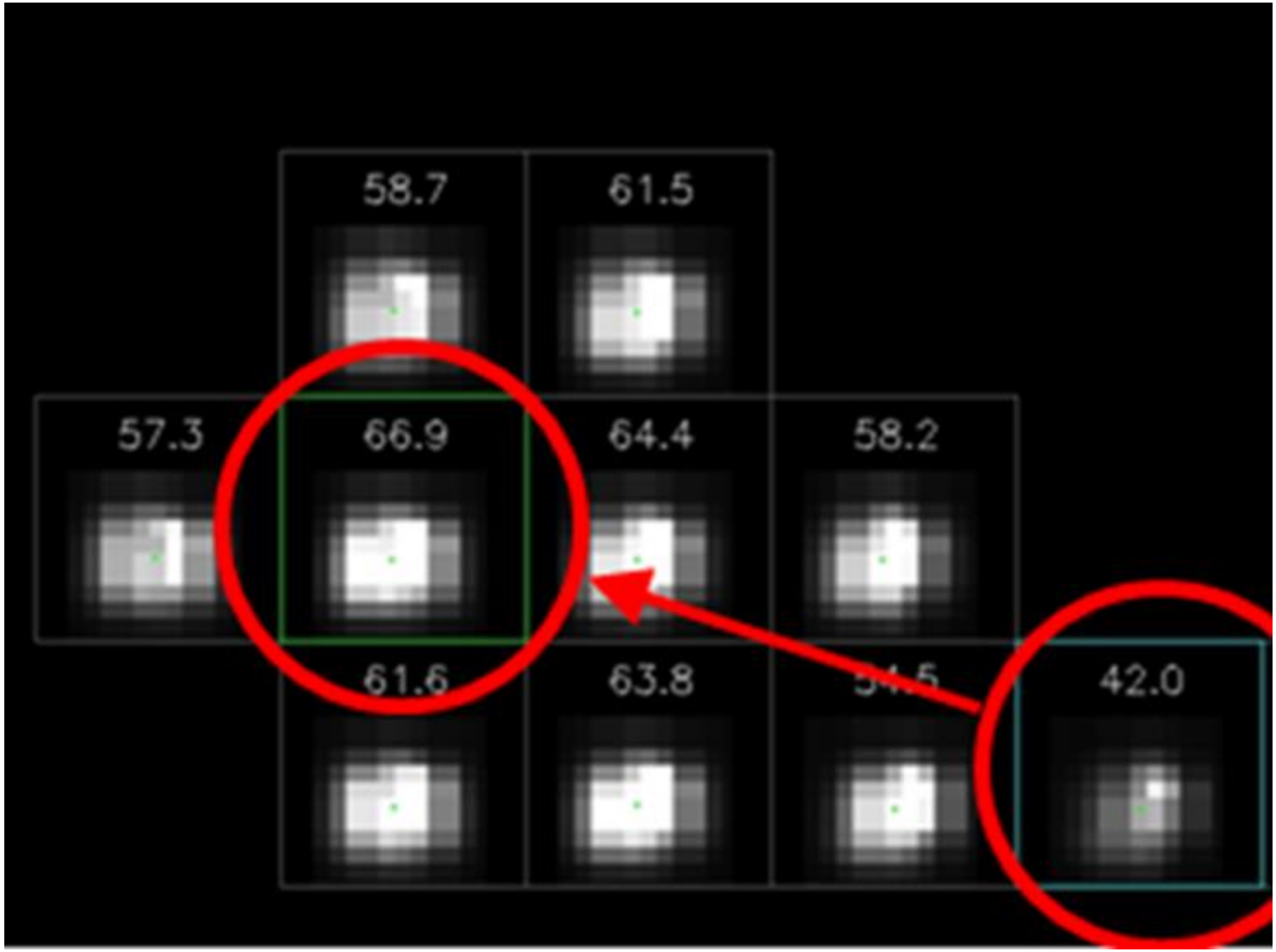

Figure 15. OpenCV and AutoHotKey Inputs Move Cursor to Maximum Intensity Location

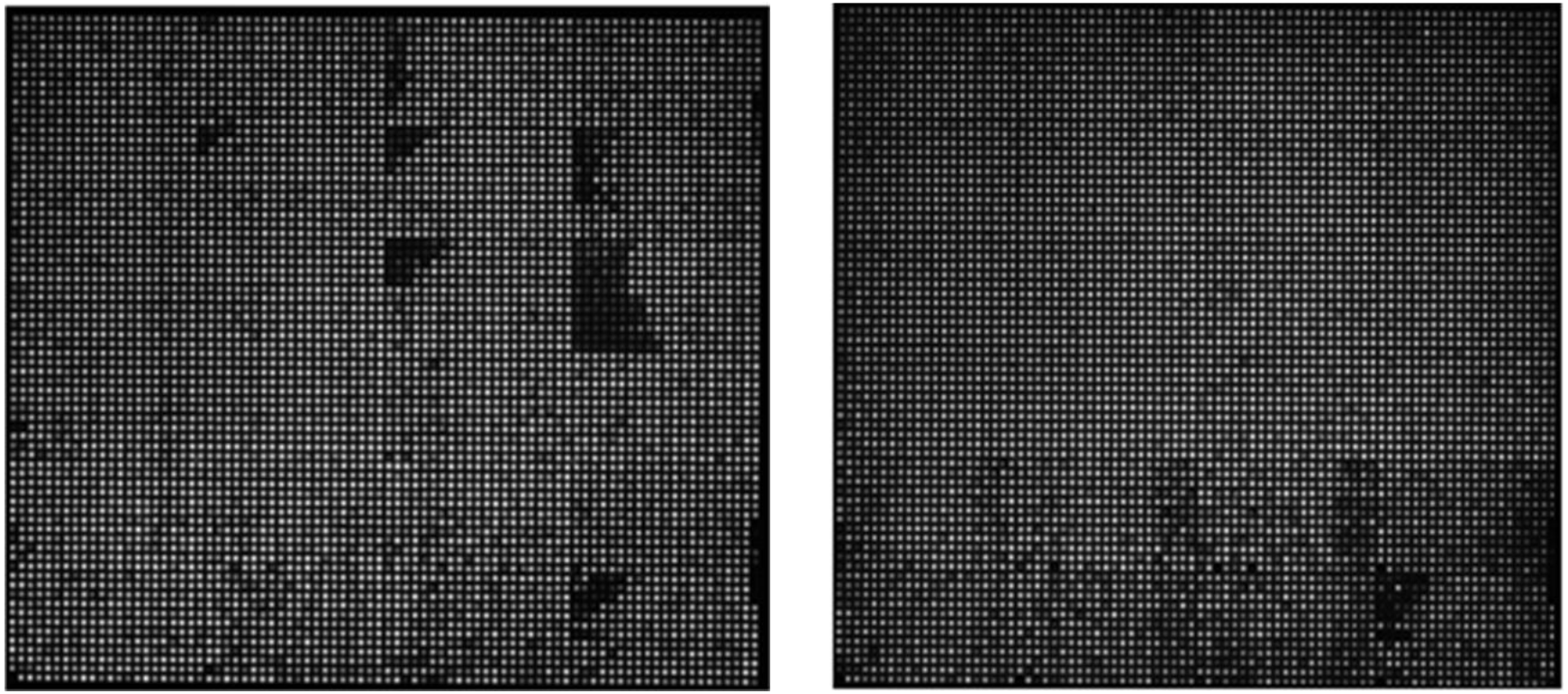

Figure 16. Hogel Calibration Pattern: Initial (Left) and Top Two-Thirds Realigned (Right)

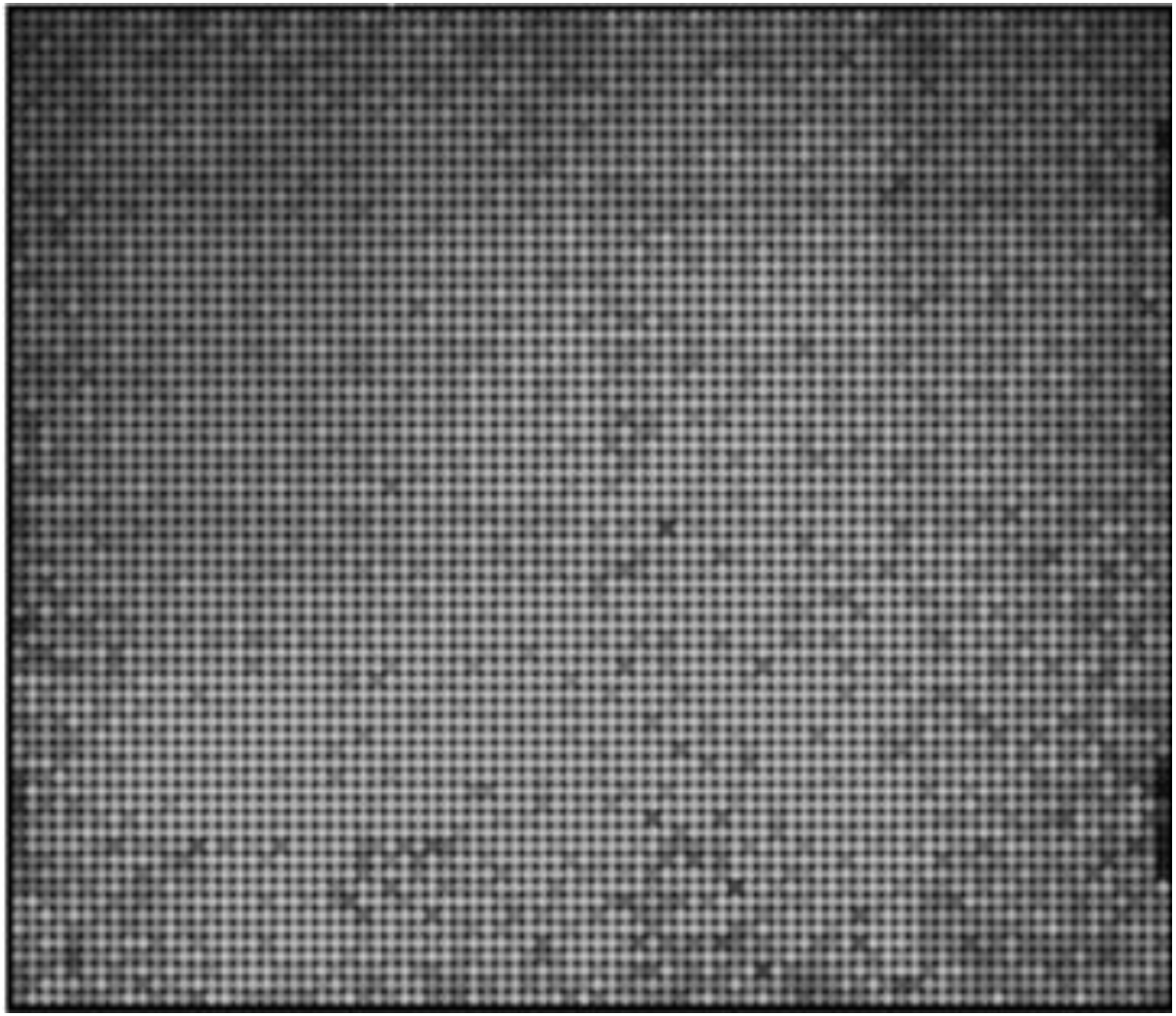

Figure 17. Calibration Pattern Appearance after Alignment

3.5.3.2 Display Volume Uniformity of the ZIR 9-Tile ZMD. To accurately reproduce the James rods, the OpenGL Euclidean space has to be sized and mapped uniformly to the ZMD display volume. To accomplish this mapping, scaling factors are calculated for each of the three primary, orthogonal dimensions: width, height and depth. The width and height dimensions are defined as being in the plane of the hogel array; and depth, perpendicular to this plane. Once calculated, there are multiple locations in the rendering path where scaling factors could be implemented. Scaling factors in width and height are easily calculated from measurements at the plane of the hogel array. An OpenGL input used to move an object in either width or height direction, and then the size of the movements are measured with a millimeter rule. Once the initial input-response ratio is determined, a simple correction factor can be calculated to scale the response to the desired size.

The calibration of depth can be conducted in a similar manner to the width and height except for one significant complication. The display produces imagery both in front of (real imagery) and behind (virtual imagery) the light emitter array surface. Items projected in front of the surface form real images, whose locations can be confirmed with a scale or gauge. However, images projected as if originating from behind the display surface are virtual and, thus, inaccessible to direct measurement.

Indirect measurement is accomplished as follows. The entire image volume (real and virtual portions) are reimaged into real image space using a spherical lens of known power mounted on an indexed optical rail as shown in Figure 18. A translucent diffusing screen is used to identify the reimaged (2nd image) locations produced by the simple optical system. Using the lens power, lens location and the secondary image locations initial displayed image locations relative to the lens can be calculated using the paraxial formula for thin lenses in air. A three bar test pattern was presented at a series of nominal command depths in OpenGL space: (-0.20, -0.15,-0.10,-0.05, 0.00, +0.05, +0.10, +0.15, +0.20). The OpenGL command depth "0.00" is assumed to correspond to the display surface (top of the miniature projection optics layer) but no other scaling or position information is known beforehand. The series of test patterns at the nominal OpenGL command depths are reimaged by the optical system and the secondary image locations are found by adjusting the screen distance from the lens to find the position of best image focus. From that measurement the initial image positions relative to the lens are calculated.

The subjective nature of determining the image location by best focus is compensated by repeating the measurement series using several different observers with each observer collecting three complete sets of data. For the present work three observers are used to take a total of nine sets of measurements; the cumulative data is plotted and fitted with a linear trend line. The resulting estimated position relative to the lens for command depth "0.00" (display surface) was within 1 mm of the measured position of the display surface. The data is then translated to report all command positions relative to the display surface. The translated data is presented in Figure 19. The slope of the linear regression line shown in Figure 19 serves as the initial input-response ratio from which the correction factor can be calculated.

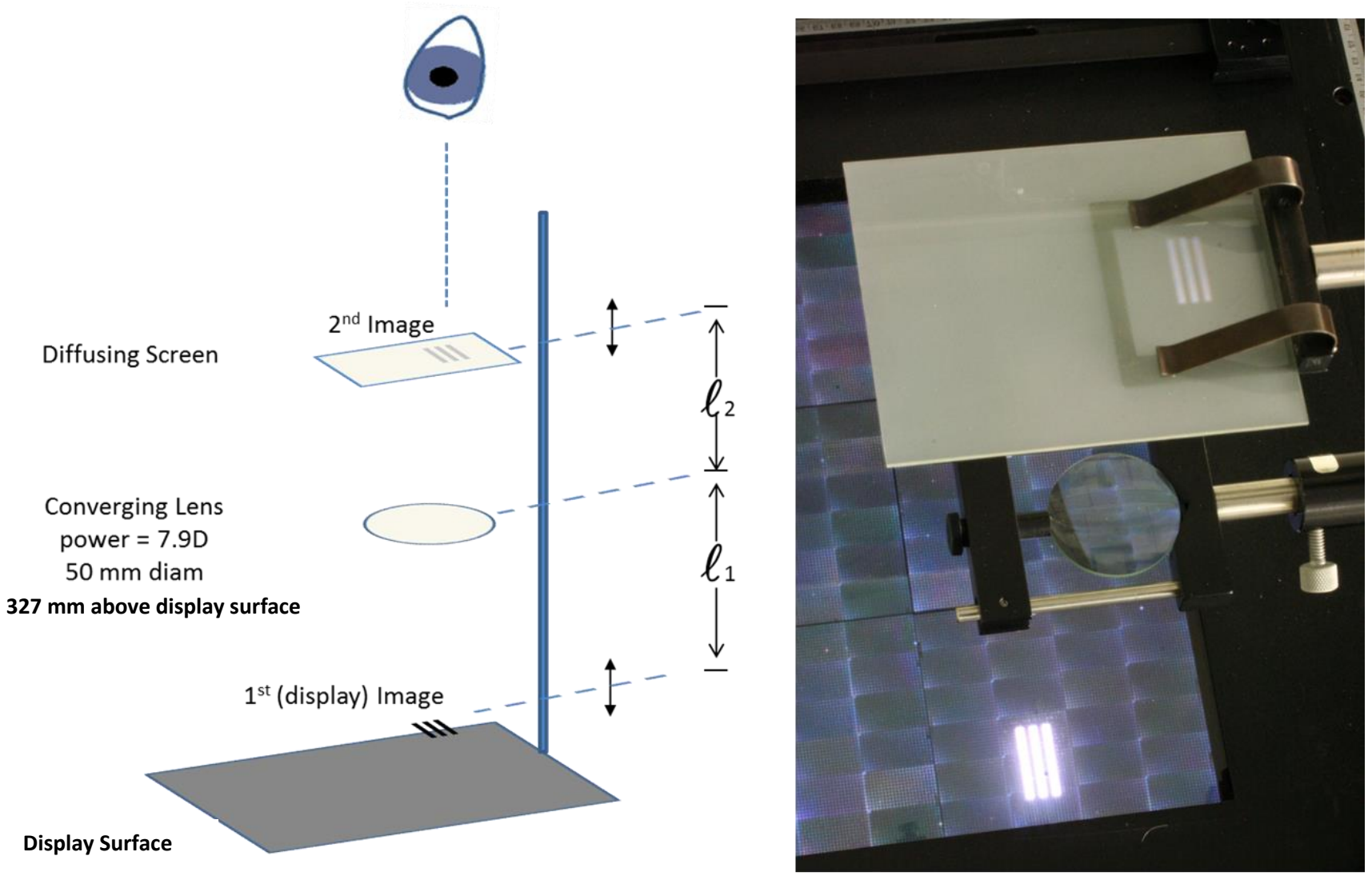

Figure 18. Optical Set-Up for Estimating Displayed Image Location from Secondary Image

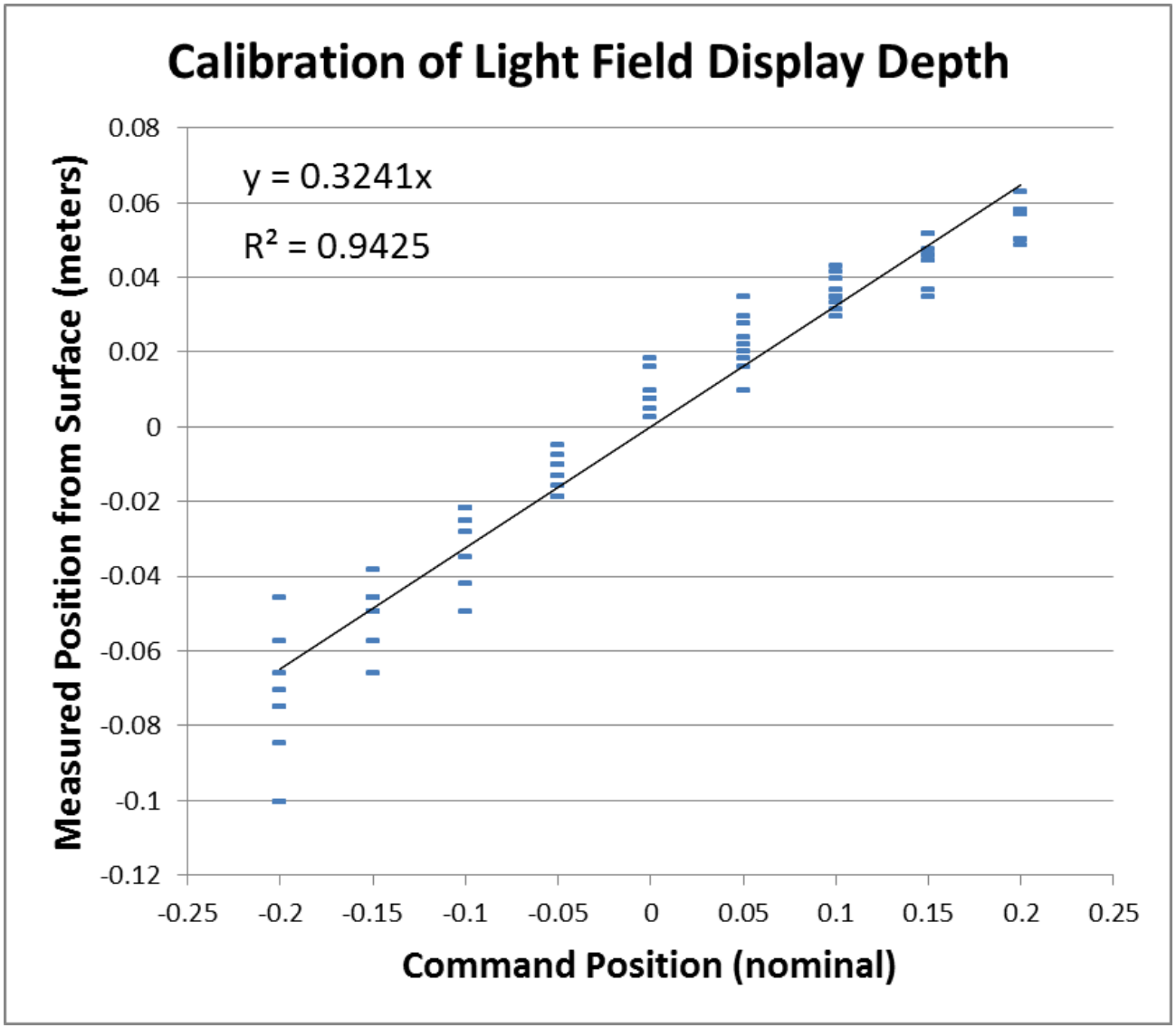

Figure 19. Scatter Plot of Perceived Depth from Commanded Depth

3.6 Objective Human Subject Evaluation of Proposed eJ Methodology

The four true 3D devices described above were arranged side-by-side for efficient sequential objective evaluation of the proposed eJ methodology by six (6) human subjects. The number of subjects is sufficient to provide an indication of the usefulness, or lack thereof, of the proposed methodology, but insufficient for statistically significant conclusions.

3.6.1 Experimental Condition for eJ Evaluation

The experimental condition for the collection of objective human subject evaluation data on the four 3D devices is illustrated in Figures 20 and 21. The subject is seated 6 m from and, sequentially, directly in front of one of the four devices under test (the other three turned off) with a hand controller to input judgments of distance.

3.6.2 Testing Approaches

Two objective human subject testing techniques are common and were both employed in the presently reported eJ experiments: the Method of Adjustment and the Method of Alternatives. The viewing distance was 6 m (20 feet) to correspond to the normal testing distance for the DPA.

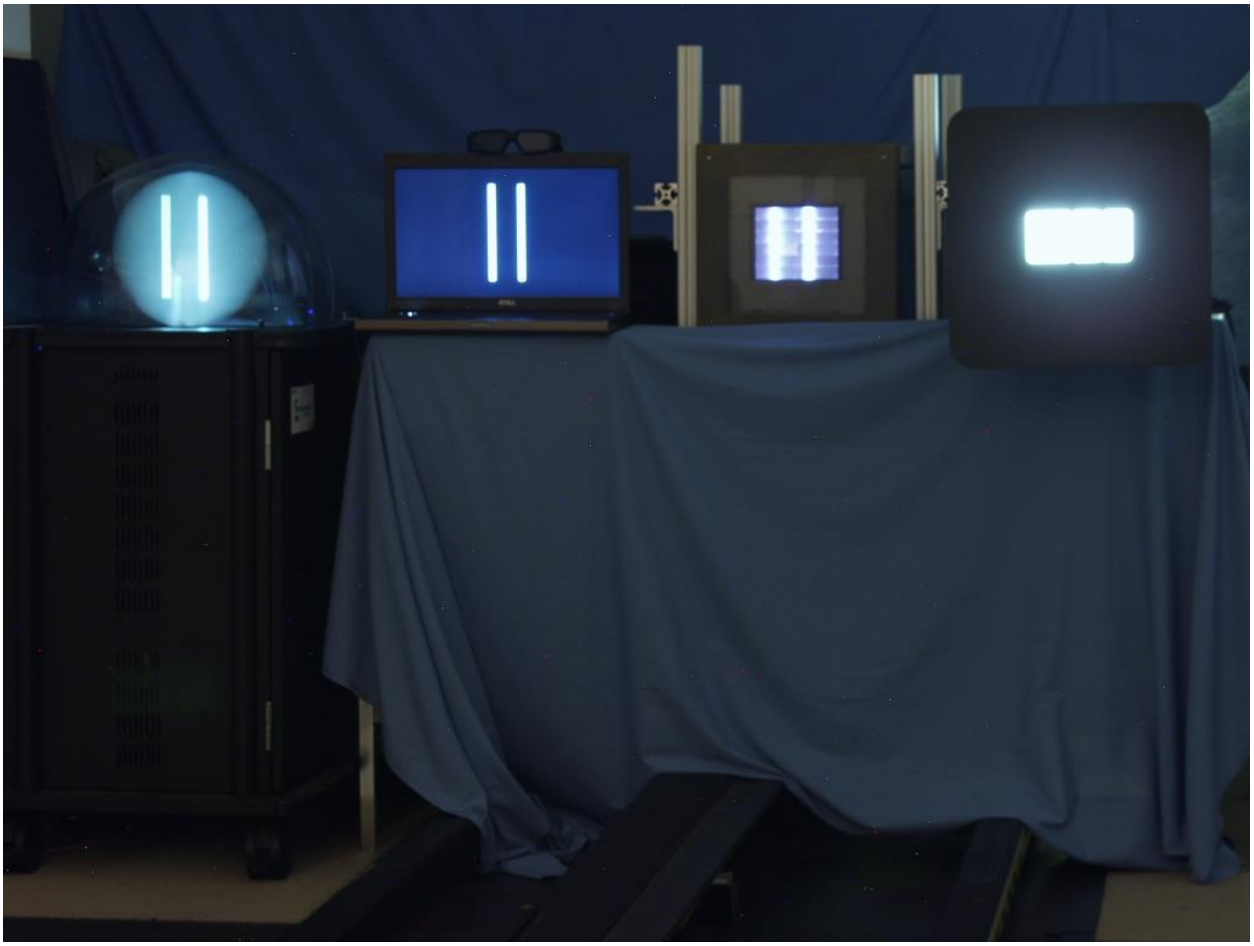

Figure 20. Close-up of Four 3D Devices Under Test as Arraigned for Subject Evaluations

Figure 21. Experimental Condition for Human Subject Evaluation of eJ Methodology

3.6.2.1 Method of Adjustment (Subject Moves Right Rod to Match Depth of Left). The well-known psycho-physical testing Method of Adjustment (MoA) was used by Deyo (1922): the stimulus depth magnitude of the right rod was under the manual control of the subject. The subject in the present work was also required to move the position of a control rod (always on right) to match the depth positioning of a fixed target rod (on left). The movement of the control rod was conducted via a wireless hand-held gamepad controller, using the forward/backward directional thumb-stick. On each trial, the participant had unlimited time to complete their alignment.

Each participant completed a total of 60 trials per display plus 12 trials on the physical DPA. The left rod was always the fixed reference target, and the right rod was always the control object whose position was under manual control of the viewer. For the electronic 3D displays, the left target rod could appear at any one of the five possible locations in depth (594, 597, 600, 603, and 606 cm) while the right rod would appear at a randomized starting location within 594 to 606 cm. With 12 repetitions per target distance per display, this gave a total of 72 trials per participant. Data collection lasted approximately 15 minutes per display condition, so a total of about 1 hour per participant.

3.6.2.2 Method of Constant Stimuli (Forced Choice: Subject Identifies the Nearer Rod). The well-known psychophysical Method of Constant Stimuli (MoCS) was used by James (1907, 1908) and Howard (1919a, 1920a). The stimuli depth magnitudes were chosen in advance at random and were not under the control of the subject. This testing procedure is also known as the Method of Alternatives and, in this case, as Two-Alternative Forced Choice (2AFC). The stimuli was suddenly revealed/flashed-on and the subject was merely required to make a forced-choice judgment about whether the left or right rod was perceived to be nearest (one was always closer than another). The answer was signaled with a button press, using a wireless hand-held gamepad controller. On each trial, the participant had unlimited time to complete their judgment.

Each participant completed a total of 200 trials on each display, with the stimulus pairs presented in a randomized order. Each stimulus pair consisted of two rods (left and right), with each rod at one of five possible locations in depth (594, 597, 600, 603, and 606 cm) but never at the same locations as the other for any given trial. All possible permutations of these pairs thus gave 20 unique stimulus pairs, with 10 repetitions of each pair (200 trials per participant). Data collection lasted approximately 15 minutes per display condition, so a total of about 1 hour per participant.

Normally, using this procedure, a psychophysical threshold is estimated by determining the intensity or magnitude of a physical stimulus required for a subject to achieve some targeted percent correct value. For a MoCS 2AFC paradigm, 75% correct is often the chosen target level of performance, midway between 50% which represents performance at chance levels, and 100% which represents perfect performance.

Poor image quality of some of the electronic 3D displays made the MoCS estimation of a depth acuity threshold difficult.

3.6.3 Description of the Subjects Used to Evaluate the eJ Methodology

A total of six (6) subjects were used to evaluate the proposed eJ methodology. All subjects were employees within the AFRL Warfighter Interface Division and have extensive experience in human subject testing of visualization systems.

3.6.3.1 Subject Selection Criteria. All participants were required to possess 20/20 distance vision (Snellen normal) or better in each eye separately (monocular), and together (binocular). Vision correction was acceptable. We also required all participants to demonstrate normal binocular depth vision, confirmed via Titmus "Stereo Fly" test (Wirt circles portion) which confirmed stereoacuity of 40 arcsec or better. There was no color vision requirement for this study.

3.6.3.2 Anonymous Demographic Vectors. The subjects were all male and aged 30-60 years.

4.0 RESULTS AND DISCUSSION

4.1 Implementation of the Two-Bar Stimuli on the Three Electronic 3D Displays

The software-defined bars presented on the three electronic 3D display systems were designed to be 10 mm wide to match the diameter of the rods in the physical DPA as illustrated in Figure 22 for the S3D system. The angle subtended by the 10 mm rod at 6.00 m is 1.67 mrad (5.74 arcmin).

Theoretically, as a bar moves towards (away) from an observer, the angle subtended at each of their pupils increases (decreases) and might provide a non-depth cue during the collection of data. For observers located at 6 m (600 cm) from the reference plane, the angle changes are slight and have been shown to have no significant effect on depth acuity measured with the physical DPA (Howard 1919) (Berry, Riggs, and Richards, 1950). However, significant visual artifacts of the electronic 3D systems employed in the present work—low contrast due to scattered light (see Figure 20); ill-defined edges due to diffusion and pixilation effects (see Figures 22-27)—might also provide non-depth perception cues regarding relative bar positions. Thus, the software-defined bars were designed to change width with their depth placement so as to maintain constant angular subtend of 1.67 mrad at the pupils of observers located at 6 m from the reference plane of the display under test.

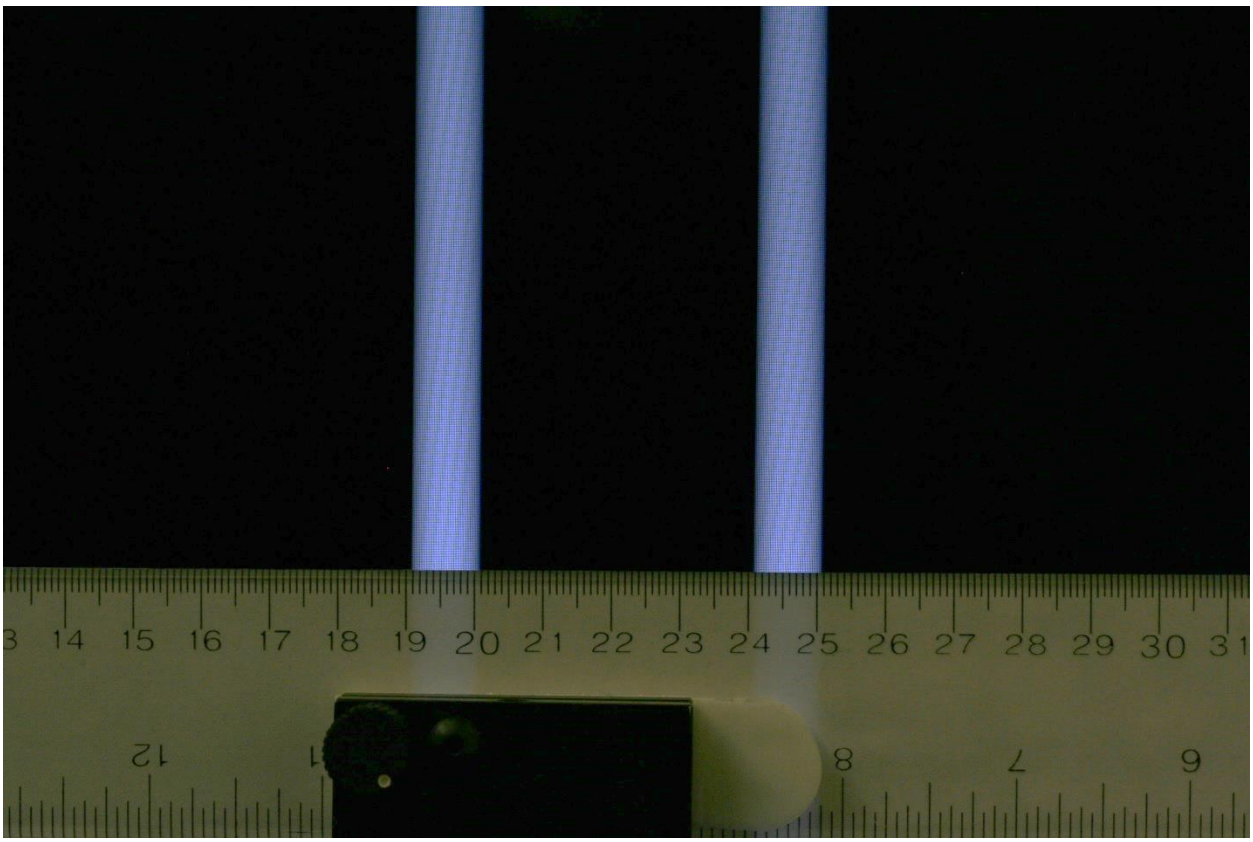

Figure 22. Rendered Bars Designed to Have 10 mm Width at Reference Depth on S3D

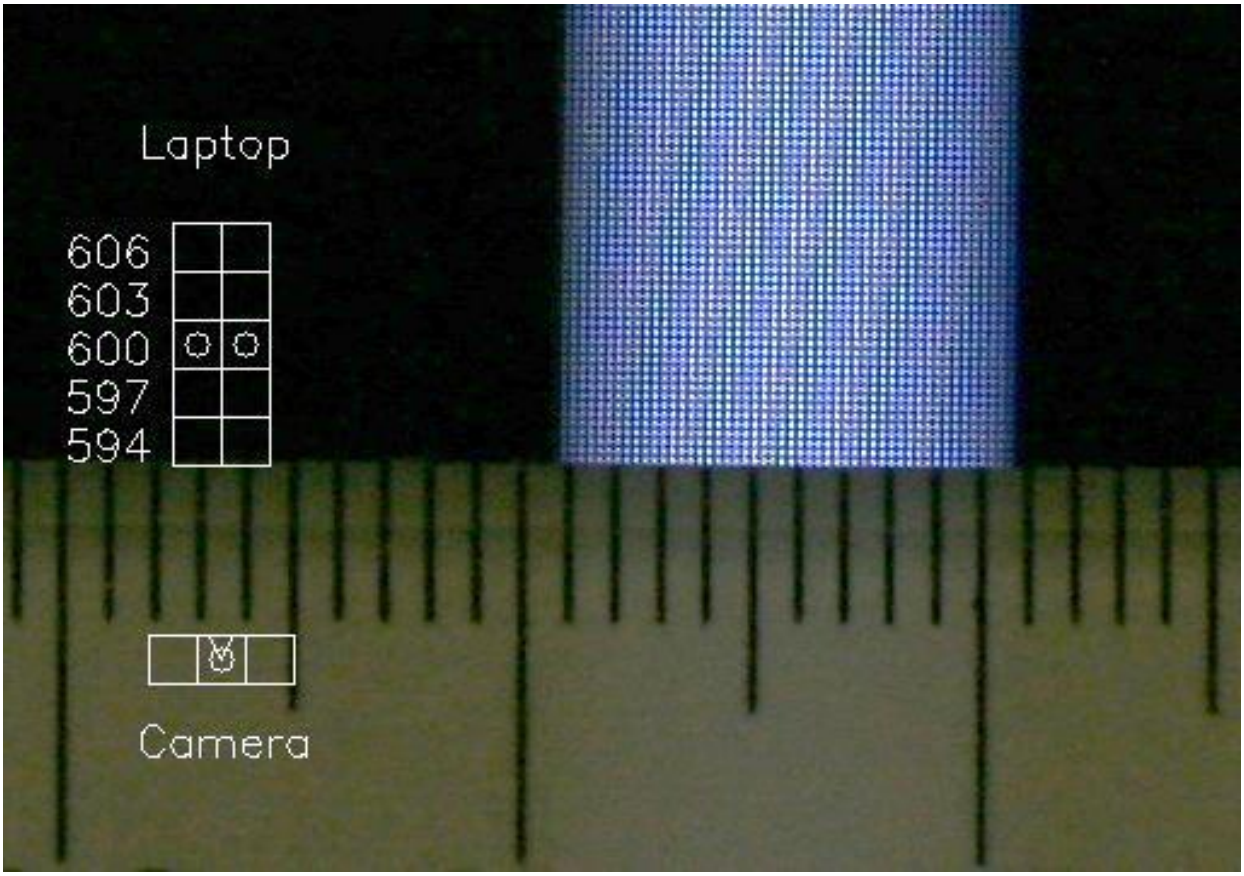

Figure 23. Ill-defined Edges of Bars on S3D Laptop Display Due to Pixellation Effects

Photograph arrays are presented in Figures 24-27 to document the appearance of the rod pairs for the physical apparatus (AFRL-Automated USAFSAM variant of the Howard DPA) and the rendered bar pairs on the three electronic 3D displays.

Figure 25 is a 1x5 array of photographs taken of the physical apparatus (Howard DPA) with camera located 6 m from reference position of the fixed left rod at 600 cm for a series of right rod distances of 606, 603, 600, 597, and 594 cm.

Figures 25-27 for the electronic 3D displays present 5x5 arrays of images of the rendered bar pairs taken with the camera located 6 m from their reference positions (600, 600 cm) for all combinations of 0, ±3, ±6 cm changes in the position of either bar**.**

The ill-defined bar edges are readily apparent in these photographs, especially for the spatially integral ray (ZIR 1-Tile ZMD) system (Figure 27). Tiling artifacts of the subcomponents used to construct the ZIR system are also readily apparent in these images.

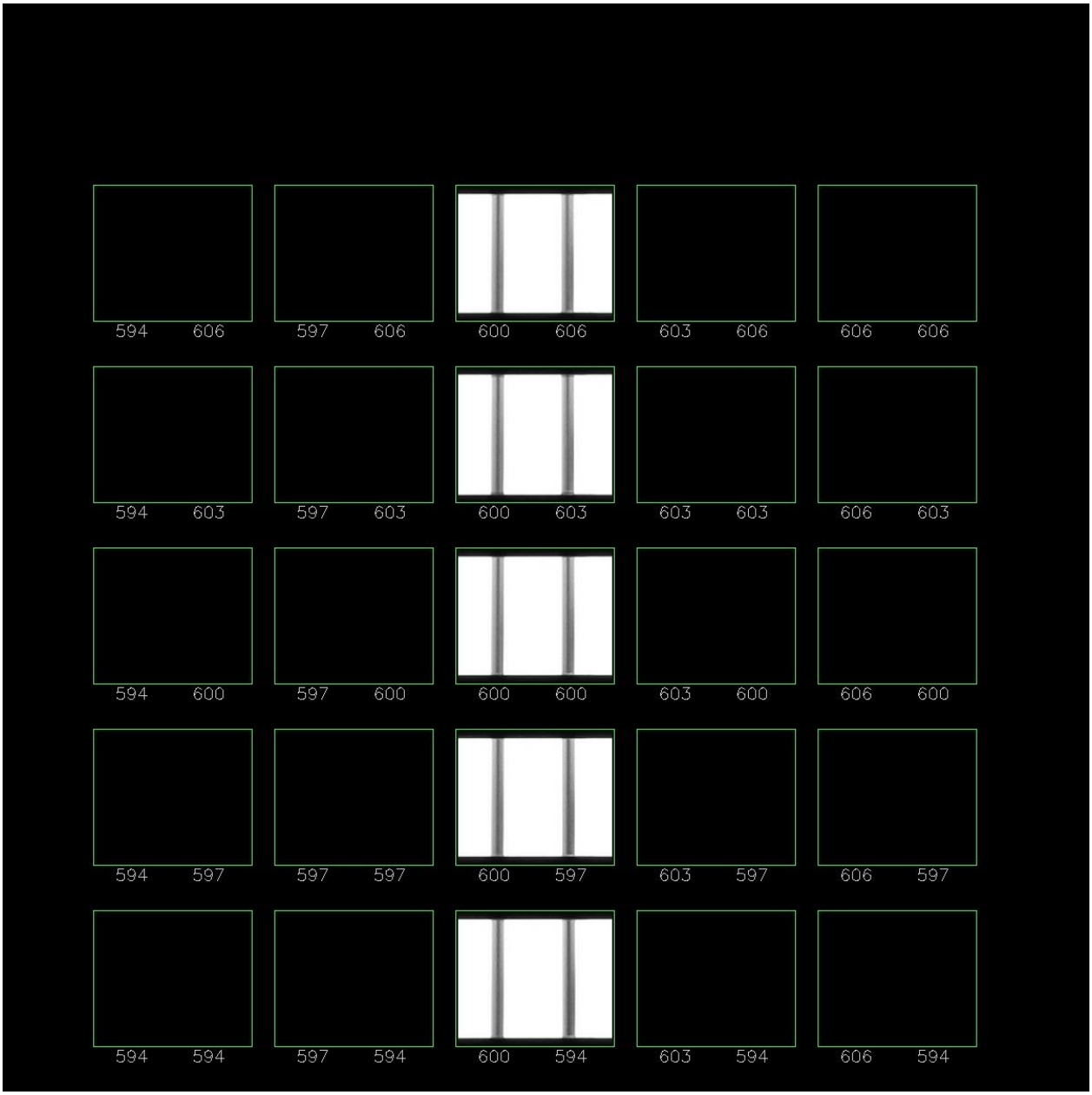

Figure 24. Photograph Array of the Physical Depth Perception Apparatus (Howard DPA) Taken with Camera Located 6 m from Reference Position of the Fixed Left Rod at 600 cm for Right Rod Distances (Top to Bottom) of 606, 603, 600, 597, and 594 cm.

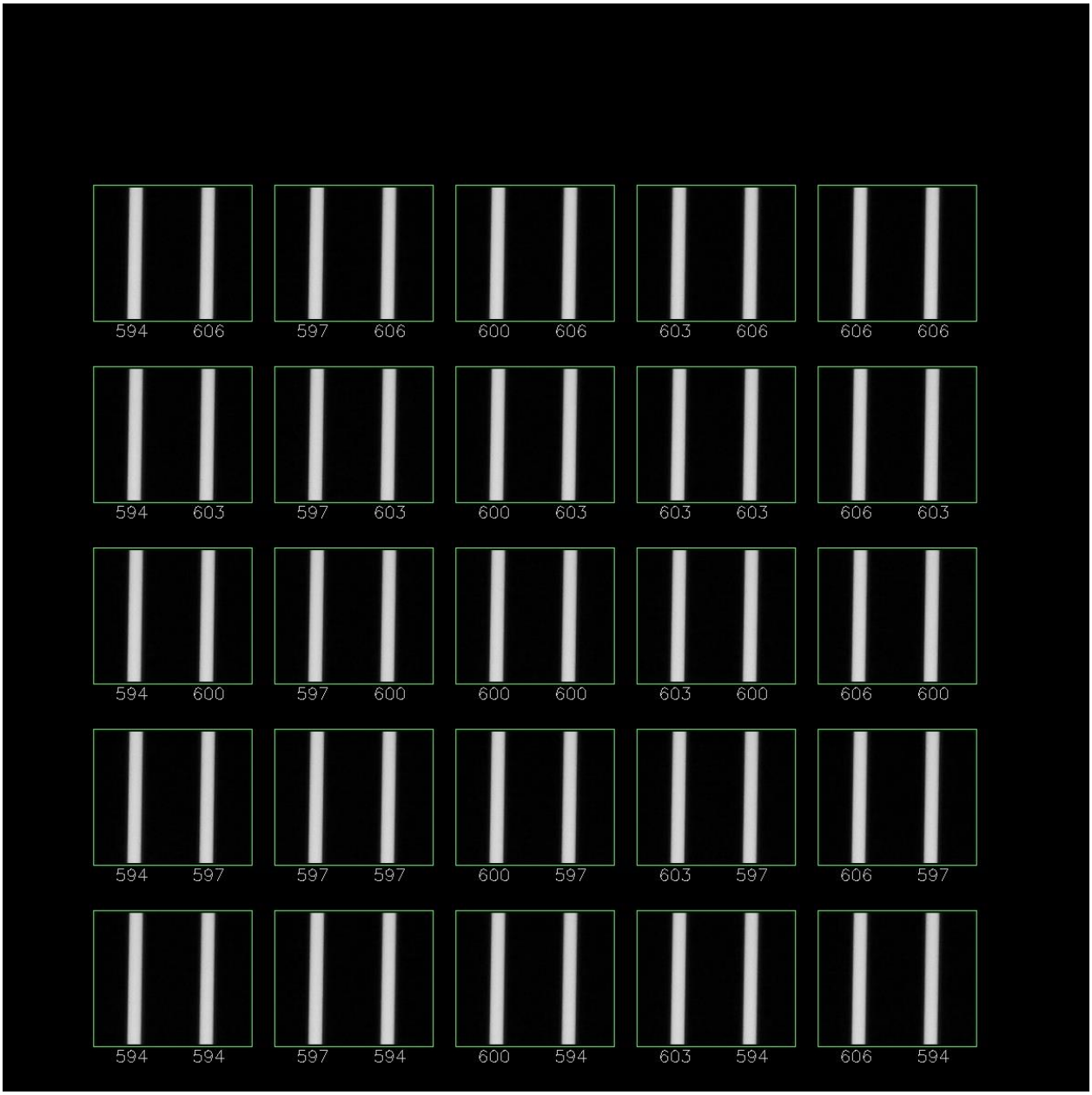

Figure 25. Photograph Array of the S3D Display (Dell M6700 Laptop) Bar Pairs Taken with Camera Located 6 m from Their Reference Position (600, 600 cm) for All Combinations of 0, ±3, ±6 cm Changes in the Position of Either Bar

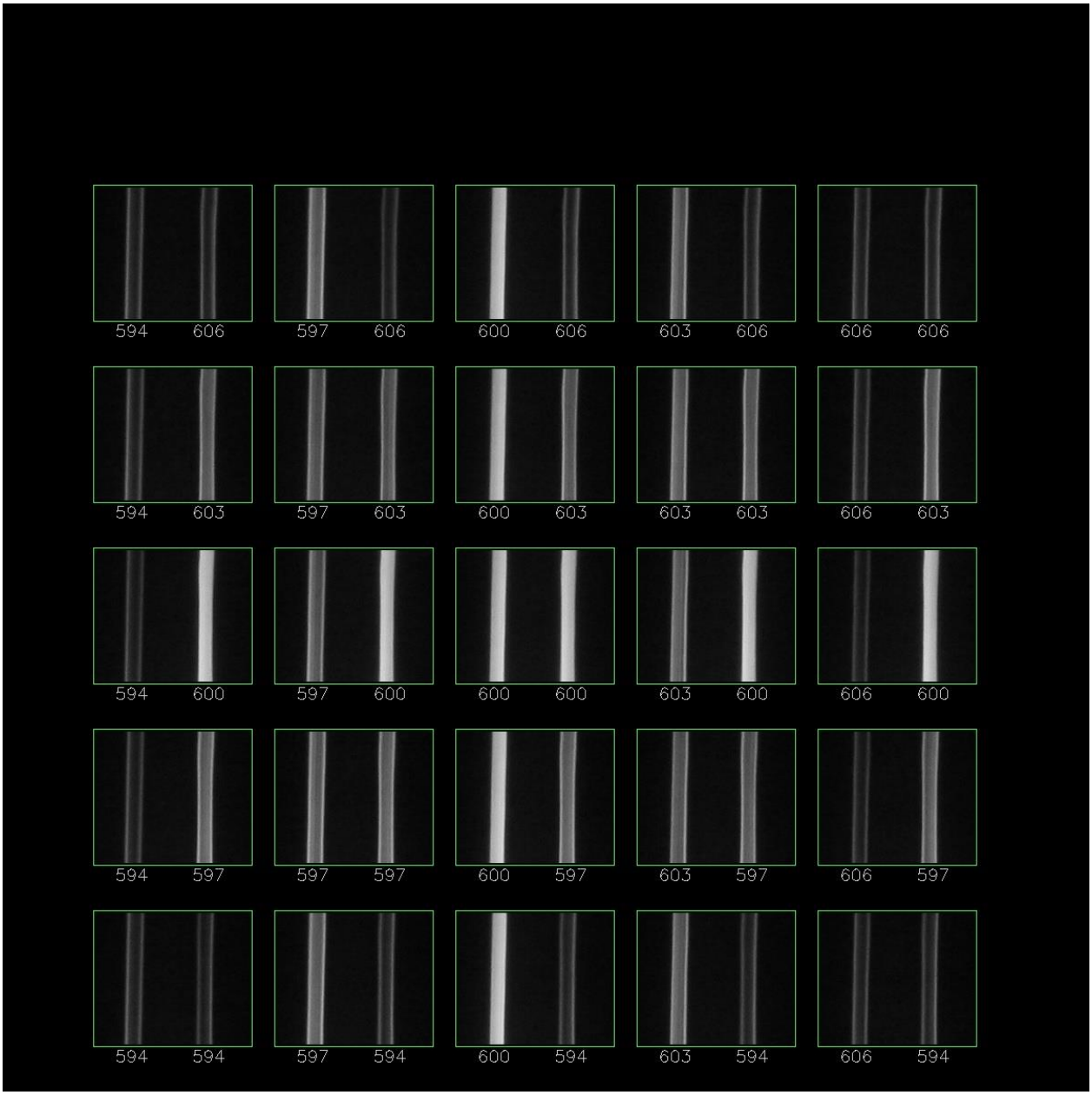

Figure 26. Photograph Array of the Volumetric (AIS Perspecta) Display Bar Pairs Taken with Camera Located 6 m from Their Reference Position (600, 600 cm) for All Combinations of 0, ±3, ±6 cm Changes in the Position of Either Bar

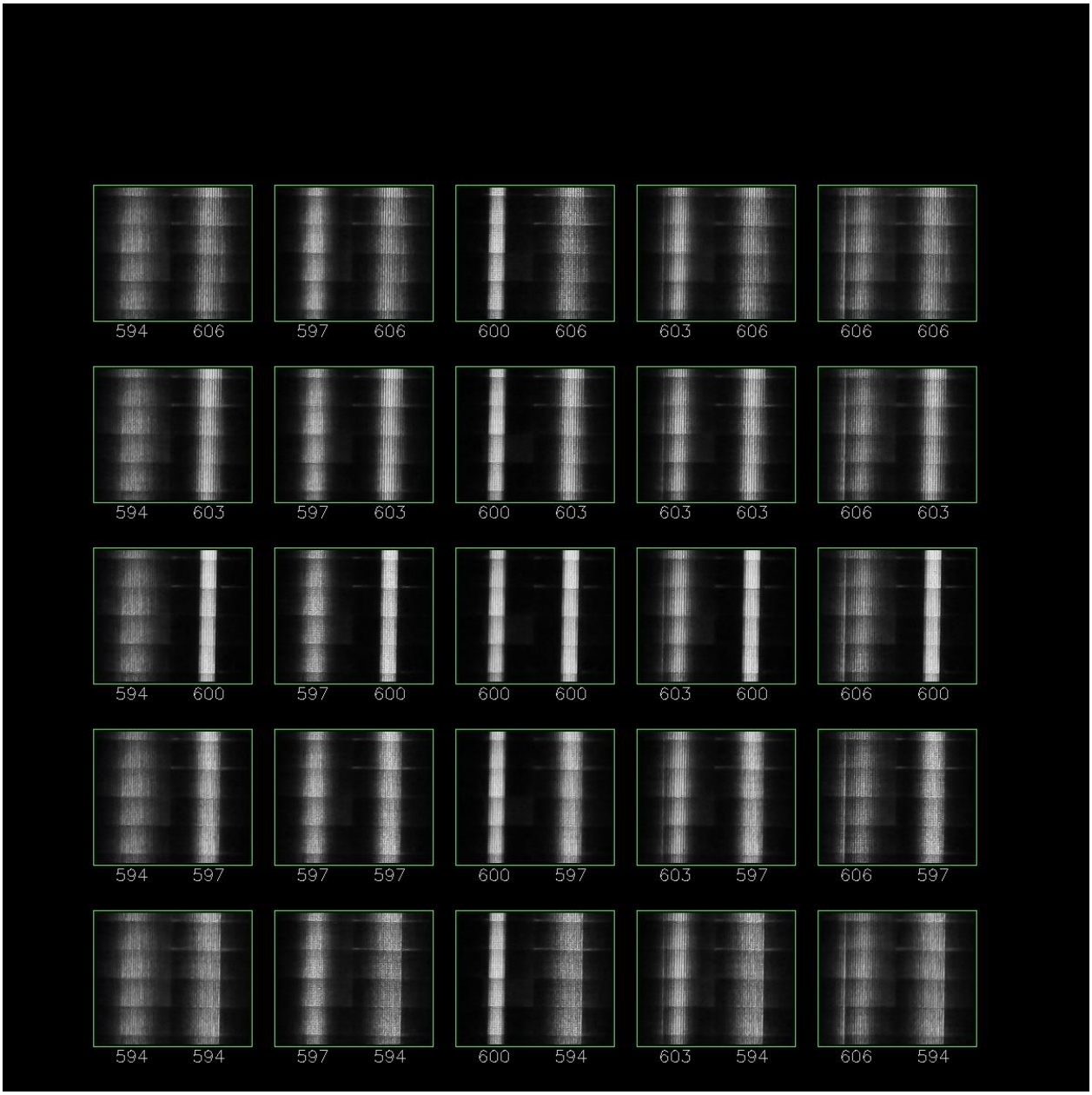

Figure 27. Photograph Array of the Integral Ray (ZIR 1-Tile ZMD) Display Bar Pairs Taken with Camera Located 6 m from Their Reference Position (600, 600 cm) for All Combinations of 0, ±3, ±6 cm Changes in the Position of Either Bar

4.2 Two-Bar Stimuli Depth Acuity Testing of Six Observers on the Four 3D Devices

Depth acuity datasets were collected and analyzed for six binocular observers using the method of adjustment (MoA) and the method of constant stimuli (MoCS). The MoCS method is also known as the method of alternatives and as the method of forced choice. A third dataset for five observers using only their dominant eye (other blocked) was collected using the MoCS method to assess monocular viewing.

The four devices presented four display conditions of the two-bar stimuli to the observers. These devices were arrayed in front of the observer (as shown in Figures 1, 20 and 21) from their left to right as follows: **AIS** ("**Perspecta**"), **S3D** ("**Laptop**"), **ZIR** ("**Zebra**"), and **DPA** ("**RealHD**"). The parenthetical names are used below to label depth threshold data collected for each device. Note: the data panels in Figures 28-37 are NOT ordered according to the experimental condition.

4.2.1 Dataset 1: Depth Acuity Threshold Measured by Method of Adjustment (MoA)

The MoA data is analyzed in several ways which are plotted in Figures 28-32. Data for all six observers are combined for each device (aka display condition) into a subpanel of each figure.

Note that a fewer numbers of trials (12/observer) were recorded for the physical device, the DPA (RealHD), due to the fixed location of the left, reference bar at the "0" position. The same number of trials (60/observer) were used for each of the three electronic 3D displays. Thus, the DPA ("RealHD") histogram contains fewer trials (72) than those for the other devices (360).

4.2.1.1 MoA Signed Positional Error Data. Figure 28 presents histograms showing the frequencies of signed errors (placement accuracy) centered on zero and normalized on the range -12 to +12. A fitted normal Gaussian curve is included for comparison within each panel.

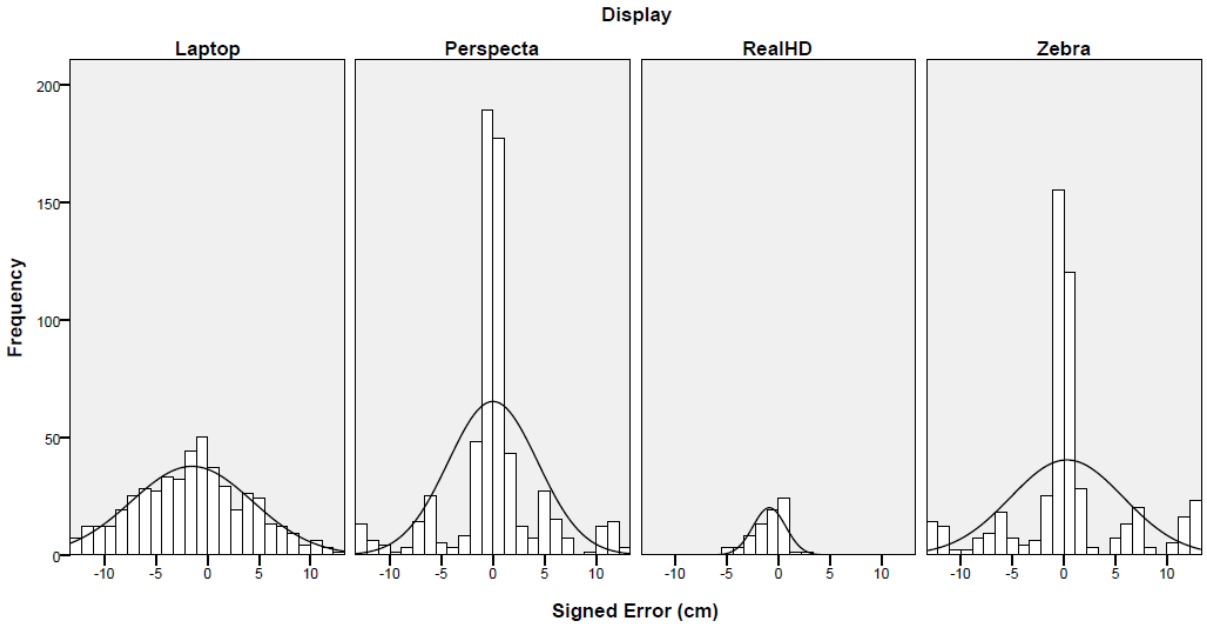

Figure 28. Method of Adjustment (MoA) Frequency Histograms of Signed Error

The positioning performance on the DPA ("RealHD") was very good with high accuracy: most observations were centered around zero, with perhaps a slight tendency to underestimate the depth position (tail towards the negative signed error range). This result seems to confirm the utility of the physical DPA for depth perception testing.

The S3D ("Laptop") performance was centered at zero, but with a wide distribution of signed errors in both the negative and positive directions. These data suggest that this stereo display generally supports depth perception but with considerably less accuracy and consistency than is offered by the DPA ("RealHD") system.

The AIS ("Perspecta") and the ZIR ("Zebra") devices had similar-looking histograms comprising a large spike in the distributions of errors centered around zero and smaller *but still-prominent spikes* at -12, -6, +6, and +12. These data suggest that perceptual confusions were systematically occurring at particular relative distances. Depth-dependent visual artifacts (luminance/contrast, and/or blur) were observed for both the Perspecta and the Zebra; the presence and intensity of these artifacts seemed to primarily depend on the depth locations of stimuli relative to the zero reference depth ("center") of the device. In other words, these systematic error spikes in the histograms likely indicate front/back positional confusions caused by the artifacts. These confusions may have impeded the ability observers to perform accurate depth alignments as desired, but only at particular relative depths. This issue is addressed in section 4.3.2.

4.2.1.2 MoA Absolute Positional Error Data. Figure 29 presents histograms of absolute positional error observed for the four test devices. Observations based on this data are similar to those for the raw signed error data from which it is derived.

For the DPA, errors tended heavily towards zero, with almost no tail observations beyond 5 cm of error, again confirming that the real apparatus allows for an accurate perception of rod locations in depth.

For the S3D, the *shape* of the distribution was very similar to the DPA, though the tail is considerably lengthier, evidencing errors as large as 10 to 15 cm in some cases.

However, the systematic confusions caused by the circular rotating screen of the AIS ("Perspecta") and the low resolution hogels of the ZIR ("Zebra") devices are even more prominent, relative to the S3D laptop and the DPA. These two FoLD systems (ZIR, AIS) again showed similar distributions to each other, with large spikes tending towards zero with prominent error "bumps" clustered at around 6 and 12 cm. This new look at the raw signed error data supports the above "artifact" interpretation of these error clusters.

These unique display quality problems, which are inherent in the circa 2005 Perspecta and circa 2010 Zebra devices used, may have unintentionally turned what was meant to be a *depth-matching task* into instead a *visual-artifact-matching task*; at least for these two FoLD systems.

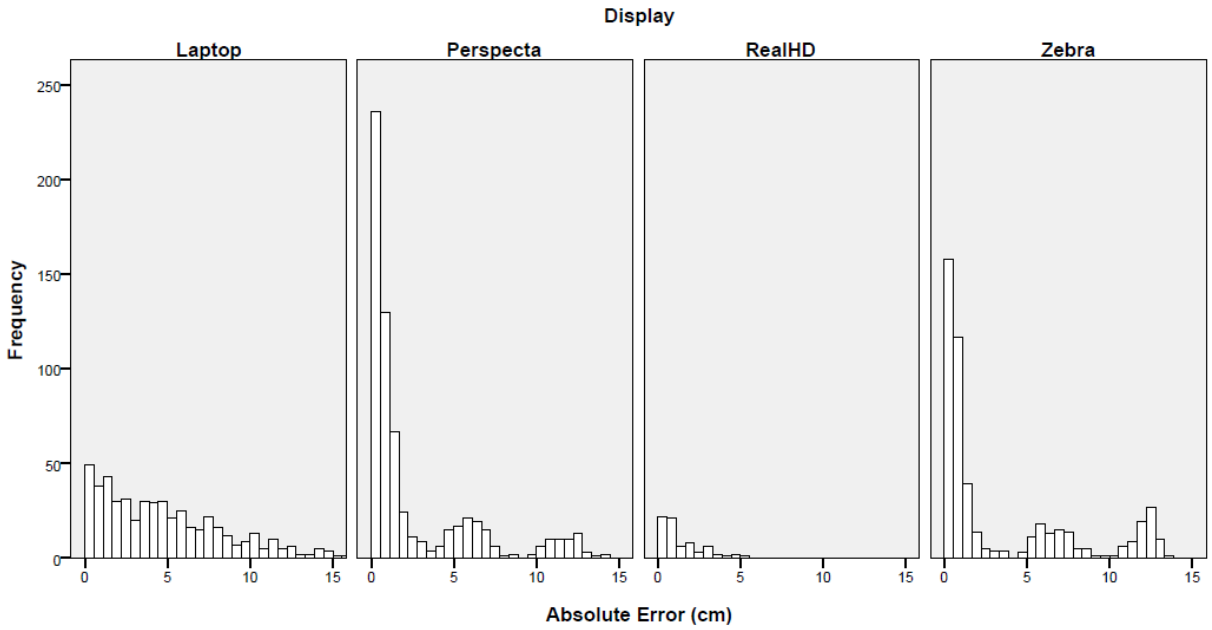

Figure 29. **Method of Adjustment (MoA) Frequency Histograms of Absolute Error**

4.2.1.2.1 Mean Placement Performance as Function of Reference Distance

Figure 30 shows the placement performance (distance observer placed the moveable pin) versus the reference distance, averaged over all trials. Theoretically optimal performance is indicated by the solid red *y=x* line; deviations from this line indicate suboptimal performance.

These plots of average performance suggest that the perception of depth location did scale with distance, as the slopes are positive and with patterns approaching linearity, though for the S3D ("Laptop"), AIS ("Perspecta"), and ZIR ("Zebra") devices the error bars were noticeably larger when compared to the DPA ("RealHD") device.

The DPA clearly resulted in extremely accurate performance with very tight error bars, for its single reference pin position.

Interestingly, the S3D ("Laptop") data indicate consistently inaccurate location judgments: observers tended to misperceive the stereo stimuli as being nearer than expected, except for the closest reference distances.

The AIS ("Perspecta") and ZIR ("Zebra") devices seemed to have particular problems portraying nearer locations. However, both the AIS and ZIR portrayed stimuli at the center (real or virtual "screen surface") positions accurately and with low variability in judgments.

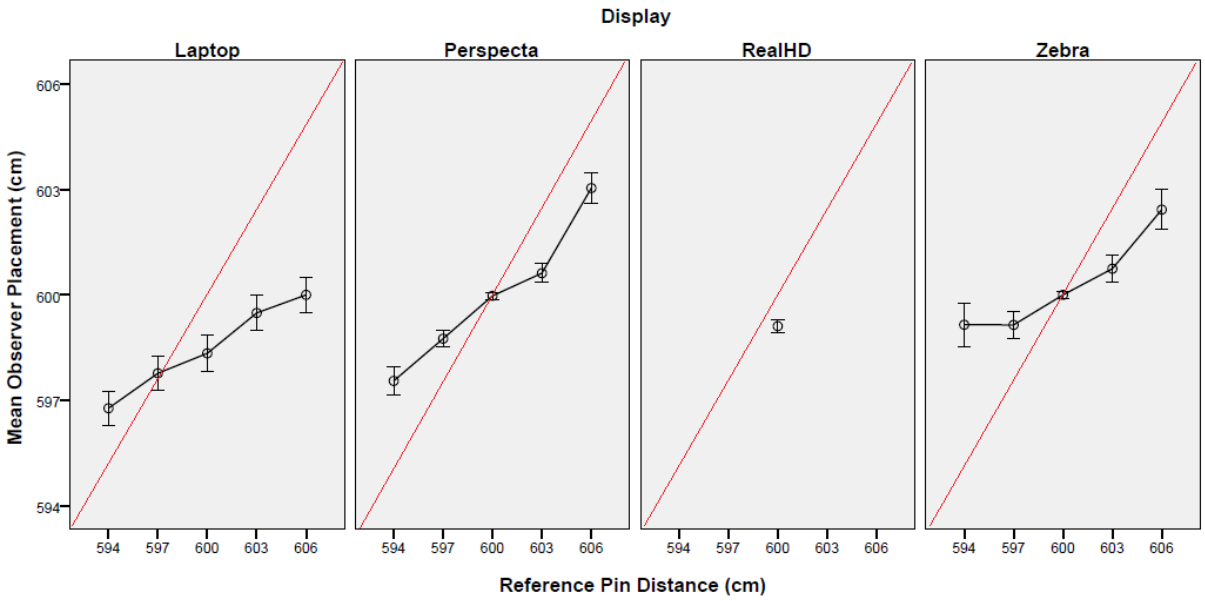

Figure 30. Placement Performance vs. Reference Distance (Mean ± 1 SEM); Straight Red Line Represents Optimal Performance

4.2.1.2.2 Per Trial Placement Performance as Function of Reference Distance

Figure 31 is a scatterplot of all MoA data. Here, instead of looking at the dataset data as averages with error bars, every single observation, every data point per trial, is plotted. The x and y variables in Figure 31 are identical to those Figure 30 and a red y=x line is used to indicate theoretically perfect performance. However, the scatterplot shows how noisy the relative performance was across the four devices. The DPA ("RealHD") had good, consistent performance in placement accuracy, with very little scatter.

The S3D ("Laptop") had extremely noisy data and inconsistent placements. The slope shown for the averaged S3D data in Figure 30 is barely perceptible in the raw data scatterplot in Figure 31.

The scatterplots for the two FoLD systems AIS ("Perspecta") and ZIR ("Zebra") demonstrated very similar patterns: clusters of data points were aligned accurately along the red y=x line (perfect performance) with shockingly remarkable precision.

However, the scatterplots for these two FoLD systems *also* resulted in clusters on an oppositely-sloped y = (-x) line, which crosses the optimal performance y=x line at the center 600 cm distance. This y = (-x) line represents "perfectly wrong performance" and is depicted as by dashed blue lines in the AIS and ZIR panels within Figure 31. The clusters on this y = (-x) dashed blue line demonstrate that front/back positional confusions or misperceptions were occurring. For instance, reference target pins at a distance of 606 cm (+6 cm from center position) were sometimes being misperceived at 594 cm (-6 cm from center), and vice versa. Likewise, reference locations of 603 cm (+3) were occasionally but consistently being misperceived at 597 cm (-3), and vice versa. This front/back confusion was not observed in the DPA or S3D data.

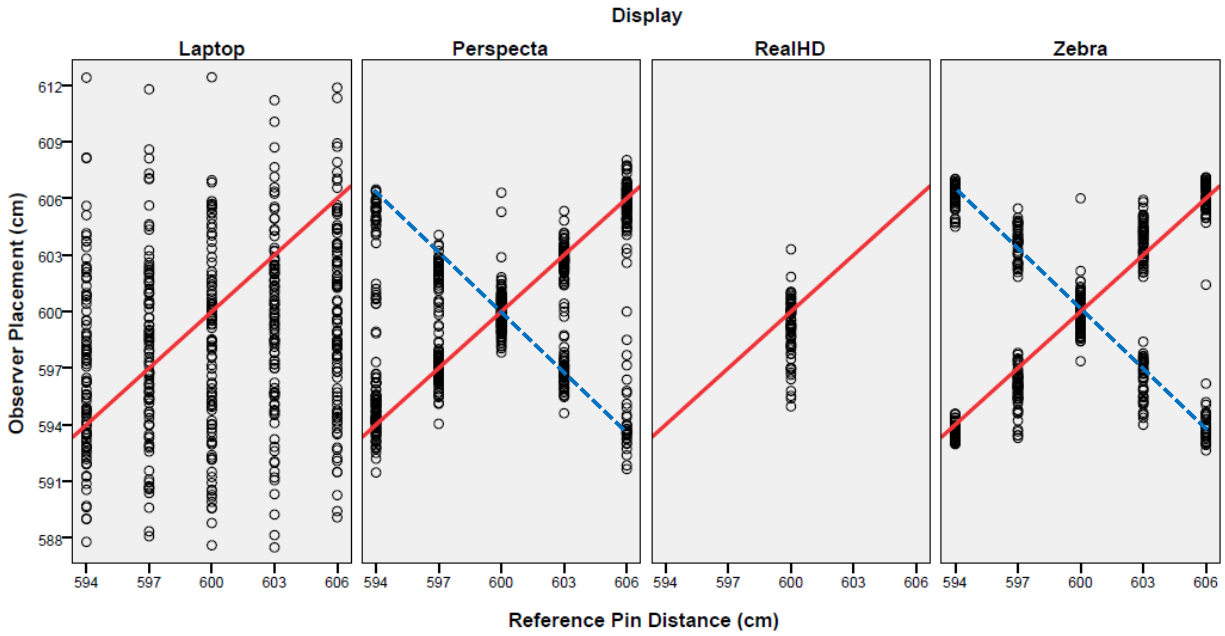

Figure 31. Per Trial Placement Performance vs. Reference Distance; Solid Red Lines Show Optimal Performance; Dashed Blue Lines Indicate Systematic Near/Far Misperceptions

The front/back confusion pattern found in the MoA dataset for the AIS ("Perspecta") and ZIR ("Zebra") devices may be caused by the aforementioned visual artifacts of these two displays. The magnitude and severity of the artifacts were observed to depend upon the magnitude of the distance a stimulus was commanded to be displayed relative to its "center" plane. The farther from this central position in either direction of depth a stimulus was placed, the more degraded the displayed image of the stimulus became (in terms of blur, intensity changes, etc.). Thus, distances of ±3 cm result in perceptually-similar displayed stimuli (suffering from similar magnitudes of artifacts). Distances of ±6 cm resulted in even worse artifacts (but again of similar magnitudes).

Analysis of the MoA dataset using only averages (similar to the way psychophysical stereoacuity threshold data are often computed) may be misleading. Table 1 summarizes averaged MoA data for the four 3D devices used in this work. The mean absolute error for the DPA ("RealHD") device was 1.32 cm was lowest (best); AIS ("Perspecta"), 2.57 cm; ZIR ("Zebra"), 3.44 cm; and S3D ("Laptop"), 4.77 cm. One might be tempted to conclude that the AIS and ZIR are capable of supporting depth stimuli that significantly outperform that offered by the stereo display. However, the presence of the visual artifacts in the AIS and ZIR devices used in this work may make this a premature and inaccurate conclusion.

Table 1. Means and Standard Deviations of Absolute Error Performance, across Participants, for Four 3D Devices Using MoA Dataset 1

Device (Viewing Condition)	Mean (cm)	Standard Deviation (cm)
S3D ("Laptop")	4.77	3.76
AIS ("Percepta")	2.57	3.50
DPA ("RealHD")	1.32	1.24
ZIR ("Zebra")	3.44	4.28

Figure 31 provides plots of the MoA standard deviation of observer placements vs. the reference distance for each of the four test devices. The DPA ("RealHD") standard deviation at 600 cm reference distance is about 1.4 cm. The S3D ("Laptop") shows consistent performance variability with a standard deviation of about 5.0±0.2 cm across rod distances. At the 600 cm reference distance the data appear to suggest that two FoLD systems (AIS and ZIR devices) support smaller (better) variability in placements at the 600 cm target distance than; however, variability climbs monotonically as the target is moved forward or backward in depth from the 600 cm until they reach levels at or just above the S3D.

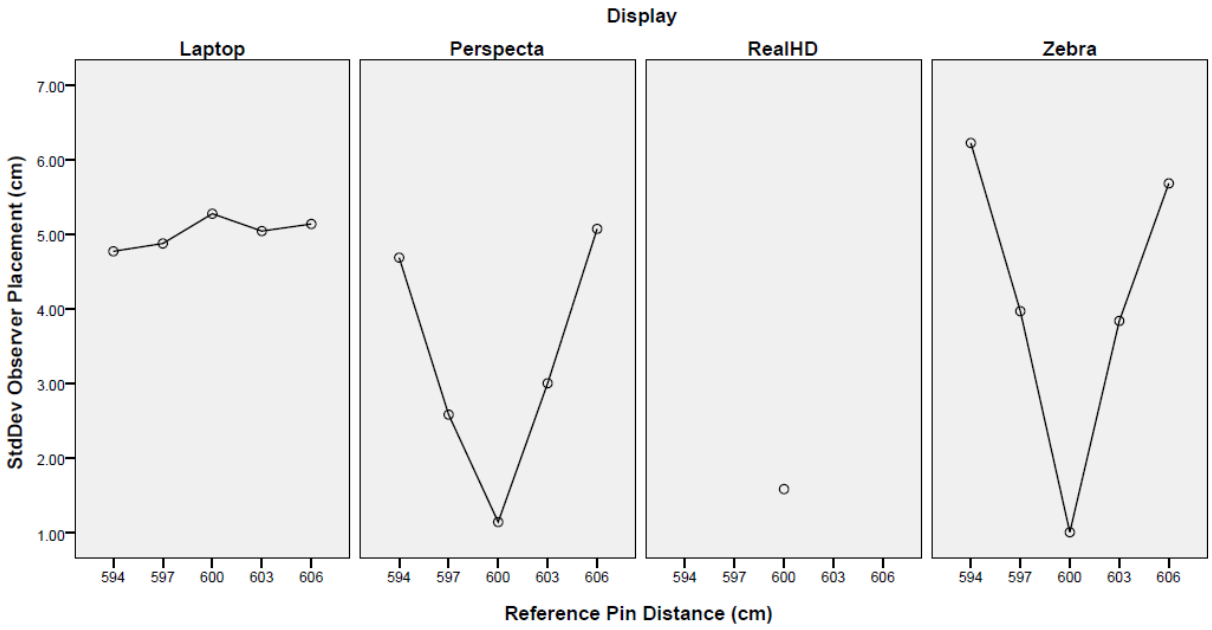

Figure 32. Variability of Placement Performance vs. Reference Distance

4.2.1.2.3 Stereoacuity Threshold Estimates Based on MoA Dataset 1

Stereoacuity threshold estimates, across participants, for each of the four devices (viewing conditions) are tabulated in Table 2. These thresholds were computed as binocular disparity values (in arcsec) from the means and standard deviations (S.D.) of absolute errors in placement performance assuming the average reference rod distance of 600 cm, an average eye separation of 6.3 cm, and crossed disparity relative to the reference rod. The threshold for the "angle of stereoscopic parallax" (ASP, aka stereoacuity threshold) is computed using the binocular disparity equation given by James (1908) and Howard (1919a) later used by Cormack & Fox (1985a): see Figure 3a and Equation 1. Thresholds were computed using both means and standard deviations, as either or both methods are commonly employed in similar evaluations and can be interpreted as accuracy (means) or as precision (standard deviations).

The computed thresholds of 4.74 (means) and 4.47 (S.D.) arcsec or the physical DPA; these values are comparable to commonly observed for experienced viewers with good vision (around 2-10 arcsec (Howard, 1919a; Deyo, 1922; Fielder & Moseley, 1996). The rods were fixed diameter. However, the actual width of the targets in the two rod case has been found to have no effect on depth acuity (Berry, Riggs, and Richards, 1950).

Values for the three electronic displays were two to three times poorer, suggesting that on average, reduced quality depth stimuli were being displayed and/or perceived.

The computed MoA stereoacuity values for the S3D ("Laptop") device were 17.08 and 13.49 arcsec. It is remarkable that the high image quality rendered by the laptop shown in Figure 25 resulted in uniformly poor results compared to the reference device, the physical DPA. Other work using different S3D devices and test conditions have, however, indicated hero results as low as 5-10 arcsec.[4]

The computed stereoacuity of the AIS ("Perspecta") was 9.24 (means) and 12.56 (S.D.) arcsec. The computed stereoacuity of the ZIR ("Zebra") was 12.35 (means) and 15.34 (S.D.) arcsec. However, the visual artifacts inherent these two display systems shown in Figure 26 (AIS) and Figure 27 (ZIR) may have affected these results.

Table 2. MoA Stereoacuity Threshold Estimates

Device Under Test	Stereoacuity Thresholds from Means (arcsec)	Stereoacuity Thresholds from S.D. (arcsec)
S3D ("Laptop")	17.08	13.49
AIS ("Perspecta")	9.24	12.56
DPA ("RealHD")	4.75	4.47
ZIR ("Zebra")	12.35	15.34

[4] *Prior work in our lab—using (a) different S3D devices, (b) a different psychophysical task (QUEST adaptive staircase method with 2AFC; McIntire, Wright, Harrington, Havig, Watamaniuk, and Heft, 2014), (c) high-quality anti-aliasing (e.g., Lloyd, 2012), and (d) different stimuli (three-bar vs. two-bar)—produced stereoacuity thresholds low as 5-10 arcsec.

4.2.2 Dataset 2: Depth Acuity Threshold Measured by Method of Constant Stimuli (MoCS)

The Method of Constant Stimuli (MoCS) two-alternative forced choice (2AFC) judgment for depth acuity threshold measurement using two rods was originally devised by James (1908) and used by Howard (1919a). Howard, and later Deyo, introduced a "Six-Meter Stereoscope" apparatus that was capable of both the MoA as well as the laborious data collection process required for large numbers of subjects using the original MoCS. Deyo (1922) demonstrated that MoA data (taken with the Howard-Deyo DPA devices shown in Figure 6) was as reliable as MoCS data reported by Howard (1919a) taken with Howard DPA device Figures 4.

The MoCS Dataset 2 for the present work was collected for the same test devices and subjects as for the MoA Dataset 1. The intent was to further investigate the location-dependent visual artifacts that seemed to give observers an unintentional cue for matching depth locations on the two FoLD systems. The goal was to ascertain if observers could simply judge which of two stimuli appeared nearer in depth, on each trial using pairs of stimuli at all pairs of the five depth locations (594, 597, 600, 603, and 606 cm) tested in the MoA experiment. In the MoA Dataset 1 experiment, viewers could have, and likely did, utilize the conspicuity and magnitude of visual artifacts to perform an *artifact-matching task* for the two FoLD systems instead of only a *depth-matching task* as originally intended. Instead of using a manually-controlled matching task (MoA), a forced depth discrimination task 2FC was utilized so that display artifacts would be of little or no help in performing the judgments, as the artifacts could appear at either near or far locations with no obvious systematic pattern. Presentation order of stimulus pairs was randomized.

The MoCS Dataset 2, presented in Table 3 and Figure 33, shows that all test devices were capable of producing subject depth discrimination at a level far above chance. However, the correct rates for the S3D (72.6%), AIS (78.8%), and ZIR (70.7%) devices were all significantly less than for the physical DPA (92.1%). The three electronic 3D displays apparently all have significant problems regarding their ability to present high-quality visual depth stimuli.

Table 3. MoCS Performance Averaged Across Subjects for Four Test Devices

Device Under Test	Percent Correct (%) *	*p*-values **
S3D ("Laptop")	72.6	<.0001
AIS ("Perspecta")	78.8	<.0001
DPA ("RealHD")	92.1	<.0001
ZIR ("Zebra")	70.7	<.0001

***** Chance performance is 50% using a 2AFC method for the MoCS.
****** Associated *p*-values significant at a <.01 level.

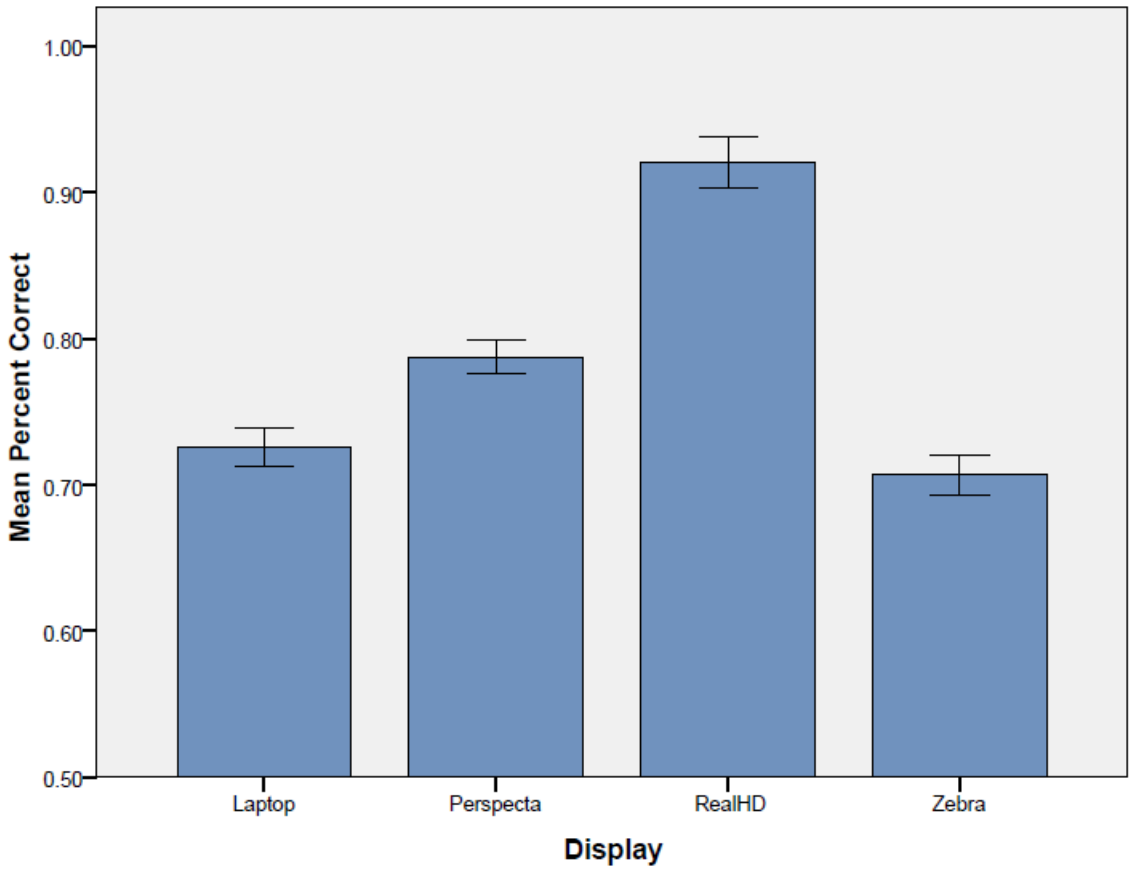

Figure 33. Performance, Averaged Across Viewers, for the S3D ("Laptop"), AIS ("Perspecta"), DPA ("RealHD") and ZIR ("Zebra") Devices Under Test; Error Bars Represent ±1 SEM

Next, we look at how the percent correct rate for each display is modulated by different stimulus separations in depth, and compare these magnitudes to the DPA results. Figure 34 shows that, for the physical DPA ("RealHD"), the smallest stimulus separations of only 3 cm allowed for 85.0% correct discriminations. If the separations were increased to a larger value of 6 cm, giving a larger depth cue, then performance essentially became perfect at 99.2% correct. The only 3D display to even reach values approaching perfect performance was the AIS ("Perspecta"), which required the largest stimulus separations of 12 cm in order to reach 99.2% correct. The stereo S3D ("Laptop") performance maxed out at only 86.7% with 12 cm separations, and the ZIR ("Zebra") maxed out even lower, at only 80.0% correct for the 12 cm separations.

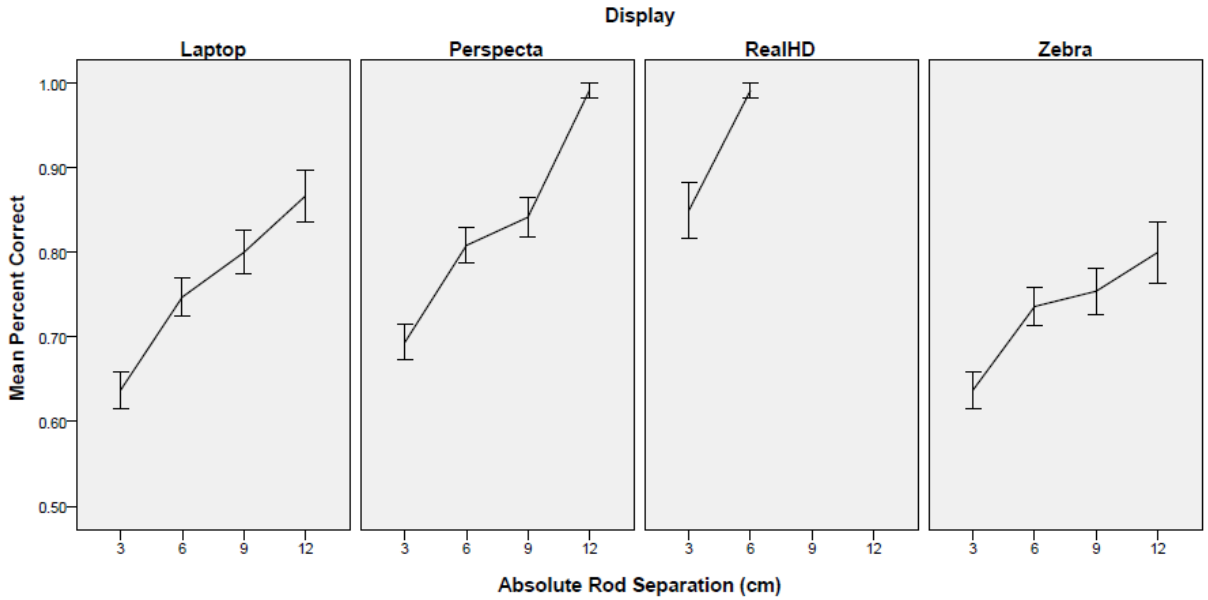

Figure 34. Performance, Averaged Across Viewers, vs. Depth Stimuli Separations for the S3D ("Laptop"), AIS ("Perspecta"), DPA ("RealHD") and ZIR ("Zebra") Devices Under Test; Error Bars Represent ±1 SEM

For the 6 cm separations the mean percentage correct performance was near-perfect on the physical DPA ("RealHD") device, but just 74.7% for the S3D ("Laptop"), 80.8% for the AIS ("Perspecta"), and 73.6% for the ZIR ("Zebra") devices.

For the 3 cm separation (the most difficult discrimination condition), the average performances were DPA (85.0%), S3D (63.8%), AIS (69.4%), and ZIR (63.8%).

Ideally, when using MoCS, percent correct judgments must reach a high-enough magnitude so that a 75% correct threshold (or some selected above-chance level of performance) can be computed, and compared across experimental manipulations. In this case, we wish to compare stereoacuity thresholds across the different display devices relative to the DPA. Unfortunately, all four devices cannot be *directly* compared, because some of the displays have non-overlapping percent correct distributions: the DPA smallest percent correct was 85.0% at 3 cm, but the highest performance for the ZIR device never reached over 80.0% correct at any separation level.

An *indirect estimate* of the threshold magnitudes from MoCS Dataset 2 can be made as indicated graphically in Figure 35, utilizing an 80% correct threshold level. This *indirect* comparison gives the following estimates for stereoacuity thresholds on each of the devices, using the MoCS at an 80% correct level (Table 4), and extrapolating the data for the DPA apparatus:
The solid red line indicates the 80% correct performance threshold. The solid blue lines represent the corresponding thresholds in terms of stimulus magnitudes (with the DPA using an extrapolated intersection with the 80% performance line).

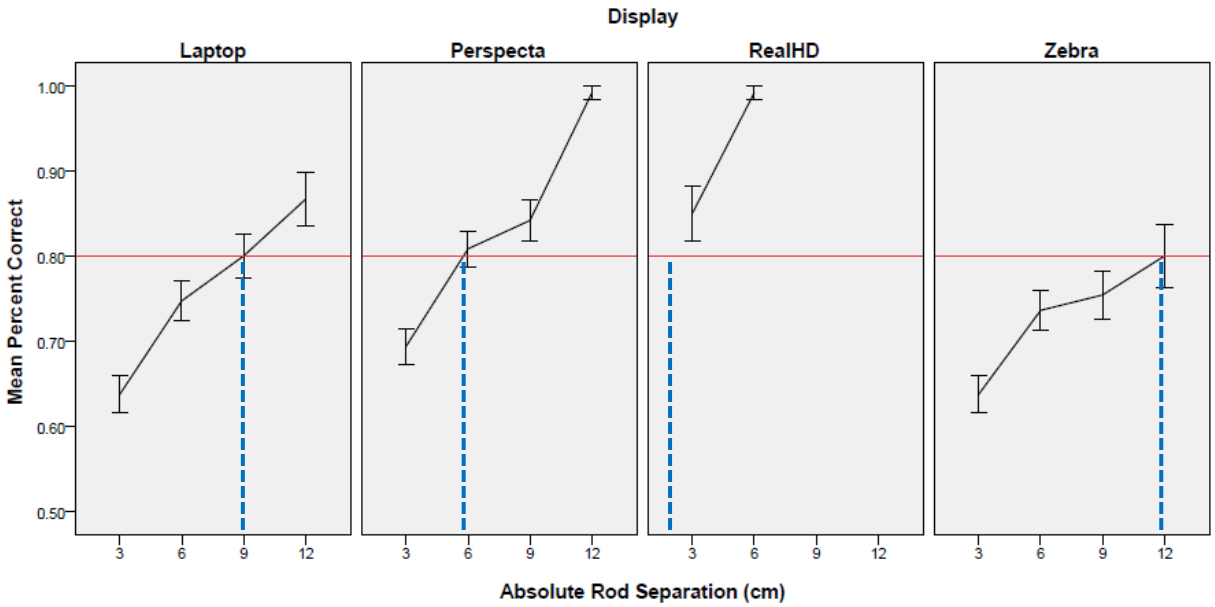

Figure 35. Indirect Estimate of Threshold Magnitudes from Data Plotted in Figure 34: Intersections of 80% Correct Performance (Horizontal Solid Red Line) with Device MoCS Dataset 2 Performance (Vertical Dashed Blue Lines); Error Bars ±1 SEM

Table 4. Estimated Stereoacuity Thresholds Supported by the Four Devices Under Test Computed Assuming an 80.0% Correct Magnitude as Indicated in Figure 35

Device Under Test	Stereoacuity Threshold Estimate (cm)	Stereoacuity Threshold Estimate (arcsec)
S3D (“Laptop”)	9	33.0
AIS (“Perspecta”)	6	21.9
DPA (“RealHD”)	~1.5	5.4
ZIR (“Zebra”)	12	44.2

The data suggest that stereoacuity thresholds were best on the DPA apparatus, of a magnitude we would expect at 5.4 arcsec, indicating high-quality depth perception. Thresholds were considerably worse on all three electronic 3D displays, ranging from 22 to 44 arcsec. These data suggest that all three of the electronic 3D displays supported depth perception at levels four to nine times worse than the DPA.

The results of this MoCS Dataset 2 experiment were generally in accord with the previous MoA Dataset 1 experiment. Interestingly, despite the change in psychophysical methodology, the present data still *appear* to suggest that the two FoLD systems were capable of producing depth stimuli of a quality comparable to the stereo laptop despite their apparently poorer image quality and presence of visual artifacts.

4.2.3 Dataset 3: Depth Acuity Threshold Measurement by MoCS for Monocular Observers. The MoCS 2AFC Dataset 3 was collected for five observers using only one eye to perform the task. The dominant eye was utilized; the non-dominant eye was occluded by an eye-patch. The purpose of this follow-up data collection was to unequivocally confirm or deny whether the two FoLD systems were providing non-stereopsis cues to depth (i.e. location-dependent visual artifacts), and to compare the FoLD systems with the S3D for which high-quality depth cues had been expected. A MoCS 2AFC stereoscopic vision task should theoretically result in performance only at the level of chance (50%) for observers using only one eye. Any deviations from chance levels would indicate the presence of unintentional but systematic monocular cues to depth/location. Similar techniques have been used by Bohr & Read (2013) and Holmes & Fawcett (2005) to control for possible monocular (non-stereo) cues present in standard optometric tests of stereo acuity, with the assumption that if binocular stereoacuity is identical to the "monocular stereoacuity" measure, then the binocular vision status should be clinically rated as "stereo-negative" or stereo-blind.

An early study comparing monocular to binocular performance on the Howard-Deyo DPA illustrated in Figure 6 showed that binocular performance was over six times more accurate (using a MoA technique) than monocular performance (Deyo, 1922).

The data in Table 5 show, somewhat surprisingly, that performance on all four viewing systems was different than chance would predict, when using a 0.05 significance level. These results appear to suggest that non-binocular (monocular) cues to depth exist in all systems. This result was thought to be (a) not possible in the case of the S3D ("Laptop") as all possible monocular cues were thought to be strictly controlled, and (b) unlikely in the case of the DPA ("RealHD") device as the theoretical possibility of horizontal size cues available from the width of the rods as a monocular depth source has been studied (e.g. Howard 1919a, Woodburne, 1934). The use of a more-conservative alpha value of 0.01 produces results that suggest that only the two FoLD systems were providing for greater-than-chance performance. Thus, the 0.01 significance level implies the FoLD systems (AIS, ZIR, but not the S3D nor the DPA apparatus, were providing non-stereoscopic but depth-related information to viewers which improved their performance above chance, perhaps because of the visual artifact cues, which are visible monocularly and whose presence and magnitude scales in depth.

Table 5. Performance across Five Subjects when Devices Were Viewed Monocularly.*

Device Under Test	Monocular Percent Correct (%)	Sample size (total trials)	*p*-values
S3D ("Laptop")	48.8	1000	.031**
AIS ("Perspecta")	55.0	1000	.003***
DPA ("RealHD")	55.5	200	.017**
ZIR ("Zebra")	54.4	1000	.005***

***** Chance performance is 50% using a 2AFC method for the MoCS.
****** Associated *p*-values significant at a <.05 level.
******* Associated *p*-values significant at a <.01 level.

While monocular performance on the AIS ("Perspecta") and ZIR ("Zebra") were significantly above chance at 55.0% and 54.4%, respectively, these were not alarmingly high percent correct values. When the same task was performed binocularly, percent correct values tended to be a bit higher using both systems (78.8% and 70.7%, respectively). This suggests that these systems were at least providing *some* stereoscopic depth cues which helped performance over the monocular condition, but only of a smaller relative magnitude than some of the previous analyses (Deyo, 1922) had documented. The binocular-to-monocular advantage for the S3D ("Laptop") and the volumetric AIS ("Perspecta") were the same on average, giving +23.8% improvements in percent correct judgments, while the binocular advantage for the ZIR ("Zebra") was only a +16.3% improvement. In contrast, the binocular improvement for the physical DPA ("RealHD") was considerably larger at +36.6%, suggesting that all three 3D devices were incapable of producing high quality *binocular* cues to depth using a virtual James task, when compared to viewing the real apparatus.

Table 6. Performance across Subjects: Binocular vs. Monocular

Device Under Test	Binocular Percent Correct (%)	Monocular Percent Correct (%)		Binocular Advantage (% difference)
S3D ("Laptop")	72.6	48.8		+23.8
AIS ("Perspecta")	78.8	55.0		+23.8
DPA ("RealHD")	92.1	55.5		+36.6
ZIR ("Zebra")	70.7	54.4		+16.3

An examination of the monocular percent correct performance as a function of reference pin position, a different story emerges. Figure 36 shows the performance data plotted in this manner. The DPA, with only one reference pin position at 600 cm, shows monocular performance at about chance level (the solid red line), which is a straightforward finding. The S3D ("Laptop") supported performance roughly at chance across all reference rod locations, with a flat performance line as would be expected. However, percent correct performance for the two FoLD systems was approximately linear, but far from flat, and systematic biases in responses are obvious. Both FoLD systems resulted in a strange performance pattern: when a reference rod was located at the nearest positions, participants almost always guessed incorrectly; when a reference rod was located at the central position, performance was at chance; and when a reference rod was located at the farther positions, performance climbed dramatically and became almost perfect. This provides further confirmation, importantly, that systematic monocular cues to depth locations were present in the FoLD systems, which biased performance (above or below chance) whenever the reference pin was located off the central depth position of the displays.

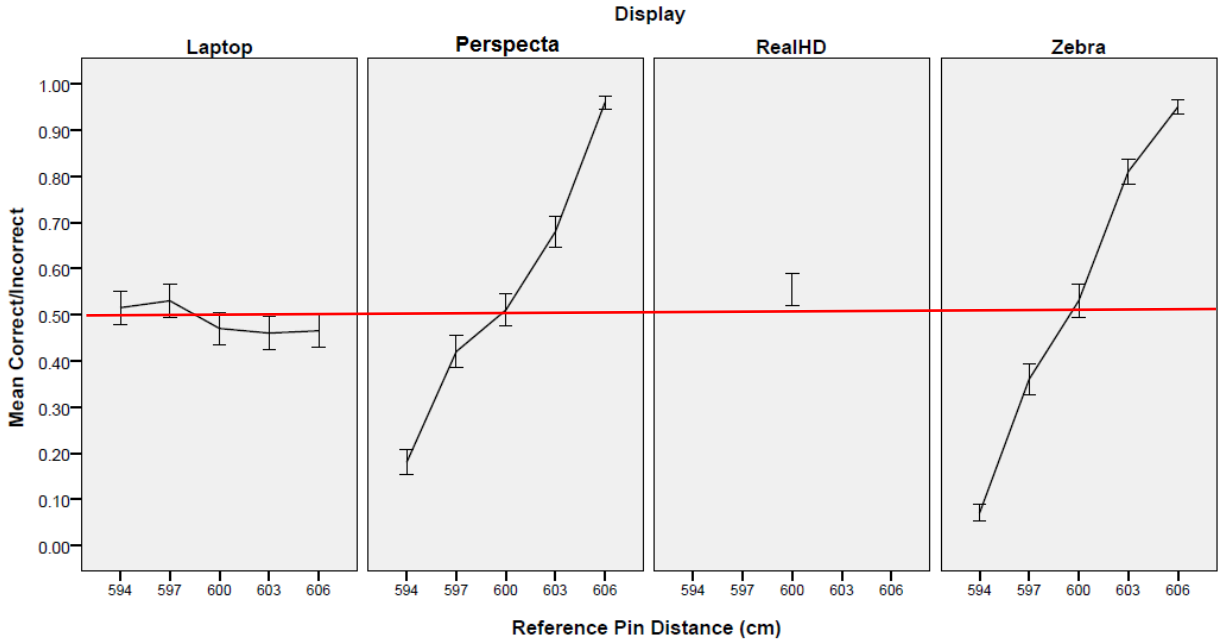

Figure 36. Performance vs. Reference Pin Location; Error Bars Represent ±1 SEM.

This pattern would manifest if observers had adopted a decision strategy like: "If the reference pin is blurrier and/or dimmer than the other pin, it must be farther away." This would result in very high accuracy when the reference pin was farther away, and very poor accuracy when the pin was near (because the blur and dimming effects occur at both near and far locations relative to the center position). Thus, this almost "perfectly-wrong" combined with almost "perfectly right" performance pattern likely resulted from mis-perceptions in the depth locations due to the location-dependent, monocular visual artifacts in these systems, as described earlier. These intriguing results explain why performance on the FoLD systems could be both noticeably better (and simultaneously worse) than chance would predict when performing a binocular depth discrimination task with only one eye.

If one next examines the binocular advantage of each display system across comparison pin locations (with reference pin always fixed at 600 cm, n=200 per display), the results again confirm that the two FoLD systems were causing systematic near/far confusions (see Table 7; data shown graphically in Figure 37). The confusions seem to be resulting in extremely large binocular advantages for near comparison pin locations, which are just too good to be true (beating out the DPA for some distances). The converse was true for far pin locations, for both FoLD systems, resulting in huge binocular *disadvantages*!

Table 7 shows performance across subjects and for each comparison pin distance (reference pin fixed at 600 cm). Sample size for each display is 200 trials; for each distance is 50 trials. Average binocular performance is compared to monocular performance, and the binocular-to-monocular advantages are provided.

Table 7. Average Binocular vs. Monocular Performance

Device Under Test	Comparison Pin Distance (cm)	Monocular Percent Correct	Binocular Percent Correct	Binocular Advantage (%)	Average Binocular Advantage
S3D ("Laptop")	594	40	68	**+28**	**+21.3%**
	597	52	52	**0**	
	603	52	70	**+18**	
	606	44	83	**+39**	
AIS ("Perspecta")	594	2	68	**+66**	**+18.5%**
	597	14	58	**+44**	
	603	92	70	**-22**	
	606	96	82	**-14**	
DPA ("RealHD")	594	58	100	**+42**	**+36.5%**
	597	62	83	**+21**	
	603	56	87	**+31**	
	606	46	98	**+52**	
ZIR ("Zebra)	594	5	72	**+67**	**+16.0%**
	597	10	73	**+63**	
	603	86	53	**-33**	
	606	96	63	**-33**	

Collapsing the average binocular advantages across pin locations gives a more general comparison of the displays (rightmost column in Table 7), with the data confirming initial, intuitive suspicions: the DPA gave the largest binocular advantage of +36.5%, followed by the S3D ("Laptop") at +21.3%. Poorer still were the two FoLD systems, with the AIS ("Perspecta") volumetric device at +18.5% just besting the ZIR ("Zebra") holographic display at +16.0%.

In Figure 37 the solid performance line indicates binocular performance on the 2AFC task; the dashed line indicates corresponding monocular performance on the same task. Regions of positive binocular advantage are shaded green; regions of binocular disadvantage (negative) are shaded red. Notice that, for monocular viewing, the AIS ("Perspecta") and ZIR ("Zebra") devices were biasing performance across pin positions, sometimes helping but sometimes hurting performance, which is likely due to the unique FoLD system artifacts such as blur and/or dimming being interpreted as depth cues for far distance.

This analysis confirms: (a) that the physical DPA ("RealHD") provides the highest quality binocular depth cues for determining pin positions; (b) that the S3D ("Laptop") was providing high quality binocular disparity cues to depth, which were not apparent in previous analyses; and (c) that the two FoLD systems provided for *some* binocular cues, with positive overall binocular-over-monocular advantages, but the quality of such cues appears to have been degraded relative to the S3D ("Laptop") and severely degraded relative to the physical DPA ("RealHD").

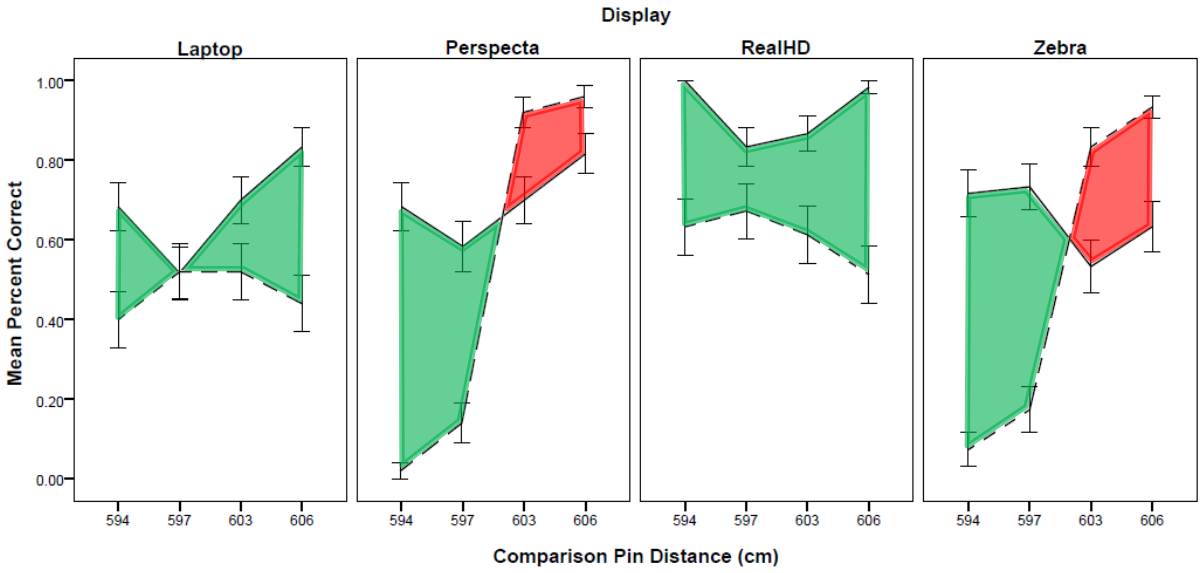

Figure 37. Performance, Averaged Across Viewers, vs. Comparison Bar Location for Reference Bar Fixed at 600 cm; Error Bars Represent ±1 SEM

Howard tried 10 men and found that the depth difference threshold varied from an average of 13 mm with both eyes open to over 285 mm when only one eye was open (Howard, 1919 TAOS, p. 234).

4.3 Effects of Rod Lighting Model Used to Render Rod Images for View on Devices

4.3.1 Unexpectedly High Stereoacuity Thresholds Observed for S3D ("Laptop") Device

Throughout the human subject data collection and analysis the comparatively poor stereoacuity thresholds supported by the S3D ("Laptop") device vs. those observed with the FoLD systems, was difficult to understand. The mean stereoacuity threshold on the S3D ("Laptop") device was measured at 17.1 arcsec by MoA and 33.0 arcsec by MoCS. These are not terrible stereoacuity values, but they are not excellent, and this was confusing/frustrating for several reasons.

First, stereoacuity thresholds measured for other S3D displays (in this and other labs) have consistently been lower (as low 5-10 arcsec), which is comparable to the lowest (best) stereoacuity thresholds (for physical DPA devices) of 2 or 3 arcsec (Howard, 1919a) (Fielder & Moseley, 1996). The mean stereoacuity threshold obtained with the physical Howard-DPA device ("RealHD") used in the present study was 4.8 arcsec by MoA and 5.4 arcsec by MoCS.

Second, the observed stereoacuities for the S3D ("Laptop") device were similar in magnitude to those for the two FoLD systems, which ranged from 9.2 arcsec by MoA for the AIS ("Perspecta") device to 44.2 arcsec by MoCS for the ZIR ("Zebra") device.

Third, the S3D ("Laptop") had image quality superior to that of either FoLD system. The observation of comparable stereoacuity thresholds was, thus, surprising and puzzling. Part of the explanation probably lies in the FoLD systems providing for monocular depth information due to their location-dependent visual artifacts. Attempts to control for differential image quality and for monocular clues were undertaken in the collection and analysis of MoCS Dataset 2 and MoCS Dataset 3; however, these attempts were only partially successful. The MoCS Dataset 3 study showed that, assuming a conservative alpha value, monocular depth cues impacted results obtained for FoLD systems, but not for the S3D ("Laptop") or physical DPA ("RealHD"). In addition, the third study showed that when the reference pin was held at a constant position, the magnitude of the binocular-to-monocular advantage was +21.3% for the S3D ("Laptop") device compared to +18.5% for the AIS ("Perspecta") and +16.0% for the ZIR ("Zebra"). Yet another notable advantage of the S3D ("Laptop"), demonstrated in the analyses of all three datasets, was that it did not suffer the problematic near-to-far perceptual confusions elicited by the FoLD systems.

Although the presence of visual artifacts in the FoLD systems might help explain their surprisingly decent stereoacuity values, it does not seem to explain the relatively poor values obtained on the S3D ("Laptop") device. This result may have been due to the nature of the visual stimuli used in our studies. Specifically, in the conceptual lighting model of the virtual rods, the virtual light source was coming from a point source directly in front of the rods (i.e from the direction of the viewer).

The use of *front-lit white rods* lit from a single point source displayed *against an empty black background* in the present work resulted in rendered images of rods "reflecting" most intensely from their centers towards the viewer, with a prominent luminance degradation moving laterally off the center of the vertical rods, going gradually from bright white, to grey, to greyer, to black

as shown for the S3D ("Laptop") stimulus pictured in Figure 38. The pixel structure of the display is visible. As can be seen, the fading from brightest to darkest at the left and right edges of the stimuli spans several pixels in width, potentially creating sub-optimal stimuli for stereoacuity threshold measurements. Additionally, thresholds are generally best when tested with image content possessing high spatial frequencies and sharp contours. However, in the present work the automatic anti-aliasing employed by the NVidia software was turned on and, although the exact specifications of the anti-aliasing function are unclear, may have "blurred" any sharp edges even further.

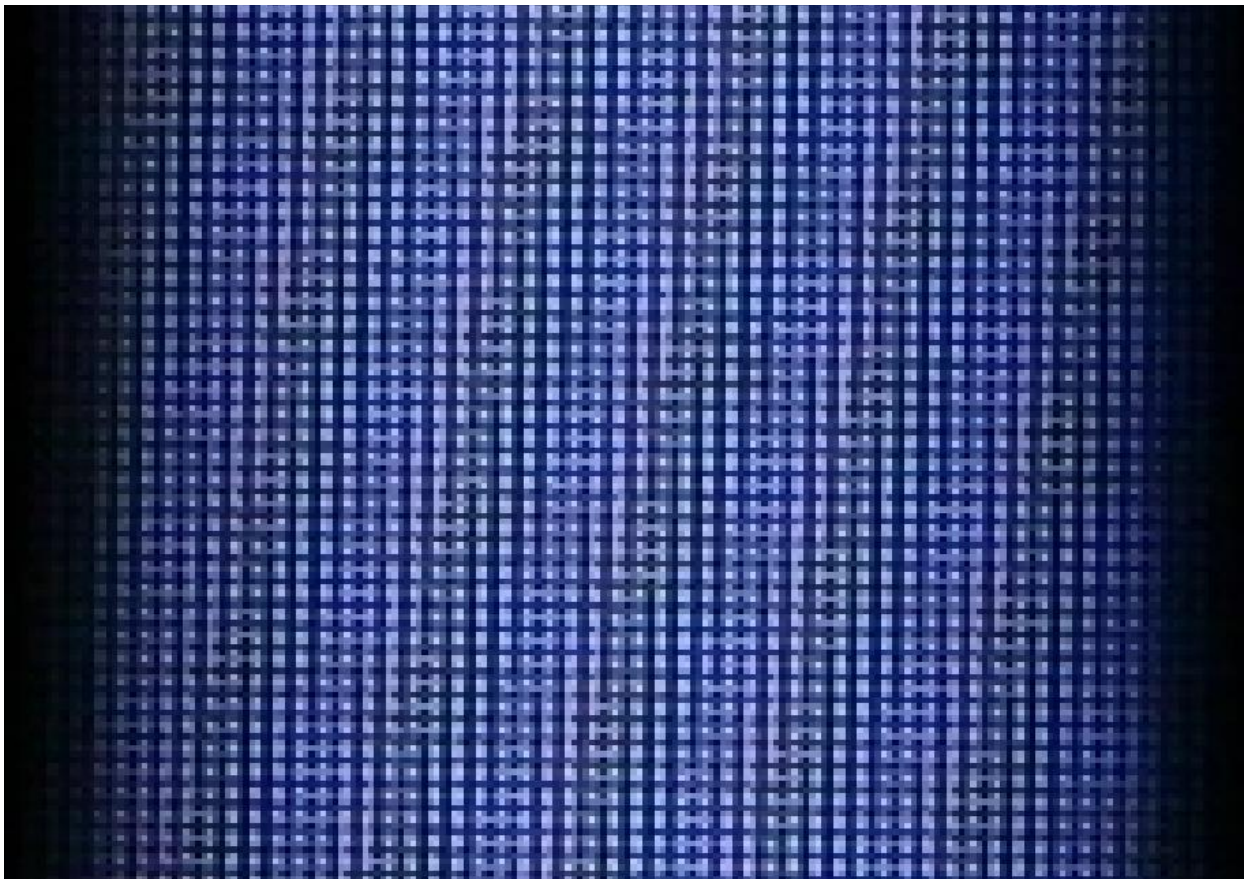

Figure 38. Close-up Photographic of Front-Lit Rod Stimulus Displayed on S3D ("Laptop")

These issues may have resulted in degradations of the crisp, sharp, high-contrast edges that the visual system needs to perform extremely precise stereoscopic localization. For instance, Patterson (2009, p. 992) notes that "fine sensitivity to small disparity differences require a high spatial frequency (fine details in an image)."

4.3.2 Follow-Up Data Collection with Lighting Model Changes

To test whether the front lighting model might have been inadvertently "blurring" the stimulus edges too much in the S3D ("Laptop") device (reducing the sharp, high spatial frequency countours), an abbreviated *follow-up data collection* was accomplished with one experienced subject with excellent stereovision. In this follow-up collection the *rod/background polarity was changed so that there were now black rods with crisp edges -- and with no grey gradations -- against a solid bright white background.* Some 40 trials were collected in this reversed polarity condition by MoA and compared to the average absolute value threshold for the same observer in the 60 trials from the MoA Dataset 1 experiment.

The stereoacuity threshold for this single observer improved dramatically, dropping nearly in half from 3.83 cm (13.7 arcsec) to 2.26 cm (8.1 arcsec), which is in line with previous experience with S3D devices.

These complicating issues are described along with a description of how they were dealt with in the present work so that lessons learned can be taken into account to control or avoid such problems in future work.

4.3.3 Lighting Approaches in Seminal Stereoacuity Research with Physical DPA Devices

It is noted that the earliest stereoacuity measurements with physical DPA devices using two vertical rods involved two white rods *lit uniformly from all subject-viewable directions* against a black velvet-covered background (James 1907, James 1908). The present electronically stimulated white rods were lit from a single modeled point source for the collection of Datasets 1, 2 and 3, which resulted in the non-uniform appearance shown in Figure 38 and in the ill-defined edges. If front-lit models of white rods are used in future depth perception research on S3D or FoLD systems (Datasets 1, 2, 3 in the present work summarized in subsection 4.3.1), care should be taken that the lighting model involve uniform illumination of the subject-side of the rods rather than a point source.

Howard (1919a) reversed the colors in his version of the James apparatus: two black rods back-lit uniformly and indirectly backlit by light reflected off a white cardboard background. The back was the only white interior surface; all other interior surfaces were painted dead black. Howard found 14 of 106 observers examined possessed an average stereoacuity threshold of 1.9 ± 0.1 arcsec (Howard, 1919a TAOS, p. 214). Howard further concluded that normal judgement of distance was ≤ 8.0 arcsec (the stereoacuity depth equivalent of 20/20 Snellen lateral acuity). The present follow-up data collection (summarized in subsection 4.3.2) is an electronic version of the Howard lighting approach.

4.4 Computer-Rendered Images Issues for the Electronic James Depth Acuity Test

The original concept of this effort was to recreate the James depth acuity test in electronic form. However, each electronic display device used in the present work encountered unique difficulties in replicating the physical DPA presentation of the two-bar stimuli. The inability to find a single virtual model that could be used across all electronic displays (three pictured in Figure 39 along with the AFRL-modified Howard DPA (Howard 1919b) was initially frustrating. The James rods used in the Howard and Howard-Deyo DPAs (Howard 1919a, 1919b; Deyo 1922) are an extremely simple research stimulus. An inability to generate easily comparable virtual rods across electronic displays suggests that cross-category display experiments using more subtle, elaborate or generalizable stimuli will be challenging.

Optimal rod appearance was dependent on the unique characteristics of each display.

The Howard DPA (Howard, 1919a, 1919b) used black rods uniformly back-lit (no side of front lighting whatsoever). However, the black rods in the AFRL-modified Howard DPA (Howard, 1919b) were sandwiched between two long fluorescent tubes so that the sides of the rods received greater illumination than the front, creating a subtle, darker in the middle, brightness change across the width of the rod. Illumination also varied with the position of the moveable rod, but the variation was deemed too small to serve as a cue to rod position. The viewing window was effective at reducing all other monocular depth cues with the possible exception of rod width (which has been discounted in prior works) and small motion parallax cues (which Howard had eliminated by use of a chin-mount). Monocular performance on the AFRL-modified Howard DPA (Howard, 1919b) was shown to be at chance level on a 2AFC near/far depth judgment, confirming the absence of monocular cues.

Automation of the Howard DPA system enabled commonality with the electronic displays on several experimental design variables to include: subject input device, trial and intra-trial duration, and psychophysical measurement method. The lack of flexibility in lighting conditions, rod reflectance and illumination non-uniformities, and background reflectance made it difficult to compare the performance of the physical AFRL-modified Howard DPA (Howard, 1919b) against electronic displays that could not replicate the physical fixed luminance relationships used in the seminal works (James, 1908) (Howard, 1919a, 1919b) (Deyo, 1922).

The S3D ("Laptop") device had good luminance, contrast, and resolution and could satisfactorily produce a wide variety of rod presentations including: black rods against a white background, white rods against a black background and every rod/background contrast in-between. In addition, the large gray scale supported a wide variety of virtual lighting presentations, enabling subtle highlighting and great flexibility in optimizing the surface appearance of the rods. Replicating the box and window of either the James DPA or the Howard DPA was more difficult.

The physical AFRL-modified Howard DPA has a flat, uniform black appearance to the front face of the box with a uniform white interior. Unfortunately, in stereo displays, uniform surface appearance produces ambiguous binocular disparity cues; without the addition of significant

surface texture, the appearance of the virtual box was unstable in depth. Thus, all S3D displays rely on a false depth cue (texture) to evoke a perception of depth. However, ultimately it was concluded that all of the electronic displays had difficulty replicating the surrounding box face and it was eventually dropped from all electronic stimulus presentations, leaving only the virtual rods.

One of the critical functions of the window on the front of the physical DPA is to eliminate vertical size as a depth cue. In the S3D device, the vertical size of the rods should not be a problem, as size is easily held constant in rod image rendering. Nevertheless, when a subject views the rods stereoscopically, changing the disparity of the rod image changes the both the perceived depth location and the perceived size (i.e., size-disparity perceptual scaling was a potential issue). The variable size perception is substantial and researchers may feel inclined to correct the perception by introducing a vertical scaling factor to counter the perceived change in size induced by changing disparity. This inclination should generally be ignored for S3D devices as it introduces a large monocular cue to depth. These effects are a potential issue for computer rendered stimuli for FoLD devices, but they were long ago ruled out in as important factors in the use of well-designed physical DPA devices.

Discrete sampling of continuous vector models creates challenges for using S3D devices in psychophysical measurements. At current display resolutions and typical viewing distances it is arguable whether a stereo display can be considered to produce a continuous image. It is commonly, but mistakenly, assumed that a display with a pixel pitch of less than 1 arcmin (60 arcsec) is "eye–limited" and, therefore, produces a perceptually continuous image. In reality, the hyperacuity threshold is 5 arcsec. Stereoacuity measured on physical DPA devices has been routinely measured at 2 to 6 arcsec. However, producing a 2 to 6 arcsec pixel pitch display for psychophysical measurements is not possible and typically is not necessary. Anti-aliasing allows a manipulation of relative pixel luminance between stereo pixel pairs. This luminance shift has been demonstrated to support sub-pixel stereoacuity measurements (Lloyd, 2012).

Unfortunately, enabling anti-aliasing introduces ambiguity into the description of the stimulus. In many instances the anti-aliasing algorithm used by a particular S3D device is proprietary and unknown. It is also unreasonable to expect display calibration to be routinely conducted at the single pixel level. But in psychophysical measurements a rigorous description of the stimulus is considered essential to the experimental process. Until a calibration process is established for anti-aliasing, researchers will be left with the choice of accepting some ambiguity in describing or controlling the stimulus, or left with limiting the stimulus presentation to undesirably coarse single-pixel steps. These coarse steps, if not identified and managed appropriately, can cause difficulty in interpreting results. For example, in the MoCS psychophysical method, if a researcher picked two disparity levels from the virtual model that were unknowingly binned to the same pixel disparity by the computer driving the S3D device, the resulting cumulative distribution function would inappropriately appear to plateau or possibly reverse. Picking a constant-stimuli interval larger than the largest pixel step of an S3D device should avoid this problem.

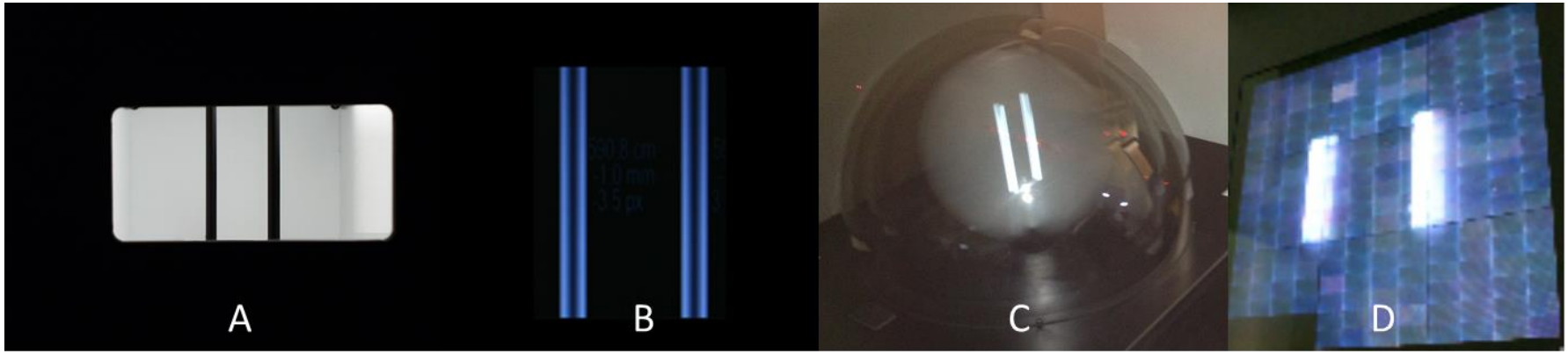

Figure 39. Close-up of Sample Images (Stimuli Viewed by Subjects at 6m) on (A) Physical Depth Perception Apparatus (DPA), (B) Active-Eyewear Stereo 3D - Samsung 22-in. Notebook Display with NVIDIA Active-Eyewear (aeS3D), (C) Actuality Rotating-Screen Integral-Slice Actuality Integral Slice (AIS) Perspecta Volumetric Display (ARS), and (D) Zebra Integral-Ray Hogel-Based Zscape Motion Display (ZIR)

After the James Test was implemented and calibrated on the S3D device, pre-experimental trials were run to explore the range of half-image pixel shifts that could be reasonably investigated using the procedure. The empty background field allowed for binocular fusion of very large pixel shifts, but at large rod half image shifts, it was noticed that the perceived depths no longer matched the predictions from the binocular disparity equations. One potential explanation for the poor correlation between predicted and perceived depth is the weakness of vergence eye movements in producing depth cues, compounded by incongruous head motion parallax, size and focus cues unchanging with vergence changes, etc. Small half image shifts can be easily seen and processed into accurate relative depth cues by the visual system but large shifts require vergence eye movements to maintain binocularity. The binocular disparity equations assume that the vergence distance is known, but vergence eye movements are weak depth cues and are ineffective in determining distance without reinforcement by monocular depth cues (Howard, I., 2008) (Mon-Williams et al., 2000). Of course the James DPA (and all incarnations since) was intentionally designed to minimize monocular depth cues (James, 1908). The inadequacy of eye vergence to support accurate depth perception is also aggravated by the inability of S3D devices to produce appropriate head motion parallax cues, a strong depth cue (Ichikawa and Saida, 1996). The larger the pixel shift presented on the display, the worse the conflict between disparity and head motion parallax cues.

S3D displays can accurately produce relative object motion parallax (just not viewer-to-object parallax without head/eye tracking). Therefore, it is essential to maintain the correct virtual camera/model and subject/display viewing geometries or else the horizontal separation between the two rods will vary with depth, creating a strong monocular depth cue. This viewing geometry sensitivity is largely ignored in the entertainment industry and may not be appreciated by researchers using electronic displays as an inexpensive tool to generat experimental stimuli.

The AIS swept volume display could not produce occlusive surfaces and consequently it was unable to display a dark rod against a white background. For the same reason, it was unable to reproduce the occlusive features of the physical DPA box and window. However, a physical window roughly analogous to the windows used in the DPA might be utilized if desired. The loss of the window results in an inability to control for vertical size cues. In a swept volume display the rod image physically moves in depth and therefore the monocular angular subtense of the rod in the visual field changes. Other monocular cues, such as head motion and object motion parallax depth cues are present in the AIS (“Perspecta”) device and need to be considered in the experimental design. The inability to produce occlusive surfaces creates novel options for rod appearance. In addition to the normal lighting options provided in the virtual model, the rod can be presented with a white surface and a hollow (dark) center or a filled in (bright) center. When viewed perpendicular to the rods axis, the luminance of the hollow rod appeared fairly uniform whereas the filled rod appeared was slightly brighter in the center and dropping off gradually towards the edge. Even after calibration, the AIS swept volume display has some residual non- uniformity in the viewing volume, and had an uncorrectable difference in brightness as the function of radial distance from the axis of rotation. Thus, change in luminance became a strong, but confusable depth cue. In the AIS, curvature and spinning screen motions, along with the variable reflections in the two concentric domes around the screen, created artifacts that also caused variable contrast as bars were moved fore or aft of the spin axis.

The ZMD ("Zebra") device is a very early proof-of-concept demonstration of a light-field display and as such it was assumed that implementing the James test on it would be difficult. For example the ZMD image quality varies with depth: the further the stimulus is presented from the display surface (as defined by the pixel layer) the blurrier images get. Consequently, blur became a strong cue to rod location in depth. This was mitigated to some extent in the present work by using a rod lighting model that resulted in a bright center but dim edge appearance to the rod. In effect, the lighting model mimicked the line spread function appearance for a poorly focused line.

The blur also impeded the ability to recreate the visual appearance of the physical DPA box. Light-field displays are similar to swept-volume displays in that a change in object distance results in a change in angular size of the retinal image, which is a very strong monocular depth cue. Unlike swept-volume, light-field displays support occlusion and theoretically the box and window approach to dealing with vertical size variations should apply. Unfortunately in the ZMD version of the light-field display, the window was so blurred that it interfered with the rod appearance and could not be used.

The inability of the FoLD systems (AIS, ZIR) to maintain contrast as the bars moved in depth limited the James stimulus presentation to white bars against a black background configuration. In the ZIR, some of the lost contrast is due to hogel lens glow. When presenting a black rod against a white background the light beam bundle (coming from pixels dispersed across several hogels) through the rod position to the eye should be very low. However, to support head motion parallax, that specific hogel must also contributes to the white background image for a very large number of alternative viewing positions. Consequently a large percentage of the 5776 potential beams generated by each hogel are illuminated. Each of these beams produces a small reflection off every optical surface it crosses in the hogel micro-lens system. The cumulative effect of the very large number of small reflections is that the hogel lens starts to glow, washing out the desired dark appearance of the rod.

Arguably the most interesting activity conducted with the ZMD in this effort was the calibration in depth. The ability to refocus display images at different depths confirms that the ZMD hogel array is producing a legitimate lightfield when viewed with a 50mm diameter aperture. In addition, the bivariate data is compatible with a wide variety of analyses. For example, a multiple regression analysis could determine whether linear or curvilinear function is a better fit to the data. In the data shown in Figure 19, adding a Command Position squared term to the regression equation raises R^2 to 0.963 with the squared term being significant at $P < 0.001$, suggesting the ZMD depth response is not entirely linear. Another potential approach for quantifying the quality of the light field would be reduce the aperture of the focusing lens until the regression curve slope is no longer distinguishable from zero.

5.0 CONCLUSIONS AND RECOMMENDATIONS

5.1 Conclusions

The report documents an initial effort to develop a quantitative metric for the perception of depth on electronic 3D displays at 6m. The metric is based on a test and physical depth perception apparatus (DPA) invented by James (1907, 1908), an ophthalmologist working in the UK. The James test and physical apparatus were subsequently used and advanced by other research ophthalmologists in The Netherlands (Schoüte 1910) and the U.S. (Howard 1919a, 1919b), and by a research psychologist in the U.S. (Deyo 1922). The 6m viewing distance was chosen to enable correlation of depth acuity to lateral acuity per Snellen (1862).

The James test (James 1908) was selected as the basis for the assessment depth perception of computer-generated (i.e. virtual) imagery on various electronic 3D displays. The foundations for an electronic James (eJ) test and methodology were established.

The Howard Six Meter Stereoscope (Howard 1919b) enabled the use of two measurement approaches: MoCS and MoA. A variant of this apparatus developed at 711 HPW/USAFSAM was automated at 711 HPW/RHCV for use as the reference device in the present work. This device served well as a reference in the present work, but the interior lighting scheme (black rods lit from front, back and sides) was found to be inferior to that of Howard DPA (black rods lit from behind only).

Three electronic 3D displays were tested and compared to this AFRL-modified Howard DPA. Two types of full-parallax prototype systems in the AFRL 711 HPW/RHCV Visualization Laboratory were among the devices under test (DUT): the Actuality Integral Slice (AIS) Perspecta spinning screen volumetric; and the Zebra hogel-based Zspace Integral Ray (ZIR). For comparison, one type of stereo 3D (S3D) device (an active eyewear laptop) was included. The AIS and ZIR are examples of two types within a display class (full parallax) that are herein called Field of Light Displays (FoLD). These FoLD systems (AIS, ZIR) were engineering prototypes, not commercial products, and both had significant visual artifacts. The S3D device also had image rendering limitations. All three electronic displays require engineering and software improvements before they can support high quality depth perception measurements. The choice of rod color (white), background color (black), and lighting direction (front side) is the same as used by James (1907, 1908); this choice was forced by the image stimuli rendering and display limitations of the AIS, ZIR, and S3D devices. And the viewing window used in all physical DPA devices was not included in the electronic stimuli for the same reasons. These engineering artifacts and rendering issues (a) impacted the design of electronically generated images that were perceptually comparable to the two-bar stimuli viewed in the DPA and (b) significantly degraded stereoacuity threshold measurements relative to the physical DPA.

During this project it was determined that the seminal work by Howard (1919a, 1919b, 1919c, 1919d, 1920a, 1920b, 1920c) was performed at the Medical Research Laboratory (MRL), Hazelhurst Field, Minneola NY (established in 1918), which is the initial version of the represent day AFRL Airmen Systems Directorate (USAF AFMC 711 HPW/RH, WPAFB OH). And the work performed by Deyo (1922) and Tefft et al. (1922, 1923) was performed at MRL and the co-located School for Flight Surgeons (SFS), the initial version of the present day USAF School of Aerospace Medicine (711 HPW/USAFSAM). That is, the authors of this report are the heirs of seminal research on the topic of depth perception. All original literature from the work performed from 1918-1925 at Hazelhurst Field was found at archival library files now located at WPAFB OH. A thorough examination of this literature showed that all literature references to a so-called "Howard-Dolman" DPA should have been to the "Howard-Deyo" apparatus.

The Howard-Deyo DPA (pictured in Figure 6) is a hybrid of the James (1907, 1908) DPA pictured in Figure 3b and the Howard (1919b) Six Meter Stereoscope illustrated in Figure 5. The Howard-Deyo DPA was *not* used in the present work.

The developmental effort, described in this report, was an attempt to apply a very simple psychophysical measurement to a variety of electronic 3D display devices in an effort to start exploring the relationship between the perception of depth and physical characteristics of the displays. Despite the simplicity of the psychophysical measurement chosen, the developmental effort immediately ran into difficulty due to the unique characteristics and limitations of each display device. No common stimulus configuration could be found that was suitable for all display types. This was initially disappointing in that the failure to create similar imagery on each display limits the ability to conduct cross display category comparisons. Ultimately, working with the unique characteristics of each display was extremely informative in regard to their current level of maturity and their theoretical potential.

Previously 3D displays have either been thought of as an entertainment device where the depth dimension is either (a) something to be manipulated by artist for content creation or (b) an information device assumed to be accurate and helpful. If an individual had difficulty extracting high quality depth information from the display it was often assumed to be a problem with the observer, not a limitation of the device; but, as the understanding of 3D displays improves, this assumption is not sustainable. The inevitable expansion of 3D display options from stereo to include holographic, volumetric, and other light-field displays, will eventually require methods for measuring the quality of a 3D display performance on their defining characteristic, depth. Developing these methods will be a challenge, as depth, in at least some of these displays, will exist only as a perception similar to brightness and color.

5.2 Recommendations

A virtual, electronic James (eJ) test was successfully demonstrated on each display type and is available for use in with-in category display comparisons.

It is recommended higher quality FoLD devices be created and the electronic James (eJ) test be further developed to guide research and, eventually, quality control in products.

All references to "Howard-Dolman" should be corrected to read "Howard-Deyo."

The automation of subject testing in this effort expedited data collection and should be used. Prior work with manual testing and data recording can be speed up dramatically using either the MoCS or MoA approaches. Research reported after the 1907-1922 period has avoided frequent use of the MoCS approach due to its labor-intensive nature for subject testing; with automated testing and data collection the MoCS approach is even faster to administer than the MoA.

In the past, psychophysical measurements have been very successfully in tying perceptions to physical measures. For example, the perception of brightness is linked to the physical measure of luminance, and color is linked to chromaticity. A similar measure of depth needs to be matured for electronic 3D displays.

6.0 REFERENCES

(Andersen and Weymouth, 1923)
Andersen, Emelie E. and Weymouth, Franck W., "VISUAL PERCEPTION AND THE RETINAL MOSAIC. I. Retinal Mean Local Sign—an Explaination of the Fineness of Binocular Perception of Distance," Am J Physiology **64** (3), 561-594 (1923).

(Bauer, 1926)
Bauer, Louis Hopewell (A.B., M.D., Major, Medical Corps, USA, Commandant, The School of Aviation Medicine), **Aviation Medicine**, 1st Edition (The Williams & Wilkins Company, Baltimore, 1926). The object of this work is a handbook for those interested in the subject. The book claims little in the way of originality and attempts to correlate results of various others. Bauer completed this book in June 1925, attended the War College in 1926, and left the Army to lead the establishment on 27 Feb 1927 of federal civil aviation medical examiners in the Aeronautics Branch of the Department of Commerce. The Army School of Aviation Medicine had been moved to Texas in 1926 over objections from Bauer.
NOTE: This book includes a confused and incomplete description of the DPA and its history.
(a) Page xi – The first two entries in the LIST OF ILLUSTRATIONS are as follows:
"Fig. 1. The depth perception apparatus"
"Fig. 2. Testing depth perception"
Photographic plates are inserted as unnumbered pages for Figures 1 and 2.
These two photographs are of the DPA and testing condition described in Deyo (1922), but Bauer fails to state that fact.
(b) On pages 13-17 (CHAPTER II, The Eye in Aviation, "Judgment of Distance" section):
The photographic plate of the DPA described by Deyo (1922) is inserted as an unnumbered page but is labeled, in contradiction to the above LIST OF ILLUSTRATIONS, as
"Fig. 1 The Howard-Dolman Depth Perception Apparatus."
Bauer provides no reference to justify the addition of the name "Dolman".
An extensive search of the government and public literature reveals no documentation of any contribution whatsoever by anyone named Dolman to depth acuity research or testing apparatus.[5]
More confusingly, on page 13, Bauer describes the so-called Dolman modification pictured in Figure 1 by reciting, verbatim, the dimensions of the Howard (1919a) version of the James (1908) DPA. The dimensions provided do not correspond to the pictures in Figures 1 and 2.
(c) Bauer did not even provide the first name of Dolman; there was a Capt Percival Dolman at MRL in 1918, but he returned to civilian live in San Francisco in late 1919 (before this research as undertaken); Percival Dolman did not author any paper on DPA and was not acknowledged by Howard (his contemporary at MRL) in any publication.

(Berry, Riggs, and Richards, 1950)
Berry, Riggs, and Richards, J. Exptl. Psychol. 40, 520 (1950).
Note: Reported actual width of targets in the two rod case had no effect on depth acuity.

[5] The library of the MRL (established in 1918) and the School of Aviation Medicine (established in 1922) are now part of the archives of the modern day version of these organizations, the USAF AFMC 711 Human Performance Wing at WPAFB OH. One of the authors (Hopper) has searched this library archive and other world literature, but no document authored by anyone named Dolman has been found to document a contribution to any DPA.

(Blaauw, 1917)
Blaauw, E.E. (M.D., Buffalo), "Binocular Single Vision. Leaving Out the Consideration of the Color Perception and the Problems of Strabismus," Transactions of the Section on Ophthalmology of the American Medical Association for 1917, pp 17-38
Paper read at AMA meeting in New York City, June 6-8, 1917.
See AMA Transactions for 1917 (Google book scan).
http://books.google.com/books?id=X5QDAAAAYAAJ&lpg=PA17&ots=Kw_59XtwVY&dq=E.%20E.%20Blaauw&pg=PA17#v=onepage&q=E.%20E.%20Blaauw&f=false

(Blaauw, 1920)
Blaauw, E.E., Binocular Discrimination of Distance (an editorial summary of G.J. Schoute 1910), AJO Series 3 Volume 3(9), 705-706 (September 1920).
http://books.google.com/books?id=8IY1AQAAMAAJ&lpg=PA705&ots=cm1oaTOeJB&dq=G.%20J.%20Schoute%20Binocular%20Vision&pg=PA705#v=onepage&q=G.%20J.%20Schoute%20Binocular%20Vision&f=false

(Bohr and Read, 2013)
Bohr, I., and Read, J. C. A., "Stereoacuity with Frisby and Revised FD2 Stereo Tests." *PLoS ONE*, 8(12), e82999. doi: 10.1371/journal.pone.0082999 (2013).

(Benton and Bove, 2008)
Benton, Steven A. and Bove Jr,, V. Michael, **Holographic Imaging** (Wiley-Interscience, 2008), 270 pages.

(Brundell et al., 1993)
Blundell, B., Schwarz, A., and Horrel, D., "Volumetric three dimensional display systems: their past, present and future." *Engineering Science and Education Journal* **2** (5), 196-200 (1993).

(Cormack and Fox, 1985)
Cormack Robert H. and Fox, Robert. "The computation of retinal disparity" *Perception & Psychophysics* **37** (2), 176-178 (Feb 1985).

(Cormack and Fox, 1986)
Cormack Robert H. and Fox Robert. "The computation of disparity and depth in stereograms" *Perception & Psychophysics* **38** (4), 375-380 (April, 1986).

(Deyo, 1922)
There are two places where this work is published, in slightly different forms, as follows:
(i) Deyo, Barbara Valette, "MONOCULAR AND BINOCULAR JUDGMENT OF DISTANCE," *American Journal of Ophthalmology*, **5** (5), 343-347 (May 1922).
(ii) Deyo, Barbara Valette, "MONOCULAR AND BINOCULAR JUDGEMENT OF DISTANCE," *Air Service Information Circular (ASIC)* Vol. **IV** No. 359, pp 25-27 (1Aug1922).

(Donelan, 2010)
Donelan, J. "The Actuality Story" *Information Display* 26:5&6, 2010 pp 24-27

(Downing et al., 1996)
Downing, Elizabeth, Hesselink, Lambertus, Ralston, John, and Macfarlane, Roger, "A Three-Color, Solid-State, Three-Dimensional Display," SCIENCE **273**, 1185-1189 (30 Aug 1996).

(Downing, 1999)
US5956172A, "System and method using layered structure for three-dimensional display of information based on two-photon upconversion,"
Inventor: Elizabeth Anne Downing, Original Assignee: 3D Technology Labs, Inc.
Published: Sep 21, 1999. This application is a continuation of U.S. Patent No. 5,684,621.

(Fidopiastis et al., 2010)
Fidopiastis, C., Rizzo, A., and Rolland, J., "User-Centered Virtual Environment Design for Virtual Rehabilitation." *Journal of NeuroEngineering and Rehabilitation* **7** (11), pages? (2010).

(Fielder and Moseley, 1996)
Fielder, A. R. and Moseley, M. J., "Does stereopsis matter in humans?," *Eye* **10**, 233-238 (1996).

(Glanz, 1996)
Glanz, James, "Three-Dimensional Images Are Conjured in a Crystal Cube," SCIENCE, **273**, 1172 (1996). This "Technology" section item is a one-page summary of Downing work

(Helmholtz, 1856, 1896, 1910)
Helmholtz, Herman von, Handbuch der **Physiologischen Optik**,
1st Edition (1856), 2nd Edition (1896), 3rd edition (1910).

(Hirsch and Weymouth, 1948a)
Hirsch, Monroe J. and Weymouth, Frank W., "Distance Discrimination I. Theoretic Considerations," Arch Ophthalmol. **39**(2), 210-223 (1948).
https://archopht.jamanetwork.com/issue.aspx?journalid=73&issueid=17371

(Hirsch and Weymouth, 1948b)
Hirsch, Monroe J. and Weymouth, Frank W., "Distance Discrimination II. Effect on Threshold of Lateral Separation of the Test Objects," Arch Ophthalmol. **39**(2), 224-231 (1948).
http://archopht.jamanetwork.com/article.aspx?articleid=619876

(Hoffman et al., 2008)
Hoffman, D., Girshick, A., Akeley K., and Banks, M. "Vergence-Accommodation Conflicts Hinder Visual Performance and Cause Visual Fatigue," *Journal of Vision* **8** (3), 1-30 (2008).

(Holmes and Fawcett, 2005)
Holmes, J. M. and Fawcett, S. L., "Testing distance stereoacuity with the Frisby-Davis 2 (FD2) test." *American Journal of Ophthalmology* **139**, 193-195 (2005).

(Hopper et al, 2016)
Hopper, Darrel G., Meyer, Frederick M., Pinkus, Alan, Liggett, Kristen K., Havig, Paul R., Ellis, Sharon A., McIntire, John P. and Heft, Eric L. *AFRL Display Test and Evaluation Methodologies (AFTEM),* AFRL-RH-WP-TR-2016-xxxx, Wright-Patterson AFB: Human Effectiveness Directorate (2016, in press).

(Howard, 1919a, 1920a)

There are three places where this work is published, in slightly different forms as follows:

(i) Howard, Harvey James, "A TEST FOR THE JUDGMENT OF DISTANCE" *Transactions of the American Ophthalmological Society* **17**, 195-235 (Nov 1919). Proceedings volume from AOS Annual Meeting held in June 1919. Paper was presented Sat, 14 Jun 1919 at the FIFTY-FIFTH ANNUAL MEETING of the American Ophthalmological Society (AOS) at THE MARLBOROUGH-BLENHEIM hotel in Atlantic City, N. J., June 14-18, 1919).
See also discussion following Howard presentation, TAOS **17**, 755-757 (Nov 1919).
http://www.ncbi.nlm.nih.gov/pmc/articles/PMC1318185/ (Accessed 8 Jul 2014).

(ii) Howard, Harvey James, "A TEST FOR THE JUDGMENT OF DISTANCE," Am. J. Ophthalmol. **2** (12) 656-675 (December, 1919).
https://archive.org/details/s3americanjournalop02chicuoft

(iii) Howard, Harvey James, "A TEST FOR THE JUDGMENT OF DISTANCE," *Air Service Information Circular* Vol. **I** No. 3 Part 13, pp. 99-115 (March 15, 1920). [File B 63/6]
http://scans.library.utoronto.ca

See also: (James, 1908) for the original design of the apparatus that Howard used "With a few modifications and addition of a head-rest…"

(Howard, 1919b)

There are two places where this work is published, in slightly different forms, as follows:

(i) http://www.ajo.com/article/S0002-9394%2819%2990253-4/pdf
Howard, Harvey J., "A SIX-METER STEREOSCOPE," *Transactions of the American Ophthalmological Society* **17**, 401-405 (published Nov 1919). Proceedings volume from AOS Annual Meeting held in June 1919. Paper presented in the session on "EXHIBITION OF NEW INSTRUMENTS AND APPARATUS" on Tues 17 Jun 1919 at the FIFTY-FIFTH ANNUAL MEETING of the American Ophthalmological Society (AOS) at THE MARLBOROUGH-BLENHEIM hotel in Atlantic City, N. J., June 14-17, 1919.

(ii) Harvey J. Howard (M.D., Oph.D., Peking, China), "A SIX METER STEREOSCOPE," American Journal of Ophthalmology Volume 2, Issue 12, 849–853, December 1919).

(Howard, 1919c, 1920b)

There are three places where this work is published, in slightly different forms, as follows:

(i) Howard, Harvey J., "A Stereomicrometer," *Transactions of the American Ophthalmological Society* **17**, 401-405 (published Nov 1919). Proceedings volume from AOS Annual Meeting held in June 1919. Paper presented in the session on "EXHIBITION OF NEW INSTRUMENTS AND APPARATUS" on Tues 17 Jun 1919 at the FIFTY-FIFTH ANNUAL MEETING of the American Ophthalmological Society (AOS) at THE MARLBOROUGH-BLENHEIM hotel in Atlantic City, N. J., June 14-17, 1919.

(ii) Howard, Harvey J., A STEREOMICROMETER, *American Journal of Ophthalmology* 3(6), 417-421 (June 1920).

(iii) Howard, Harvey J., A STEREOMICROMETER, *Air Service Information Circular (ASIC)* Vol. **I** No. 99 Part 16, pp 90-93 (15Aug1920)

(Howard, 1919d, 1920c)
There are two places where this work is published, in slightly different forms as follows:
(i) Howard, Harvey J., "JUDGMENT OF DISTANCE WITH SEMAPHORES AND A SCREEN AT 100 METERS," Arch. Ophthal. XLVIII, 461-474 (1919).
(Captain, M.C., Medical Research Laboratory, Hazelhurst Field, Mineola, Long Island, N.Y.)
(ii) Howard, Harvey J., JUDGMENT OF DISTANCE WITH SEMAPHORES AND A SCREEN AT 100 METERS, *Air Service Information Circular (ASIC)* Vol. **I** No. 99 Part 17, pp 94-99 (15Aug1920).

(Howard, I., 2008)
Howard, I. "Vergence Modulation as a Cue to Movement in Depth" *Spatial Vision* **21** (6), 581–592 (2008).

(Ichikawa and Saida, 1996)
Ichikawa, M. and Saida, S. "How is Motion Disparity Integrated with Binocular Disparity in Depth Perception?," *Perception & Psychophysics* **58** (2), 271-282 (1996).

(Ito et al., 2007)
Ito, Akinori, Yamaguchi, Takuni, and Sakamoto, Yasutada, "Turn-Type Color 3-D Display System Using Scanned Arrays of LEDs," SID 2007 DIGEST, paper P-61, 418-421 (2007).

(James, 1907)
James, G.T. Brooksbank, "Some Notes on Stereoscopic Vision," *The Lancet*, p. 430 (February 16, 1907).
Note: paper read at the Ophthalmological Society meeting

(James 1908)
James, G. T. Brooksbank, "On the Measurement of Stereoscopic Visual Acuity," *The Lancet*, 1763-1766 (June 20, 1908). Note: (Howard, 1919) references this paper as providing the description for apparatus that he modified and used in his work.

(Johnston, 1991)
Johnston, E., "Systematic Distortions of Shape from Stereopsis." *Vision Research* **31**, 1351–1360 (1991).

(Lafayette 2014)
Depth Perception Apparatus, Model 14012A, Lafayette Instrument Company, Lafayette IN, www.lafayetteevaluation.com/printview.asp?id=2141 (accessed 27 Aug 2014).
"The Depth Perception Apparatus represents the state-of-the-art in sensation and perception measurement technology."
Tests depth perception acuity for pilots, crane operators, bus drivers, athletes, etc. for use in the employment selection process. Also used for laboratory research and teaching demonstrations. Dimensions (HxWxD): 11 x 10 x 27 in. (279 x 254 x 686 mm). Accuracy: 1 mm. Power: 10A Controls: LCD and keypad control plus digital joystick for controlling displacement.

(Lloyd, 2012)
Lloyd, Charles, J. "On the Utility of Stereoscopic Displays for Simulation Training," Proceedings of the Interservice/Industry Training, Simulation, and Education Conference (I/ITSEC), paper 12301, 9 pp (2012).

(Klug et al., 2013)
Klug M, Burnett T, Fancello A, Heath A, Gardner K,O'Connell S, Newswanger C. A Scalable, Collaborative, Interactive Light-field Display System. Society of Information Display Symposium Digest of Technical Papers 2013 pp. 412-415

(Lafayette Instrument Co., 2016)
Commercial automated depth perception apparatus is available $3,427.00 from the Lafayette Instrument Company in Lafayette IN. The Lafayette Depth Perception Apparatus, Model 14012A is a closed internally LED-illuminated box with dimensions 254Wx279Hx686L mm, rod motion accuracy 1mm, power 10A for 110/220 60Hz and an LCD and keypad control plus digital joystick for controlling displacement. Lafayette states that "The Depth Perception Apparatus represents the state-of-the-art in sensation and perception measurement technology" and is used to test depth perception acuity for pilots, crane operators, bus drivers, and athletes for use in the employment selection process. The DPA is also used in laboratory research and teaching demonstrations.
(www.lafayetteevaluation.com/printview.asp?id=2141, accessed 24 Jul 2016).

(McKee and Taylor, 2010)
McKee, S. and Taylor, D., "The Precision of Binocular and Monocular Depth Judgments in Natural Settings," *Journal of Vision* **10** (10):5, 1-13- (2010).
Note: re-discovers results published in 1907, 1908, 1919, 1922, etc.

(Meyer et al., 2016)
Meyer, Frederick M., Heft, Eric L., and Hopper, Darrel G., "*Computer Automated Electronics for Howard Depth Perception Apparatus,"* AFRL-RH-WP-TR-2016-xxxx, Wright-Patterson AFB: Human Effectiveness Directorate (2016, in preparation).

(Mon-Williams et al., 2000)
Mon-Williams, M., Tresilian, J., and Roberts, A., "Vergence provides veridical depth perception from horizontal retinal image disparities," *Exp Brain Res* **133**, 407–413 (2000).

(Osmanis, 2016)
LightSpace Technologies, Ilmars Osmanis, CEO, ilmars.osmanis@lightspace3d.com
Sales: **Lightspace Technologies Inc.,** P.O. Box 242, Twinsburg OH 44087, USA);
R&D & Mfg: **Lightspace Technologies SIA**, Lielirbes iela 17A, Riga, LV-1046, Latvia, phone (+371) 6780 0009. Email info3d@lightspace3d.com |
Website: www.lightspace3d.com (accessed 23 Jul 2016)
Current product: x1405B

(Patterson, 2009)
Patterson, Robert, "Human factors of 3-D displays," *Journal of the Society for Information Display (JSID)* **17** (12), 987-996 (2009).

(Rolland et al., 1995)
Rolland, J., Gibson, W., and Ariely, D., "Toward Quantifying Depth and Size Perception in Virtual Environments." *Presence* **4**, 24-49 (1995).

(Scarfe and Hibbard, 2006)
Scarfe, P. and Hibbard, P., "Disparity-defined objects moving in depth do not elicit three-dimensional shape constancy." *Vision Research* **46**, 1599–1610 (2006).

(Schoute, 1910)
Schoute, G. J., "Binocular Vision," Nederl. Tydschr. v. Geneesk (1910).
This paper is in Dutch; for a summary in English see (Blaauw, 1920)

(Sechrist, 2014)
Sechrist, Steve, "TVs, 3-D, and Holograms at Display Week 2014," *Information Display* **30** (5), 14-18 (2014). See page 17 for discussion and photograph of QPI demonstration at SID 2014 exhibition.

(Sloane and Gallagher, 1946)
Sloane, Albert E., and Gallagher, J. Roswell, "Evaluation of Stereopsis: A Comparision of the Howard-Dolman and the Verhoeff Test," Archives of Ophthalmology **34** (5), 357-359 (1946).

(Soltan et al., 1992)
Soltan, Parviz, Trias, John, Robinson, Waldo, and Dahlke, Weldon, "Laser Based 3D Volumetric Display System, SPIE 1664, Paper 23, 133-137 (1992). This paper is also available from DTIC: Accession No. AD-A264285 (June 1993).

(Soltan et al., 1994)
Soltan, P., et al., "Laser-based 3-D Volumetric Display System (2nd Generation)," SID Digest of Papers (1994). Published?

(Soltan et al., 1996)
Soltan, Parvis, Trias, John, Dahlke, Weldon, Lasher, Mark, and McDonald, Malvyn, "Laser-Based 3-D Volumetric Display System (The Improved Second Generation)," American Society of Navel Engineering (April 1995). This paper is also available as DTIC Accession No. ADA306215 (March 1996).
"Using a novel Acousto-Optic (AO) Random Access Scanner, up to 40 thousand laser-generated voxels refreshed at 20 Hz per color are projected onto the reflective surface of the rotating helix." "The device incorporates a 36-inch diameter (and 18-inch high) double helix that spins at approximately 10 revolutions per second, providing a means to address the cylindrical volume."

(Stanford Lightfield Workshop, 2015)
https://scien.stanford.edu/index.php/workshop-on-light-field-imaging/

(Surman et al., 2006)
Surman, P., Sexton, I., Hopf, K., Lee, W.K., Bates, R., IJsselsteijn, W., and Buckley, E., Head Tracked Single and Multi-user Autostereoscopic displays," Proceedings of the 3rd European IEEE Conference on Visual Media Production, pp. 144-152 (29-30 Nov 2006).

(Tefft and Stark, 1922)
Tefft, Lloyd E. (M.D., Major) and Stark, Elizabeth, K., "SPEED OF ACCOMMODATION AS A PRACTICABLE TEST FOR FLIERS," Am J Ophthal 5(5) 339-342 (May 1922).
NOTE: This work seeks to ascertain the relationship of accommodation speed, if any, to several standard eye tests then in use. The paper contains the phrase "depth perception as elucidated by the Howard-Dolman depth perception apparatus," but provides no description of, nor any reference to documentation for, this apparatus. This is the earliest paper found to date that even uses name Dolman in association with the perception of depth. There is no evidence that any person named Dolman made any contribution to depth acuity testing or measurement apparatus. Tefft and Stark did not even provide the first name of Dolman; there was a Capt Percival Dolman at MRL in 1918, but he returned to civilian live in San Francisco in late 1919 (before this research as undertaken); Percival Dolman did not author any paper on DPA and was not acknowledged by Howard (his contemporary at MRL) in any publication.

(Thorne, 1928)
Thorne, Frederick Hamilton (Capt, Medical Corps, Dir Dept Ophthal and Otology, School of Aviation Medicine, "A REVIEW OF DEPTH PERCEPTION," *The Military Surgeon* pp 693-657 (1928).

(Westheimer, 2011)
Westheimer, G., "Depth rendition of three-dimensional displays." *J. Opt. Soc. Am. A.* **28** (6), 1185-1190 (2011).

(Wheatstone, 1838)
Wheatstone, "Contributions to the Physiology of Vision," *Philosophical Transactions* (1838).

(Woodburne, 1934)
Woodburne, L. S., "The effect of constant visual angle upon the binocular discrimination of depth differences." *American Journal of Psychology* **46**, 273-286 (1934).

(Zalevski et al., 2007)
Zalevski, Anna M., Henning, G. Bruce, and Hill, N. Jeremy, "Cue combination and the effect of horizontal disparity and perspective on stereoacuity," Spatial Vision **20** (1-2), 107-138 (2007).

LIST OF SYMBOLS, ABBREVIATIONS AND ACRONYMS

2AFC	Two Alternative Forced Choice
2D	Two dimensional
3D	Three dimensional
9-tile	Configured ZMD with 9 tileable units to create 21" diagonal display
x	Linear lateral displacement in the image plane for object moved from that plane
x_{retina}	Linear projection on the retina for xx
z	Linear depth displacement of line of sight to an object moved from that plane
Actuality	Volumetric 3D based DMD image slices projected onto spinning screen
AFRL	Air Force Research Laboratory
AIS	Actuality Integral Slice ("Perspecta"), a volumetric FoLD system
AJO	American Journal of Ophthalmology
AMOLED	Active Matrix Organic Light Emitting Diode
AOC	Air Force Air Operations Center
AOI	Area of interest
AOS	American Ophthalmology Society
API	Application programming interface
ASP	Angle of Stereoscopic Parallax = angle subtended at eye nodal point by x=SP = BPA = difference between apex angles subtended at two objects by the IPD baseline. Example: for (IPD, z) = (63mm, 5mm), ASP = 8.74 μrad = 1.803 arcsec.
AVE	Augmented virtual environment
BP	Binocular Parallax (same as Linear Stereocopic Parallax = linear SP)
BPA	Binocular Parallactic Angle (term used by Howard 1919a) ≡ ASP
BSV	Binocular Single Vision ≡ the perception of a single image for an object seen with both eyes
BSD	Berkley Software Distribution
CAD	Computer-aided design
COTS	Custom off-the-shelf
CREST	Center for Research in Education and Simulation Technologies
CT	Computerized tomography
DARPA	Defense Agency Research Projects Agency
Dim	Dimension
DLP	Digital Light Processing
DMD	Digital micromirror device
DoD	Department of Defense
DPS	Display updates per second
DXT	Compression algorithm
eJSS	eJ Software Suite
EMD	High Resolution Affordable Emissive Micro Display (a DARPA program)
FMHD	Full Multiplex Holographic Display (an AFRL program)
FOB	Forward operating base

FoLD	Field of Light Display (volumetric integral slice, hogel-based integral ray,
FOV	etc.)
	Field of views
FPGA	Field programmable gate array
FPS	Frames per second
FPS	Frames per second
FRU	Field replaceable unit
GL/ES	Graphical language / Embedded systems
GPS	Global positioning system
GRIN	Gradient Index Lens
GUI	Graphical user interface
GWOT	Global War on Terror
HL3DM	Holographic Lightfield 3D Display Metrology (an AFRL program)
HD	High definition
HDDPA	Howard-Devo Depth Perception Apparatus
	Howard-Dolman Depth Perception Apparatus (Dolman should be Devo)
Hogel	Holographic Element
HPO	Horizontal parallax only
HPS	Hogels per second
HVD	Holographic Video Display (an AFRL program)
Hz	Hertz
I/O	Input/output
ISSO	Information Services Support Office
IVIR	Information Visualization and Innovative Research
LCOS	Liquid crystal on silicon
LDAM	Light Distribution Array Modification
LED	Light emitting diode
LiDAR	Light detection and ranging
Linear SP	Same as SP
Matlab	Tool for doing numerical computations with matrices and vectors
MEMS	Micro-electro-mechanical syste,
mopel	micro-optical element (aka hogel)
Mpx	Megapixel
MRI	Magnetic resonance imaging
MTF	Modulation transfer function
MVP	Model View Projection Matrix
OGC	Open Geospatial Consortium
OIF	Operation Iraqi Freedom
OS	Operating system
OTS	Off-the-shelf
PBM	Performance Based Metrics
PC	Personal computer
PCB	Printed circuit board
PCI-e	Peripheral Component Interconnect Express
PM/CM	Project Management / Contracts Management

PMO	Project Management Office
POC	Proof-of-concept
POV	Point of view
PRISM	Parallel Ray Interpolation for Stereo Mosaicing
PRS	Actuality Integral Slice (AIS) Perspecta Rotating-Screen system (a FoLD system developed by Actuality Integral Slice (AIS) Perspecta … that creates a temporally-averaged perspective 3D image at each ~5mm pupil position in the design 360x120-deg HxV near-spherical viewing volume via rapid sequential projection of circular slices of the 3D model data as the screen spins; each slice must be refreshed at ≥30 Hz
PSF	Point-spread function
RDECOM	Army Research, Development and Engineering Command
RGB (+D)	Red, blue, green, plus depth
RMS	Root mean squared
S3D	Stereo 3D (display device)
SAR	Synthetic aperture ranging
SBIR	Small Business Innovative Research (a government program)
SD	Standard Deviation (σ), defined if Gaussian statistical model applies (n>8)
SEM	Standard Error Measure, for n = 6 (Gaussian statistics not applicable)-this
SHO	report
SIR	Synthetic Holographic Observation (an IARPA program)
SLM	Spatially Integrated Ray (a type of light field Spatial light modulator (modulation)
SOC	Systems-on-a-chip
SOCOM	Special Operations Command
SP	Stereoscopic Parallax = the linear distance (in the image plane) between two lines projected from one eye nodal point to two object points (one in and one beyond the image plane); also called linear SP, or Binocular Parallax The two object points are both on line projected from the other eye nodal point. The image plane is parallel to the IPD line between the two nodal points.
SPDU	Second per display update
Stereo 3D	Left/right eye images projected sequentially viewed with special viewing glasses (eye selection wear, active shutter or left/right circularly polarized)
SVO	Sparse voxel octree
SWaP	Size, weight, and power
TAOS	Transactions of the Americal Ophthalmological Society
TBV	Tactical Battlefield Visualization
TCPIP	Transmission Control Protocol/Internet Protocol
TDH	Tactical Digital Holograms
TI	Texas Instruments
UPSD	Urban Photonic Sandtable Display
USSOCOM	United States Special Operations Command
VE	Virtual environment

ZIR	Zebra Integral-Ray system (a full-parallax FoLD system developed by Zebra Imaging, Inc. that creates an image at each ~5mm pupil position in the design 90-deg. conical viewing zone as from rays emanating from widely distributed, non-adjacent 2D pixels, each projected in a fixed direction by a microoptics array)
ZMD	ZScape® Motion Display